

Electronic Theses and Dissertations, 2004-2019

2018

Brain Stethoscope: A Non-invasive Method for Monitoring Intracranial Pressure

Md Khurshidul Azad
University of Central Florida

 Part of the [Electro-Mechanical Systems Commons](#)
Find similar works at: <https://stars.library.ucf.edu/etd>
University of Central Florida Libraries <http://library.ucf.edu>

This Masters Thesis (Open Access) is brought to you for free and open access by STARS. It has been accepted for inclusion in Electronic Theses and Dissertations, 2004-2019 by an authorized administrator of STARS. For more information, please contact STARS@ucf.edu.

STARS Citation

Azad, Md Khurshidul, "Brain Stethoscope: A Non-invasive Method for Monitoring Intracranial Pressure" (2018). *Electronic Theses and Dissertations, 2004-2019*. 5824.
<https://stars.library.ucf.edu/etd/5824>

BRAIN STETHOSCOPE: A NON-INVASIVE METHOD FOR MONITORING
INTRACRANIAL PRESSURE

By

MD KHURSHIDUL AZAD
B.S RAJSHAHI UNIVERSITY OF ENGINEERING & TECHNOLOGY, BANGLADESH
2009

A thesis submitted in partial fulfillment of the requirements
for the degree of Master of Science
in the Department of Mechanical and Aerospace Engineering
in the College of Engineering and Computer Science
at the University of Central Florida
Orlando, Florida

Spring Term
2018

Major Professor: Hansen A. Mansy

© 2018 Md Khurshidul Azad

ABSTRACT

Monitoring intracranial pressure (ICP) is important for patients with increased intracranial pressure. Invasive methods of ICP monitoring include lumbar puncture manometry, which requires high precision, is costly, and can lead to complications. Non-invasive monitoring of ICP using tympanic membrane pulse (TMp) measurement can provide an alternative monitoring method that avoids such complications. In the current study, a piezo based sensor was designed, constructed and used to acquire TMp signals. The results showed that tympanic membrane waveform changed in morphology and amplitude with increased ICP, which was induced by changing subject position using a tilt table. In addition, the results suggest that TMp are affected by breathing, which has small effects on ICP. The newly developed piezo based brain stethoscope may be a way to monitor patients with increased intracranial pressure thus avoiding invasive ICP monitoring and reducing associated risk and cost.

ACKNOWLEDGMENTS

I am extremely grateful to Dr. Hansen Mansy, my thesis advisor, who has continuously inspired and mentored me to achieve my research goals. He helped me understand the motivation of the research and supported me with his ideas and guidance throughout this research. I would like to thank Dr. Kassab and Dr. Bhattacharya for their valuable inputs. In addition, I would like to thank Andrew Spiewak as well as my other colleagues in Biomedical Acoustic Research Laboratory for their continuous support.

TABLE OF CONTENTS

LIST OF FIGURES	viii
CHAPTER 1 : INTRODUCTION	1
1.1 Cerebrospinal Fluid and Intracranial Pressure	2
1.2 Inner Ear	4
1.3 Relation Between CSF Pressure and Cochlear Fluid Pressure	6
1.4 Middle Ear	6
1.5 Tympanic Membrane and External Ear	7
1.6 Variation of CSF Pressure and ICP with Respect to Body Posture	8
1.7 Effect of Tympanic Membrane Movement on Intracranial Pressure	10
1.8 Measurement of Tympanic Membrane movement using volume displacement	11
1.9 Relation between CSF Flow and Cerebral Blood Flow	14
CHAPTER 2 : METHODS	17
2.1 Building the Sensor Assembly	17
2.2 Data acquisition, Post Processing and Analyzing the Acquired TMp Data	18
2.2.1 Data Acquisition, Plotting the Acquired Tympanic Membrane Waveform with Earlobe Pulse and Airflow	18
2.2.2 Filtering the acquired signals	19
2.2.3 Identifying the Peaks of Ear lobe pulse	20

2.2.4	Finding the Nadirs (start and end points) of Individual TMp waveforms	21
2.2.5	Separating the Individual TMp Events	22
2.2.6	Average TMp Waveform and Normalized Deviation from Mean.....	23
2.2.7	Effect of Breathing on Tympanic Membrane Pulsations.....	25
2.2.8	Separating the TMp Events Based on Lung Volume.....	26
2.2.9	Mean TMp for High and Low Lung Volume	29
2.3	Testing the TMp Sensor Output Using Mechanical Setup.....	30
2.3.1	Experimental Setup.....	30
2.3.2	Testing the sensor output with multiple input signals	32
2.3.3	Testing Repeatability of the Piezo based TMp Sensor Output	35
2.3.4	Testing the Repeatability of LASER Doppler Vibrometer Output.....	36
2.3.5	Testing the Effect of External Pressure on TMp Sensor Output	37
2.4	Testing the Effect of Dead Space in the System on TMp Signal Output.....	38
2.5	Testing the effect of leakage on TMp Signals.....	41
2.6	Testing the repeatability of the TMp signal	44
2.7	Investigating the difference between contralateral ears	45
2.8	Testing the Effect of External Pressures on TMp Signals	46
CHAPTER 3 : TYMPANIC MEMBRANE PULSATIONS AT VARYING TILT ANGLE.....		48
3.1	Experimental Procedure	48

3.2	Results	49
3.3	TMp changes with title angle for shorter acquisition and settling times	56
CHAPTER 4 : SIMPLIFIED MODEL OF TYMPANIC MEMBRANE PULSATIONS		62
4.1	Model Geometry	62
4.2	Results	64
CHAPTER 5 : DISCUSSION AND CONCLUSION		67
5.1	Discussion	67
5.1.1	Other Approaches of TMp Measurement	67
5.1.2	Repeatability of the Piezo Sensor Output	70
5.1.3	Repeatability of TMp signals in Human Subjects	71
5.1.4	Effect of Body Posture on TMp.....	71
5.1.5	Simplified Numerical Model	72
5.2	Future Work	73
5.3	Conclusion.....	74
LIST OF REFERENCES		75

LIST OF FIGURES

Figure 1-1 CSF System Showing the CSF fluid in cranial subarachnoid space as well as ventricular places. [2].....	2
Figure 1-2 ICP waveform acquired by inserting ICP sensor through subdural cavity. (a) the whole duration of the signal (b) zoomed in version of 6 second time window. [5]	3
Figure 1-3 Inner ear showing Cochlea and the vestibular system. The inner ear is filled with Perilymph and Endolymph. Both fluid is connected to CSF through cochlear aqueduct and endolymphatic sac respectively. [6].....	4
Figure 1-4(a): Cross sectional area of human inner ear [8].(b) Cross sectional area of cochlea. [9]	5
Figure 1-5 Human middle ear. [9]	7
Figure 1-6 Human tympanic membrane along with An: Annulus fibrosus, Lpi: Long process of incus; Um: Umbo, the end of malleus; Lr: Light reflex; Lp: Lateral process of the malleus; At: Pars flaccida; Hm-handle of the malleus. [13].....	7
Figure 1-7 Cerebrospinal fluid pressure in dog at different body posture. [14]	8
Figure 1-8 CSF pressure in man with varying body posture. [14].....	9
Figure 1-9 Tympanic membrane displacement for pre-and post-operative condition for a patient with elevated ICP with a stimulus signal of 1000 Hz. While the negative volume indicates in-ward going movement, the positive volume indicates out-ward going movement of the tympanic membrane. [19].....	11
Figure 1-10 Tympanic membrane displacement system showing the ear canal connected to a cavity using a tube. The microphone measures the pressure fluctuations due to tympanic membrane	

movement. The microphone output is then sent to reference diaphragm driver unit to move the diaphragm and keep a constant pressure in the cavity. The microphone output is a measure of tympanic membrane movement. [20] 12

Figure 1-11 Tympanic membrane volume displacement waveform due to stapedius reflex excitation. [20] 13

Figure 1-12 Relation between blood and CSF volume in the brain. As the blood volume increases, the CSF volume decreases. The caudal flow indicates CSF flow towards spinal cord while the cranial flow indicates cerebral blood flow towards brain. [21] 14

Figure 1-13 Blood and CSF flow rate in the cranium. There is a time delay between the peak flow of the two systems. [21] 15

Figure 2-1(a) 0.6 kHz 44 mm piezo disc (b) Piezo sensor along with a side pressure tap and a long tube to be put in external ear canal. 17

Figure 2-2 (a) Ear lobe pulse sensor (b) TMp sensor assembly. The piezo sensors and the ear lobe sensors are inside the right and left ear muffs. The while valves are used to test sealing between ear canal and piezo disc by connecting the valve outlet to a manometer 18

Figure 2-3 Tympanic membrane pulse (top), earlobe pulse (middle) and breathing airflow (bottom). The tympanic membrane waveform changed with airflow. 19

Figure 2-4 Filtered TMp, earlobe pulse and airflow data 20

Figure 2-5 Earlobe pulses with their peaks marked with red circles 21

Figure 2-6 TMp and earlobe pulse waveforms are plotted. The peak locations of earlobe pulses are marked with black circles. The start and end points of corresponding TMp waveforms are marked with red and green circles 22

Figure 2-7 Twenty Individual TMp events plotted on top of each other. Although all the events were synchronized around their peaks, some of the events had steeper valley than the others.... 23

Figure 2-8 Mean TMp waveform. This waveform is the mean of 55 individual TMp waveforms 24

Figure 2-9 Normalized deviation from mean TMp waveforms are plotted. The values range between .25 and .8. The change in TMp waveform with respect to time might be related to breathing 25

Figure 2-10 Normalized deviation from the settled TMp for all TMp waveform (blue line) is plotted along with subject's respiration airflow data (green line). It is evident that the variation in TMp waveform synchronize with subject breathing 26

Figure 2-11 Normalized deviation from mean and airflow was plotted together. The red line indicates the regions of inspiration and expiration. The upper flat lines are inspiration region while the lower flat line indicates expiration..... 27

Figure 2-12 Normalized deviation from mean and lung volume data are showed. Red line indicates separation of high and low lung volume event. The regions of upper flat line indicate high lung volume effects while the lower flat line indicates low lung volume events 27

Figure 2-13 Identifying the pulse peaks based on high and low lung volume. The green circle indicates high lung volume event while the red circle indicates low lung volume event..... 29

Figure 2-14 Mean TMp waveforms for high and low lung volume events. Normalized deviation between the two mean waveforms was 0.5102..... 30

Figure 2-15 Mechanical setup for testing the TMp sensor output independent of human factor . 31

Figure 2-16 Piezo output plotted against piezo disc displacement and membrane displacement at 1Hz cosine input signal. The normalized deviation from mean of piezo displacement was 0.883 and the sensitivity was found to be 0.2117 V/mm..... 32

Figure 2-17 Piezo output plotted against piezo disc displacement and membrane displacement at 2Hz cosine input signal. The normalized deviation from mean of piezo displacement was 0.8421 and the sensitivity was 0.2274 V/mm..... 33

Figure 2-18 Piezo output plotted against piezo disc displacement and membrane displacement at 5Hz cosine input signal. The normalized deviation from mean of piezo displacement was 0.7865 and sensitivity was 0.3358 V/mm..... 33

Figure 2-19 Piezo output plotted against piezo disc displacement and membrane displacement at 10Hz cosine input signal. The normalized deviation from mean of piezo displacement was 0.7858 and the sensitivity was 0.3228 V/mm..... 34

Figure 2-20 Piezo output plotted against piezo disc displacement and membrane displacement at 20Hz cosine input signal. The normalized deviation from mean of piezo displacement was 0.8273 and the sensitivity was 0.3166 V/mm..... 34

Figure 2-21 Left: Filtered piezo output with 5 hz cosine input. Right Mean Piezo output waveform at different time. The acquired TMP sensor output is comparable to the input signal. The normalized deviation from mean is about 0.0736..... 35

Figure 2-22 Left: Filtered piezo output with 5 hz cosine input.Right: Mean LDV waveform at different time.. The normalized deviation from mean is 0.0135 36

Figure 2-23 TMP sensor output at different external pressure. The normalized deviation from mean of zero pressure for +8, +4, -8 and -4 were 0.144, 0.102, 0.165, 0.118 respectively. 37

Figure 2-24 TMp data when both leak testing valve closed and plugged to provide complete seal from the environment. Both left and right TMp waveform have similarity in shape compared left and right ear lobe pulse. 39

Figure 2-25 TMp data when left valve is closed and right valve opened and plugged to provide a little dead space. Results show that adding a little dead space didn't significantly change the waveform. 40

Figure 2-26 TMp data when right valve is opened and connected to manometer. Although the system is sealed, results show that adding a lot of dead space changed the right TMp waveform. 40

Figure 2-27 Mean waveform showing significant change in waveform when there is considerable dead space between the sensor and tympanic membrane, the amplitude of the waveform decreased and the shape of TMp waveform changed. The normalized deviation relative to mean for closed and plugged case for open and plugged was 0.0780 and for open and connected to manometer was 0.8825..... 41

Figure 2-28 TMp data when both valves are closed. Results show that both TMp waveform showing similarity in comparison to left and right ear pulse. This waveform with sharp single peak may be an indicator of a sealed system..... 42

Figure 2-29 TMp data when the right valve is opened by half a turn. These results show that the right TMp waveform started to lose its original shape and amplitude due to leakage of the system. 42

Figure 2-30 TMp data when the right valve is opened completely to provide a leakage to the right side. The waveform lost in terms of shape and magnitude. This can be an indicator of leakage in the system..... 43

Figure 2-31 Mean TMp waveform showing the amplitude of the TMp waveform significantly reduced as the valve position changed from closed to open. The shape of the waveform also changed as leakage introduced to the system. The normalized deviation relative to the mean of completely sealed system for half open and fully open condition was found to be 0.93 and 1.11 respectively. 43

Figure 2-32 Repeatability testing of the TMp signal for left and right ear for same subject over a period. The normalized deviation from mean TMp for left and right 0.216 and 0.194 respectively 44

Figure 2-33 TMp waveform at contralateral ear canal (right sensor in left ear and left sensor in right ear) and ipsilateral (left sensor left ear and right sensor right ear) at different time period. The normalized deviation for left sensor at contralateral and ipsilateral was 0.08 and 0.22 while for right sensor in contralateral and ipsilateral ear was 0.19 and 0.19 respectively. 45

Figure 2-34 Mean Right TMp waveforms at varying external pressure applied in right external ear canal-TMp sensor cavity. The maximum peak to peak amplitude difference was about 3 mV found between zero pressure and positive 8 cm of water. This was about 20 % of the peak-to-peak amplitude at zero pressure. The normalized deviations from zero pressure were, 0.3039, 0.1693, 0.2513 and 0.1296 for pressures of 8, 4, -8, and -4 of water, respectively. 46

Figure 2-35 Mean TMp waveforms at different external pressures. The maximum peak to peak amplitude difference was about .3 mV found between zero pressure and positive 4 cm of water.

This was about 9 % of the peak to peak amplitude at zero pressure. The normalized deviations from zero pressure were, 0.1743, 0.2047, 0.1454, 0.1471 for pressures of 8, 4, -8, and -4 of water, respectively. 47

Figure 3-1 Experimental setup showing: the data acquisition system, the Piezo sensor assembly, and spirometer assembly (top row). The bottom picture shows the subject wearing piezo sensor headset while the spirometer is put into subject's mouth to acquire the breathing data. 49

Figure 3-2 TMp waveform (black continuous line) along with ear lobe pulse (red dotted line) at different tilt positions. Starting at left top figure showing TMp and Pulse waveform for Supine position followed by 15 degrees, 30 degrees, 45 degrees, after hyper-ventilation at 45 degrees, 30 degrees, 15 degrees, supine again. As ICP increased (by increasing tilt angle) a detectable effect on TMp waveform was seen. Hyperventilation (which is known to reduce ICP) also affects the TMp waveform. TMp appeared to return its supine morphology as the subject was returned to the supine position. (Subject 1)..... 50

Figure 3-3 TMp and Ear pulse signal was filtered (bandpass: 1-2 Hz) to calculate the time delay at fundamental frequency. As the tilt angle increased the amplitude of the TMp waveform increased and the corresponding time delay increased as well. 51

Figure 3-4 Time delay between TMp signal and earlobe pulse signal at different angle. Time delay changed with tilt angle. 52

Figure 3-5 TMp along with earlobe pulse at different tilt angle. The amplitude of the TMp increased as the tilt angle increased. (Subject 2) 53

Figure 3-6 TMp and earlobe pulse filtered at fundamental frequency for different tilt angle(subject 2) 53

Figure 3-7 Time delay at different tilt angle (subject 2) 54

Figure 3-8 Tmp along with earlobe pulse at different tilt angle. The amplitude of the Tmp increased as the tilt angle increased. (Subject 3) 54

Figure 3-9 Tmp and earlobe pulse filtered at fundamental frequency for different tilt angle (subject 3) 55

Figure 3-10 Time delay at different tilt angle (subject 3) 55

Figure 3-11 Tmp along with earlobe pulse at different tilt angle, when the latter changed rapidly. The amplitude of the Tmp increased as the tilt angle increased. (Subject 1) 57

Figure 3-12 Tmp waveform along with pulse as the tilt angle increased quickly the amplitude of the waveform increased. (Subject 1) 57

Figure 3-13 Time delay between Tmp and Pulse signal at different tilt angle (subject 1). The tilt angle was changed rapidly with a 15 second data acquisition at each angle. 58

Figure 3-14 Tmp along with earlobe pulse at different tilt angle changed rapidly. The amplitude of the Tmp increased as the tilt angle increased. (Subject 2) 58

Figure 3-15 Variation of Tmp waveform with change in tilt angle (Subject 2). The amplitude and time delay increased with tilt angle 59

Figure 3-16 Time delay between Tmp and Pulse signal at different tilt angle (subject 2). The tilt angle was changed rapidly with a 15 second data acquisition at each angle. 59

Figure 3-17 Tmp along with earlobe pulse at different tilt angle changed rapidly. The amplitude of the Tmp increased as the tilt angle increased (Subject 3) 60

Figure 3-18 Variation of Tmp waveform with change in tilt angle (Subject 3). The amplitude and time delay increased with tilt angle 60

Figure 3-19 Time delay between Tmp and Pulse signal at different tilt angle (subject 3). The tilt angle was changed rapidly with a 15 second data acquisition at each angle. 61

Figure 4-1 Schematic diagram of simplified model of CSF-Cochlea-Middle Ear-Tympanic Membrane. The red color showing the Soft tissue wall mimicking brain tissue, blue color corresponds to CSF fluid. The long bony channel represented by yellow is cochlear aqueduct. After cochlear aqueduct is cochlea surrounded by soft tissue. The green rectangle at the right end is the tympanic membrane. The yellow area between tympanic membrane and the cochlea is middle ear bones. The input is applied at left wall of CSF fluid 63

Figure 4-2 The maximum input deformation of the left CSF wall. The other boundaries of the fluid wall also deformed as the pressure travel towards cochlear aqueduct..... 64

Figure 4-3 Deformation of CSF wall due to pressure input..... 64

Figure 4-4 Maximum deformation of the TM. Since the edge of the TM is fixed, maximum deformation happened at the center. 65

Figure 4-5 Output deformation of tympanic membrane is plotted with input deformation. The output deformation is scaled. Results shows a delay of 250 millisecond between the input deformation and output deformation 66

Figure 5-1 Tympanic membrane pulsations using LED & photo resistor assembly. The top figure indicates the raw data from photo resistor output. The middle figure indicates the filtered data (bandpass: 1-95 Hz). The bottom plot corresponds to optical pulse sensor at right hand thumb. 67

Figure 5-2 Tympanic membrane pulsation using LDV. The top figure shows the raw LDV output. Second from the top figure showing the filtered Tmp data. Third from the top figure showing blood pulsations and bottom figure shows the filtered blood pulse data 68

Figure 5-3 Tmp signal using probe microphone along with blood pulse at right thumb. The top figure shows the raw microphone data. The second from the top shows the filtered data. The third figure from the top shows the envelope of the signal using Hilbert transform. The bottom plot shows the blood pulsations at right thumb..... 69

CHAPTER 1: INTRODUCTION

Increased intracranial pressure (ICP) can cause brain injury if left untreated. Elevated intracranial pressure is one of the outcomes of severe traumatic brain injury (TBI), hydrocephalus or intracerebral hemorrhage [1]. Hence, monitoring ICP is a useful tool for management of these cases. Invasive methods of monitoring the ICP includes lumbar puncture manometry, placing ICP transducer at certain locations, e.g., subdural or parenchymal. Although invasive methods of monitoring ICP are considered the gold standard, they come with certain risks and may require hospital or clinic visits. They require high clinical skill and can be costly. Hence, non-invasive methods of monitoring ICP can be advantageous for patients at risk of elevated intracranial pressure. The objective of this study is to develop a non-invasive way of monitoring ICP using tympanic membrane “pulses” (TMp) measurements. These pulses are vibratory movements of the membrane that occur naturally without external excitations.

1.1 Cerebrospinal Fluid and Intracranial Pressure

The cerebrospinal fluid (CSF) is a fluid that surrounds the brain ventricles, cranial and spinal subarachnoid spaces.

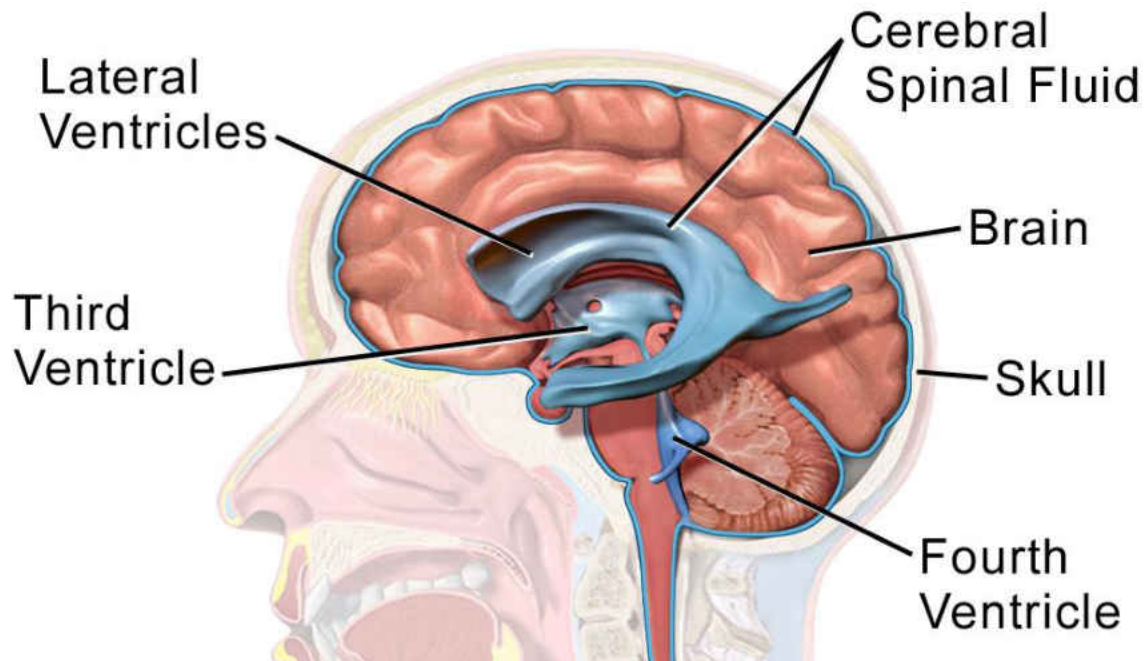


Figure 1-1 CSF System Showing the CSF fluid in cranial subarachnoid space as well as ventricular places. [2]

Figure 1-1 shows the CSF locations in the cranium. CSF is formed mainly in the choroid plexuses which is a network of cells that produces CSF in the ventricles of the brain. The mean CSF volume is approximately 150 ml where 25 ml contains in the ventricles and the remaining 125 ml is found in the subarachnoid spaces and spinal cord. The balance between CSF secretion and absorption and flow resistance determines the CSF pressure, which can be measured invasively by placing a pressure transducer in the brain parenchyma or in the CSF spaces via external lumbar drain or ventricular drain. The value of the CSF pressure varies between 10 and 15 mm Hg in normal adults

and 3 and 4 mm Hg in healthy infants [3]. According to Monro-Kellie hypothesis [4], the cranium is a rigid structure surrounding the brain, which is assumed to be incompressible. The volume inside the skull is constant. Therefore, the components of the cranium (volume of CSF, brain, blood, cerebral perfusion pressure) creates a homeostasis (a stable equilibrium between inter dependent elements) such that the increase in volume of one element leads to a decrease in other. This process keeps the ICP stable in normal humans. Figure 1-2 shows the typical ICP waveform obtained by placing an ICP sensor in the frontal brain parenchyma through dura [5].

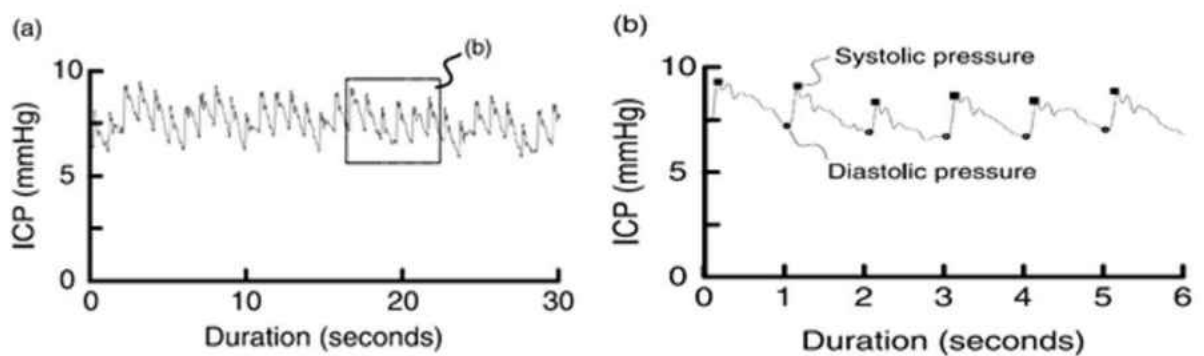


Figure 1-2 ICP waveform acquired by inserting ICP sensor through subdural cavity. (a) the whole duration of the signal (b) zoomed in version of 6 second time window. [5]

1.2 Inner Ear

The human inner ear (figure 1-3) consists of two regions: the vestibular system and the cochlea. The vestibular system consists of saccule, utricle and semi-circular canals, which are the human balance organs [6].

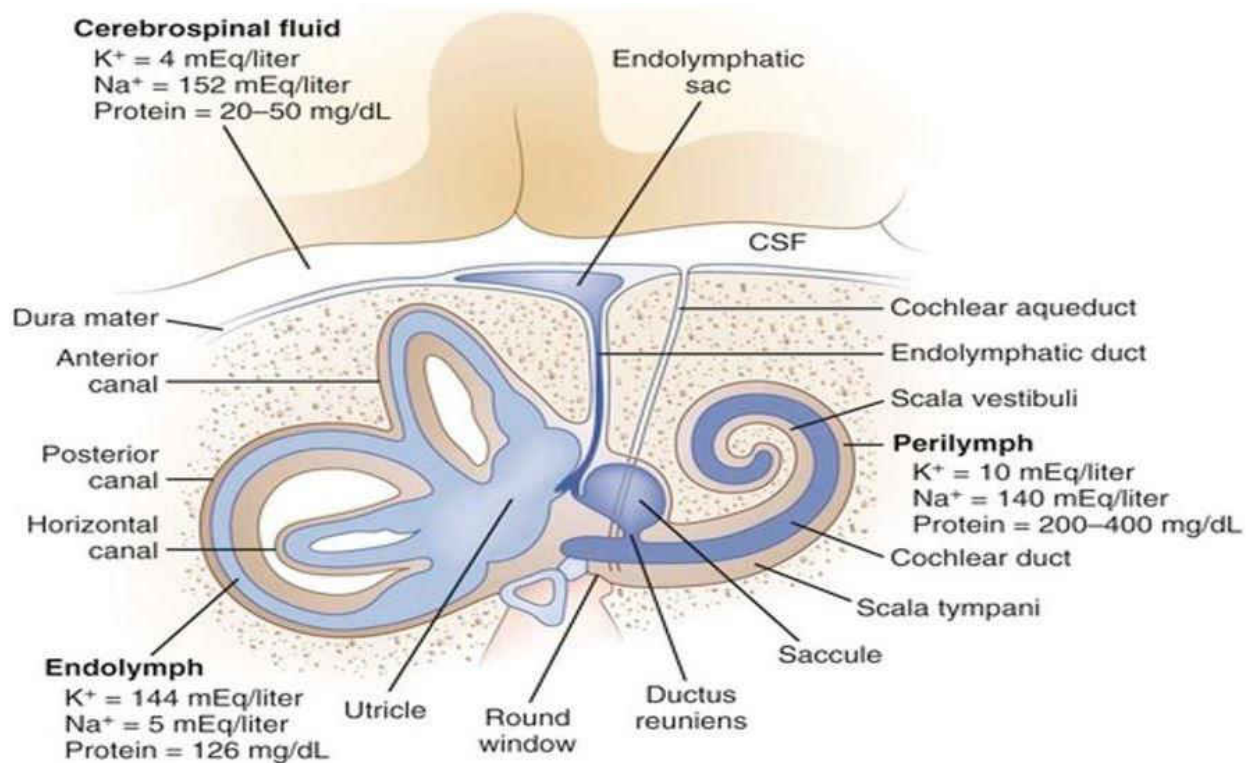


Figure 1-3 Inner ear showing Cochlea and the vestibular system. The inner ear is filled with Perilymph and Endolymph. Both fluid is connected to CSF through cochlear aqueduct and endolymphatic sac respectively. [6]

The cochlear fluid system consists of perilymph and endolymph and have similar properties [7]. While the Scala tympani and Scala Vestibuli contains perilymph, the cochlear duct contains endolymph.

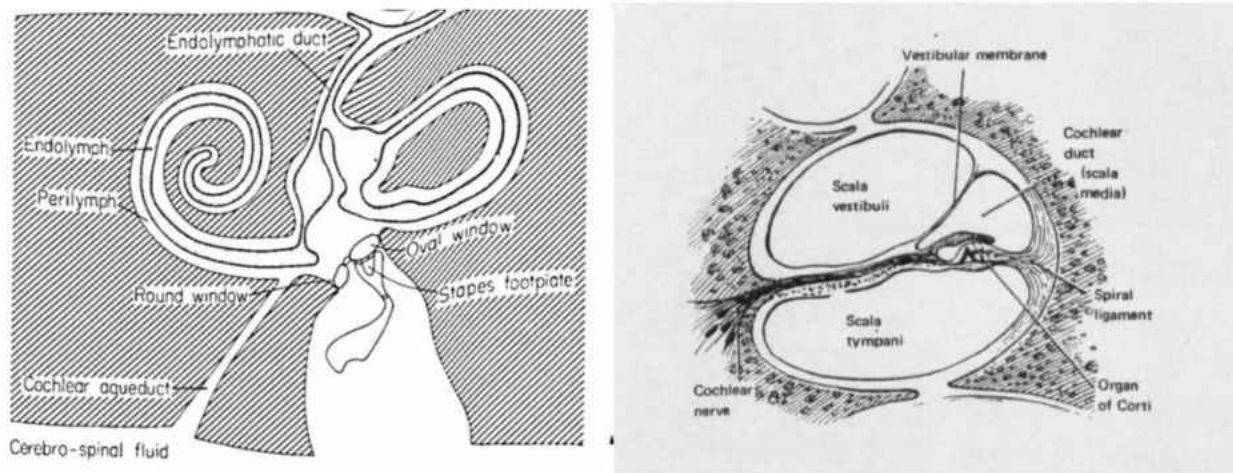


Figure 1-4(a): Cross sectional area of human inner ear [8].(b) Cross sectional area of cochlea. [9]

Outside of the cochlear wall close to the semi-circular canals is the oval window, which is attached to a bone called stapes (figure 1-4(a)) [8]. The cochlea consists of three long tubular chambers: scala vestibuli, scala tympani and cochlear duct (Scala media) (figure 1-4b) separated by basilar membrane and Reissner's membrane [9]. The cochlear aqueduct, which is a bony channel between the Scala tympani and subarachnoid space establishes communication between the subarachnoid space and perilymphatic space.

1.3 Relation Between CSF Pressure and Cochlear Fluid Pressure

Earlier study [10] suggest that pressure of the perilymph and CSF are equal in the cat. Another study [11] examined the transmission of CSF pressure to middle ear fluid pressure in the cat by increasing the CSF pressure quickly. Results showed that both perilymphatic and endolymphatic pressure increased accordingly. The study suggested that in the cat the rapid change in CSF pressure transmitted to the cochlear fluid through the cochlear aqueduct. Other study [12] varied the CSF by changing blood pressure, posture, and blood gas content in the cat. Results showed that the change in CSF pressure were comparable to the change in perilymph pressure in all cases. The findings of these experimental studies suggest that changes in CSF pressure are transmitted to the cochlear fluid.

1.4 Middle Ear

The air-filled space between ear drum and the oval window of the cochlea is middle ear cavity or tympanic cavity. Within this cavity, there are three small connected bones forming the middle ear. These are known as stapes, incus and malleus. The ‘hammer’ shaped malleus is attached to the tympanic membrane at one end and the ‘anvil’ shaped incus the other. The third bone is connected to the incus and oval window of the cochlea. The vibration of the tympanic membrane pushes the malleus which vibrates against incus. This vibration is then transmitted to the stapes through incus. The stapes which is attached to the oval window vibrates creating pressure wave in the cochlear fluid. At the base of the tympanic cavity, there is a tube that connects the tympanic cavity to nasal cavity called Eustachian tube. The tube allows the pressure in the tympanic cavity to be vented to atmosphere. Figure 1-5 shows the middle ear bones along with the tympanic membrane [9].

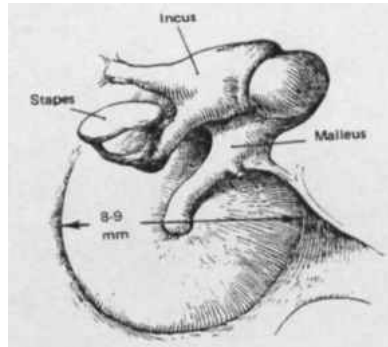


Figure 1-5 Human middle ear. [9]

1.5 Tympanic Membrane and External Ear

The tympanic membrane (TM) is a circular membrane that is connected to the malleus of the middle ear and separates the middle ear from external ear. Earlier study [13] showed that the average thickness of the tympanic membrane is approximately 0.074 mm. The tympanic membrane transmits the vibration caused by the sound energy in the external ear to the middle ear ossicles. The tympanic membrane is slightly inclined at an angle of approximately 40 degree with the floor of the ear canal [13].

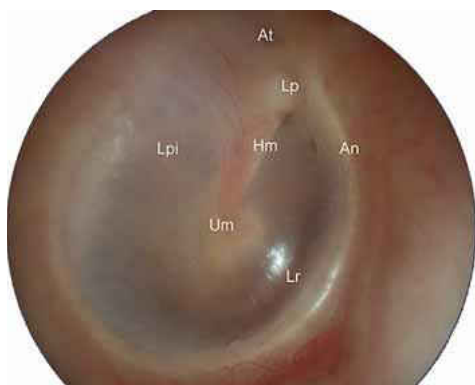


Figure 1-6 Human tympanic membrane along with An: Annulus fibrosus, Lpi: Long process of incus; Um: Umbo, the end of malleus; Lr: Light reflex; Lp: Lateral process of the malleus; At: Pars flaccida; Hm-handle of the malleus. [13]

Figure (1-6) showed a photo of tympanic membrane annotating different locations of the membrane [13].

1.6 Variation of CSF Pressure and ICP with Respect to Body Posture

Earlier study [14] suggested that changing body posture by tilting can lead to significant variations of CSF pressure. The study was done on a subject with artificial respiration. CSF pressure measurement was done by inserting a catheter into lateral ventricle of the brain. Another investigation [15] done on a dog showed that the CSF pressure varies with change in body position.

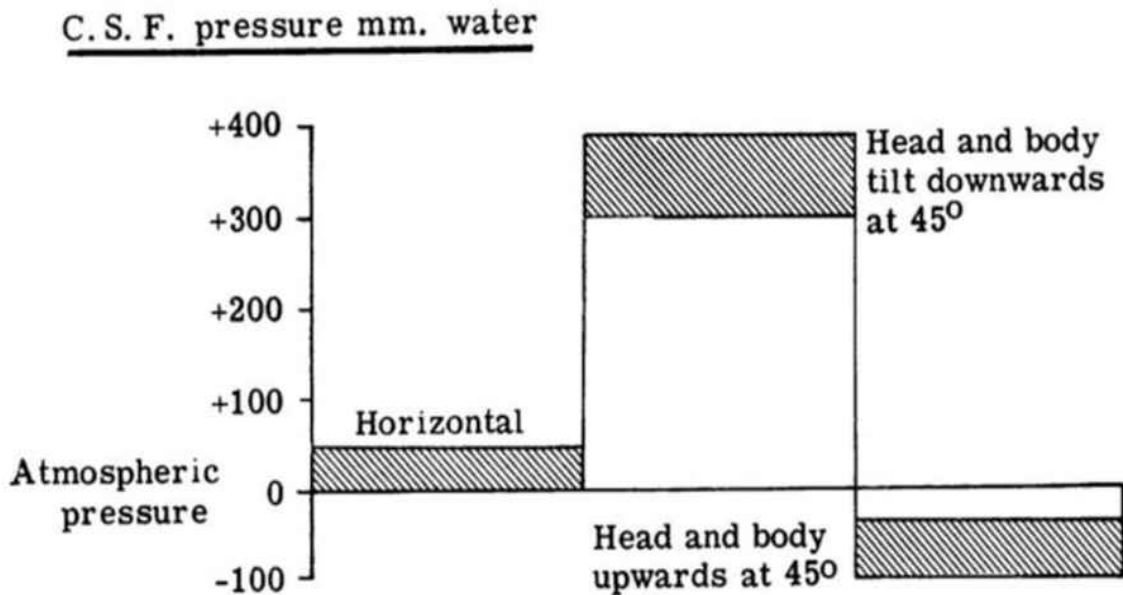


Figure 1-7 Cerebrospinal fluid pressure in dog at different body posture. [14]

Results (figure1-7) showed that the CSF pressure increased considerably as the head and body tilted downward by 45 degrees while the pressure decreased slightly when the body was tilted by 45 in the head up direction.

In addition, the study performed variation of CSF pressure on human with pre-senile dementia and dilated ventricles (figure 1-8). Results showed that the CSF pressure decreased considerably as the subject's body posture changed from supine to 90 degrees.

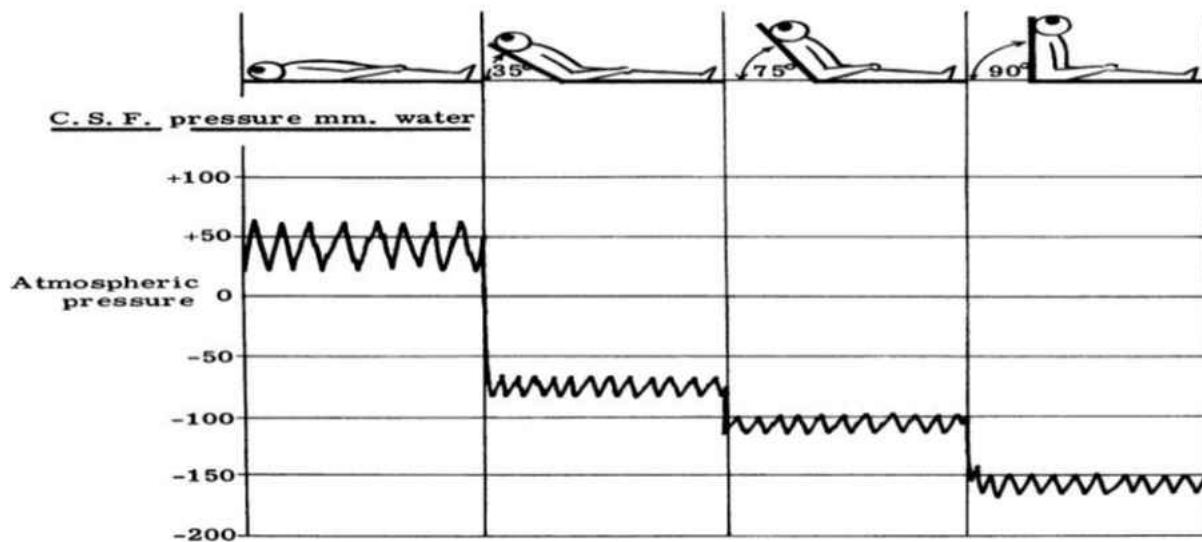


Figure 1-8 CSF pressure in man with varying body posture. [14]

Another previous study [16] on humans, where a butterfly needle was inserted into Ommya reservoir (an intraventricular catheter system used for the delivery of drugs into CSF in brain) and connected to a pressure transducer to measure the ICP. Results showed that at microgravity, ICP was lower in upright sitting positions than that of supine.

Earlier study [17] showed that in sitting position the difference between ICP and lumbar CSF pressure is identical to the height of hydrostatic column. When the body position moved from recumbent to sitting position, the corresponding change in lumbar CSF pressure is only about 40% of that predicted hydrostatic column. In addition, when the body postural position moved vertically head down, the change in ICP was about 3-fold higher than that of head up position. The study suggested that in addition to hydrostatic pressure, the elasticity of lumbar thecal sac and venous collapse influence the change in ICP due to variation in body postures.

1.7 Effect of Tympanic Membrane Movement on Intracranial Pressure

Earlier studies [1], [18] suggested that ICP is related to pressure of the cochlear fluid (fluid in the cochlea of inner ear). In addition, CSF is connected to the inner ear via perilymphatic duct. Thus, ICP can be transmitted to the inner ear via CSF or cochlear fluid and finally, then through the middle ear bone structure to the tympanic membrane. Therefore, it may be possible to monitor changes in ICP by measuring the changes in the tympanic membrane pulsations (TMp). A previous study [19] investigated the movement of tympanic membrane induced by the stimulation of stapedial reflex. The study introduced a 1000 Hz stimulus signal with varying loudness into subject's external ear canal. This induced a controlled stapedial muscle contraction and corresponding ossicular and tympanic membrane movement.

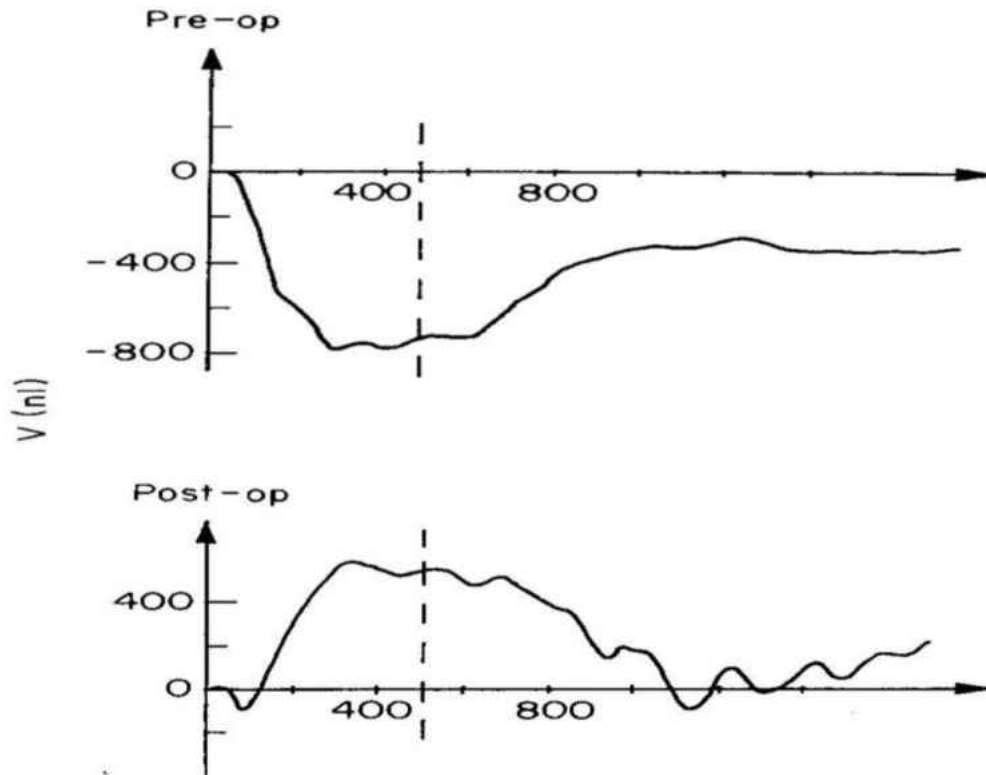


Figure 1-9 Tympanic membrane displacement for pre-and post-operative condition for a patient with elevated ICP with a stimulus signal of 1000 Hz. While the negative volume indicates in-ward going movement, the positive volume indicates out-ward going movement of the tympanic membrane. [19]

Figure 1-9 showing tympanic membrane volume displacement with a 1000 Hz stimulus signal for a patient with elevated intracranial pressure before and after placing a ventriculo-peritoneal shunt [19]. According to the study the pre-operative tympanic membrane movement showing negative volume displacement indicative of elevated intracranial pressure which shifted to positive volume after placement of the shunt indicating reduced intracranial pressure.

1.8 Measurement of Tympanic Membrane movement using volume displacement

Earlier study [20] described a technique of measuring variations in volume in the external ear due to the movement of tympanic membrane.

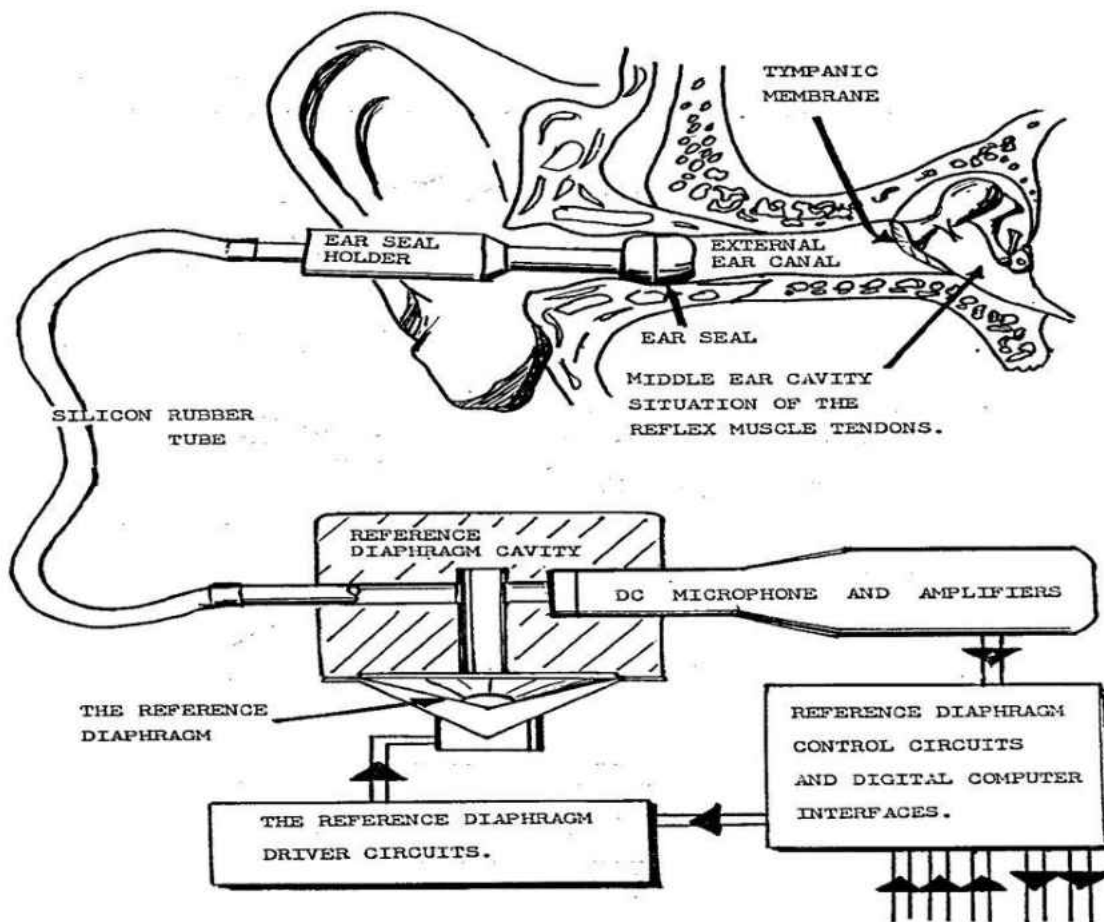


Figure 1-10 Tympanic membrane displacement system showing the ear canal connected to a cavity using a tube. The microphone measures the pressure fluctuations due to tympanic membrane movement. The microphone output is then sent to reference diaphragm driver unit to move the diaphragm and keep a constant pressure in the cavity. The microphone output is a measure of tympanic membrane movement. [20]

In this system, subject's ear canal is connected to an external cavity (TMD servo cavity). Inside the cavity, there is a microphone which measures the pressure fluctuation within the space between tympanic membrane and the cavity. In addition, there is a reference diaphragm at one of the cavity wall which is driven by an external driver circuit and can induce a subtle change in the ear canal-TMD system cavity volume (Approximately 0.04 microliters). The pressure fluctuation due to the

movement of the tympanic membrane is sensed by the microphone inside the cavity. The microphone output is sent to reference diaphragm driver circuit which move the diaphragm to cancel out the pressure fluctuation and thus keeping a constant pressure in the cavity. The volume displacement of the tympanic membrane is nullified by an equal and opposite volume displacement of the reference diaphragm. The microphone output voltage is then used as a measure of the tympanic membrane volume displacement. In addition, the input to the reference diaphragm is connected to an audiometer which can generate a range of frequencies with varying loudness. This is used to stimulate the system and excite the stapedius reflex in the ipsilateral (i.e., same side) middle ear. Figure 1-11 shows the tympanic membrane volume displacement due to excitation of stapedius reflex.

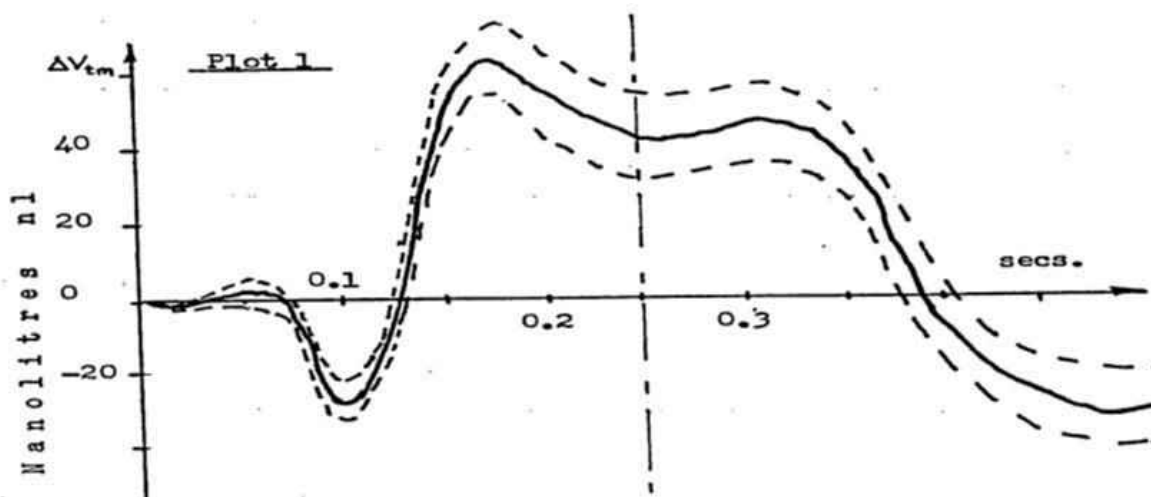


Figure 1-11 Tympanic membrane volume displacement waveform due to stapedius reflex excitation. [20]

The TMD system is used in several studies [8], [19], [20] to investigate ICP changes in normal humans and patients. The system output depends on the movement of reference diaphragm. The

property of the reference diaphragm is not the same as tympanic membrane therefore, it cannot mimic the exact movement of the tympanic membrane hence, it may not completely nullify the pressure changes due to the movement of the tympanic membrane may cause buildup of back pressure on the TM itself. Hence a passive approach (without using a stimulus signal to induce stapedial reflex) of measuring the TM movement would therefore provide better understanding of how the TM moves under different physiological conditions.

1.9 Relation between CSF Flow and Cerebral Blood Flow

Earlier study [21] described the relation between blood and CSF volume in the skull. CSF volume was obtained by integrating the CSF flow while the blood volume in the cranium was obtained by the integration of the summation of the blood flow in the internal carotid artery, the venous and vertebral artery.

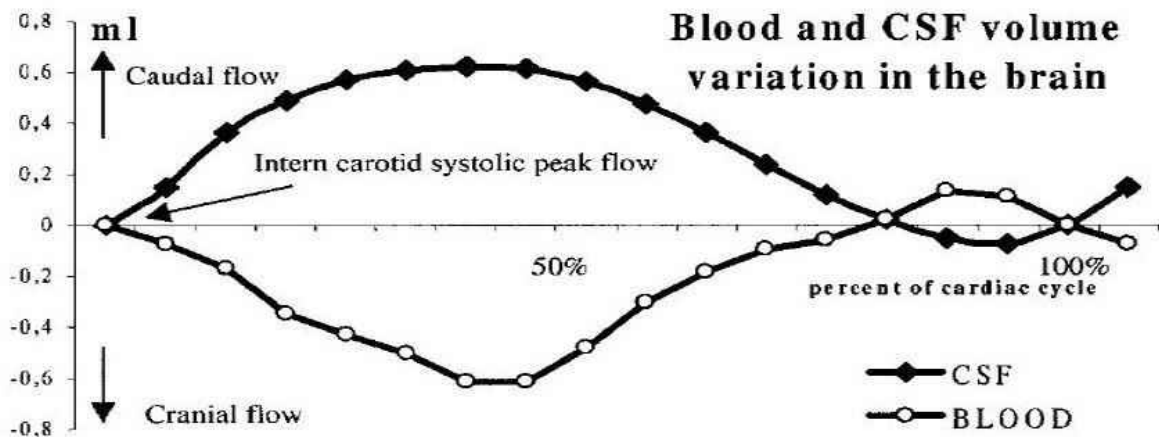


Figure 1-12 Relation between blood and CSF volume in the brain. As the blood volume increases, the CSF volume decreases. The caudal flow indicates CSF flow towards spinal cord while the cranial flow indicates cerebral blood flow towards brain. [21]

In addition, the study discussed that the peak subarachnoid outflow of CSF (Maximum flow at subarachnoid space towards spinal cord) occurs at 15% of the cardiac cycle. Figure 1-13 shows the CSF and blood flow in two consecutive cardiac cycles.

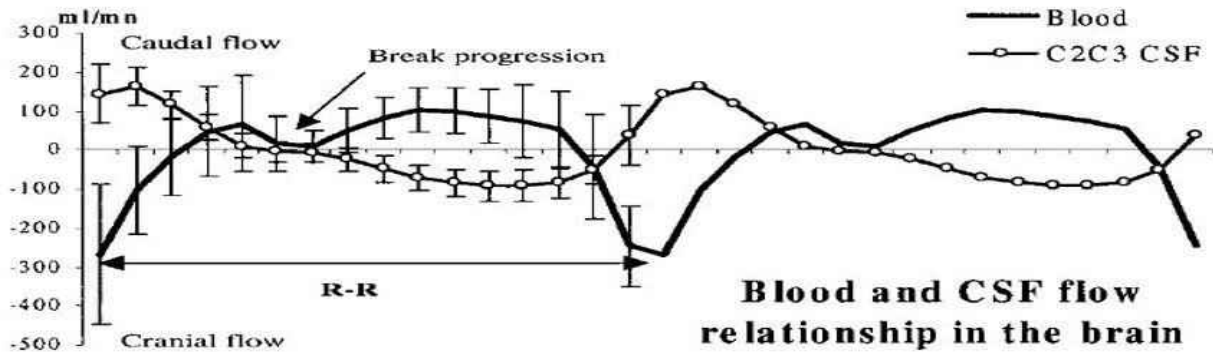


Figure 1-13 Blood and CSF flow rate in the cranium. There is a time delay between the peak flow of the two systems. [21]

The vertebral and internal carotid systolic peak flow (ICSPF) happens approximately at 88% of the cardiac cycle. This suggests that there is a delay between the peak flow of the two systems. In addition, raised ICP changes the intracranial compliance (change in volume (ΔV) per unit change in ICP (ΔP) and is the inverse of elastance) of the cranium [17]. In normal condition, if intracranial volume (CSF, brain or blood volume) increases, the ICP will rise accordingly. This then triggers enhanced CSF absorption which will reduce ICP overtime. If CSF absorption process is obstructed due to medical conditions (traumatic brain injury, hydrocephalus), the ICP will rise leading to decrement of the compliance as well as the cerebral blood flow [17]. As the intracranial compliance changes the time interval between the cerebral blood flow and CSF peak flow may change. This may lead to a change in time interval between the CSF pulsations and earlobe pulsations from the

external carotid artery which supplies blood to earlobe. Hence a change in the CSF-earlobe pulsation time interval may reflect ICP variation in the cranium.

The TMp sensor system (will be discussed in the following chapters) can acquire TMp signal and the earlobe blood pulsations simultaneously. The ear lobe pulse signal depicts the pulsation of external carotid artery due cardiac activity. The earlobe pulse signal will be used to analysis the effect of ICP variation on TMp signal induced by postural changes. In addition, the pulse signal will be used to investigate changes in time delay between TMp and blood pulse signal due to variation of ICP.

CHAPTER 2: METHODS

2.1 Building the Sensor Assembly

The tympanic membrane pulsation sensor setup has two components: 1. Piezo sensor 2. Ear lobe pulse sensor. A Buzzer Element Piezo of resonant frequency 0.6 kHz and 44 mm diameter piezo disc (CUI inc, Tualatin, OR 97062, USA) was used to build the piezo sensor. The piezo disc was inside a 3-d printed circular chamber. There is a 3.5 mm opening at the center of the top surface of the chamber. A 38-mm long tube (inner diameter 3.5 mm) is attached at the opening of the chamber. The tube is tapered to allow easy insertion and removal of ear plug. A pressure tap was installed at the base of the tube to allow testing the seal (i.e. air tightness) of the connection between the tympanic membrane and piezo disc. Figure 2-1 shows (a) the photo of piezo element and (b) the constructed sensor.

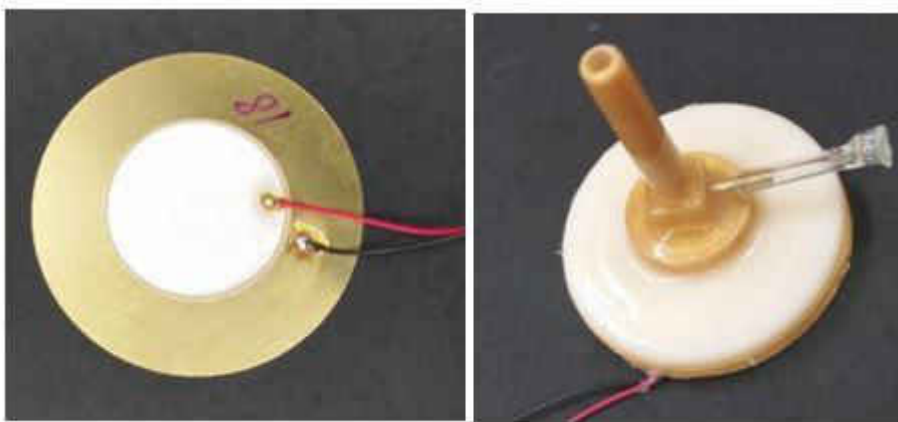


Figure 2-1(a) 0.6 kHz 44 mm piezo disc (b) Piezo sensor along with a side pressure tap and a long tube to be put in external ear canal.

The ear lobe optical pulse sensor (Sparkfun Electronics, Niwot, CO) was attached to a small 3-d printed chamber to cover the electronics of the pulse sensor. An ear clip was attached to back of the pulse sensor to attach the sensor to the ear lobe. Both piezo and pulse sensor were placed inside the right and left ear muffs (Fnova, 34 dB, Shenzhen, Guangdong, China). The seal testing port at the base of the long tube was connected to flexible tube, which was connected to a valve that would allow releasing the pressure in the connection between TM and piezo disc to atmosphere. Figure 2-2 shows (a) the ear lobe pulse sensor along with (b) the TMp sensor assembly.



Figure 2-2 (a) Ear lobe pulse sensor (b) TMp sensor assembly. The piezo sensors and the ear lobe sensors are inside the right and left ear muffs. The while valves are used to test air tightness between ear canal and piezo disc by connecting the valve outlet to a manometer

2.2 Data acquisition, Post Processing and Analyzing the Acquired TMp Data

2.2.1 Data Acquisition, Plotting the Acquired Tympanic Membrane Waveform with Earlobe Pulse and Airflow

The piezo sensor, the ear lobe pulse sensor, and the spirometer outputs were connected to a data acquisition system (IX-RA 834, IWORX, Dover, NH, USA) which allowed real time data

monitoring while acquiring the data. Acquired data were saved in CSV files for later analysis. During post processing, acquired tympanic membrane data along with earlobe pulsation and airflow data are read and plotted (Matlab 2013, Mathworks, Natick, MA). Figure 2-3 shows the TMp waveform (top row), earlobe pulse (middle row) and airflow rate (bottom row). It can be seen in the figure that the TMp waveform tended to vary during the respiratory cycle.

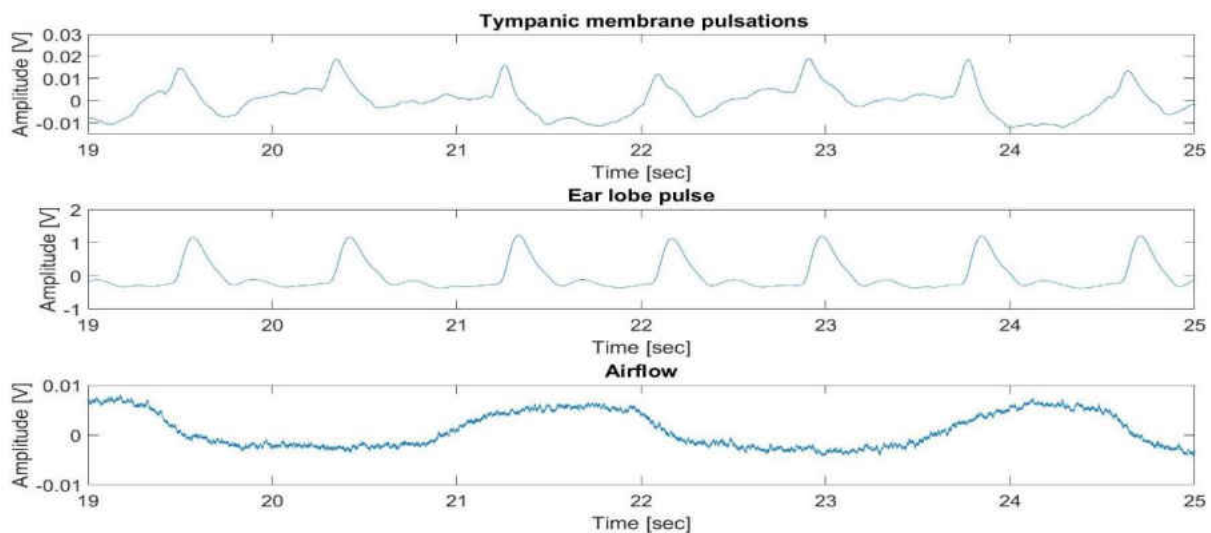


Figure 2-3 Tympanic membrane pulse (top), earlobe pulse (middle) and breathing airflow (bottom). The tympanic membrane waveform changed with airflow.

2.2.2 Filtering the acquired signals

The acquired raw signals are filtered (bandpass: 1-20 Hz) to remove noise (e.g., of environmental, electronic, and respiratory origins).

Figure 2-4 shows the filtered TMp, earlobe pulse and airflow signals corresponding to those shown in figure 2-3.

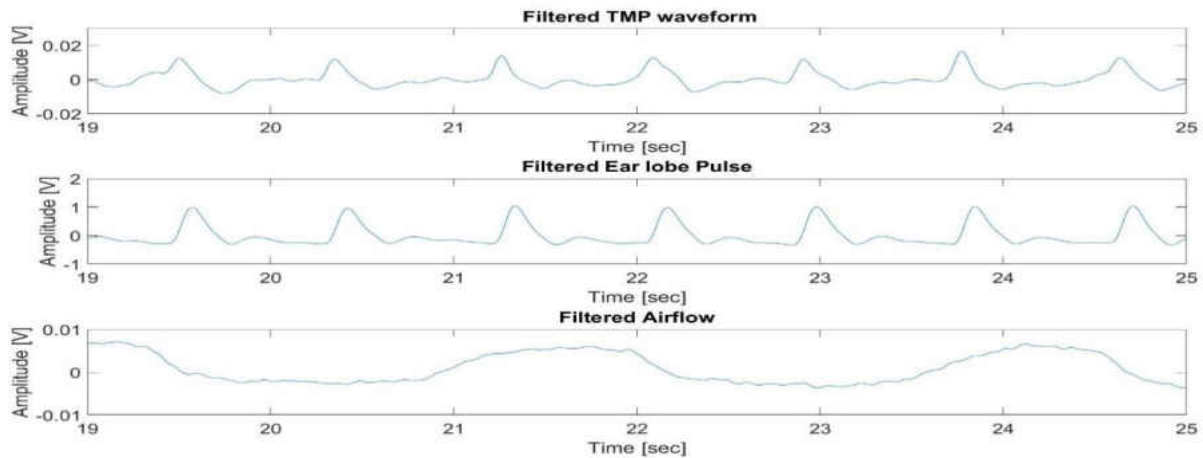


Figure 2-4 Filtered TMP, earlobe pulse and airflow data

2.2.3 Identifying the Peaks of Ear lobe pulse

Next step in analyzing the data is to find the peak locations of earlobe pulse peaks. The ear lobe pulses are relatively repeatable under same condition. Hence ear lobe pulse peak locations are used as a reference to mark corresponding TMP waveforms. These peaks were identified using methods similar to previous studies [22], [23]. This process involved setting a threshold amplitude above which peaks of all individual the ear lobe pulse signal are assumed to lie. Matlab “findpeaks” function was then used to find all the pulse peaks above mean peak height (threshold amplitude). Since the heart rate was typically between 50-90 beats/minute, if there were multiple peaks within the corresponding pulse period, only the peak with higher amplitude was chosen and other peaks will be defined as false peaks and was removed. Figure 2-5 shows the ear lobe pulse peaks with their peaks marked with red circles.

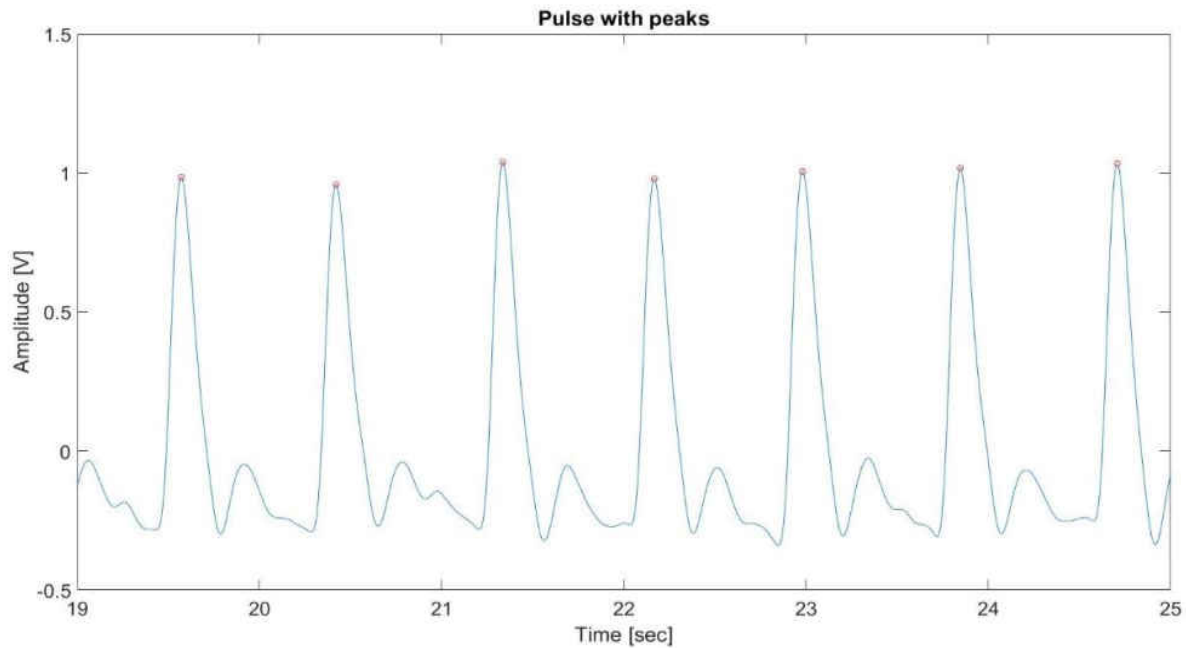


Figure 2-5 Ear lobe pulses with their peaks marked with red circles

2.2.4 Finding the Nadirs (start and end points) of Individual Tmp waveforms

Following the identifications of pulse peak locations, the MATLAB program finds the nadirs (start and end points) of corresponding Tmp waveforms. Since period of ear lobe pulses are identical for each pulse, the Tmp cycles are assumed to be similar. The algorithm finds the start and end points by going a specified location in the Tmp data before and after corresponding ear lobe pulse peak locations. This method is similar to the above section (using the findpeaks Matlab function after multiplying the signal by “-1”), which is also similar to previous studies [24], [25].

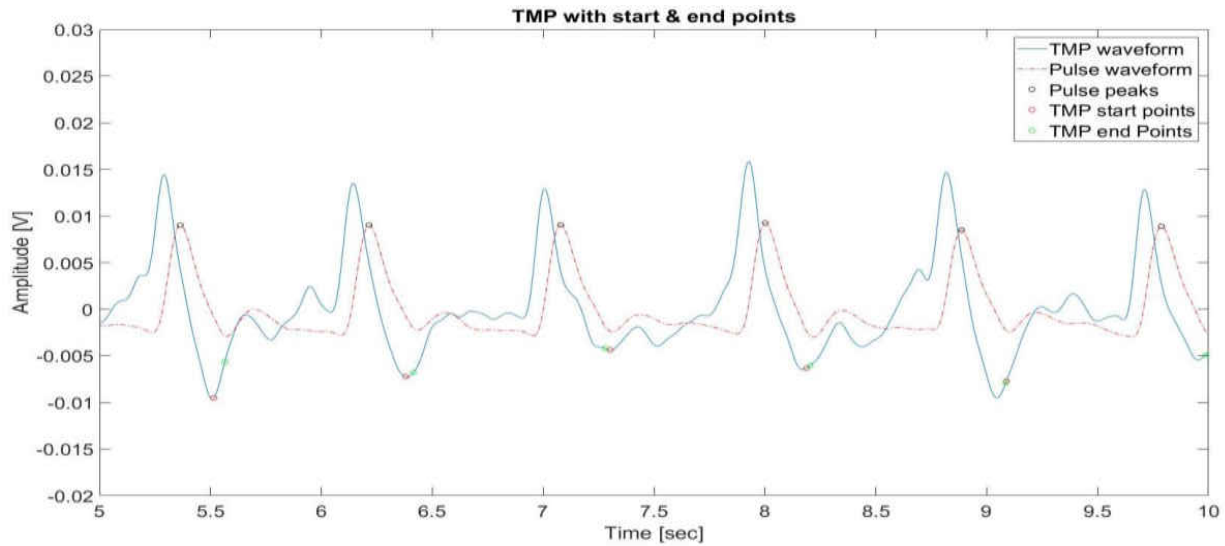


Figure 2-6 TMP and earlobe pulse waveforms are plotted. The peak locations of earlobe pulses are marked with black circles. The start and end points of corresponding TMP waveforms are marked with red and green circles

Figure 2-6 shows the TMP nadirs along with pulse peaks.

2.2.5 Separating the Individual TMP Events

Once the start and end points of individual TMP waveforms are identified, the TMP waveforms are stored in an array. Next, these waveforms are plotted (figure 2-7) on top of each other. This help looking at individual TMP waveforms and identify the noise in the stored data.

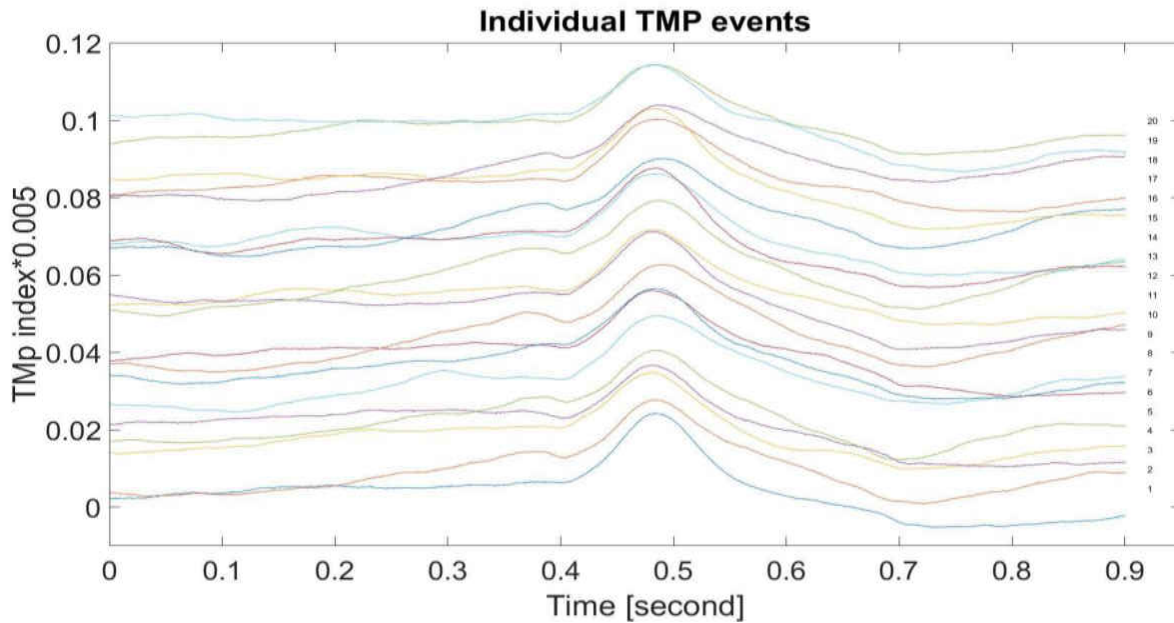


Figure 2-7 Twenty Individual Tmp events plotted on top of each other. Although all the events were synchronized around their peaks, some of the events had steeper valley than the others.

2.2.6 Average Tmp Waveform and Normalized Deviation from Mean

The average of the individual Tmp waveforms is calculated using methods described in previous studies [26].

The mean waveform is calculated as:

$$Mean_{T_{Mp}} = \sum_i^n \frac{T_{Mp}(i)}{N} \quad (1)$$

Here N is the number of Tmp waveform.

Figure 2-8 shows an average Tmp waveform of 55 Tmp individual waveforms.

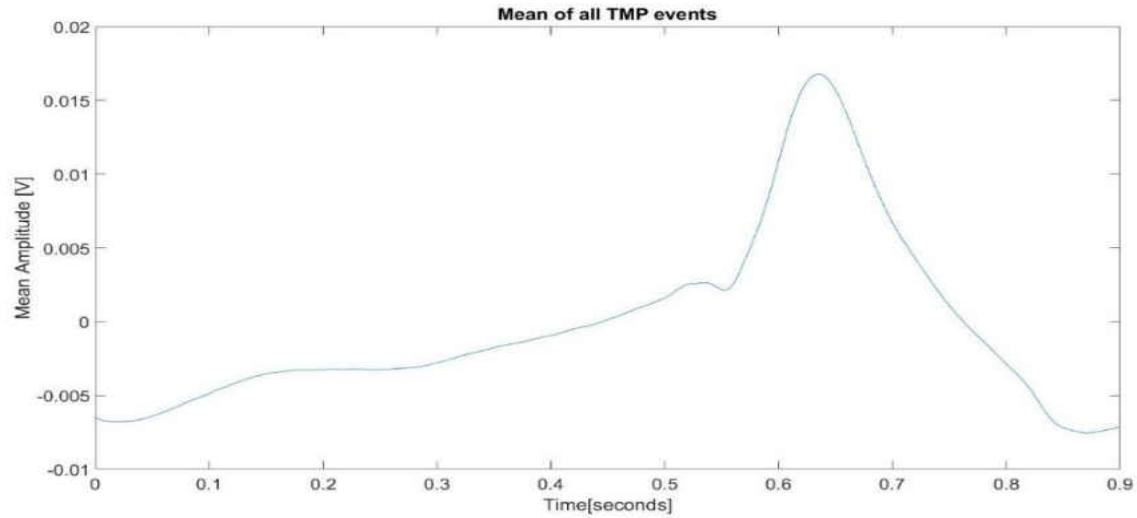


Figure 2-8 Mean TMP waveform. This waveform is the mean of 55 individual TMP waveforms

The mean TMP waveform is then used to calculate the “normalized deviation from the mean waveform” for each individual wave, which is similar to normalized relative difference described in earlier studies [27].

$$\text{Normalized deviation from mean}(i) = \frac{\text{Standard deviation}(TMP(i) - \text{Mean}_{TMP})}{\text{Standard deviation}(TMP(i))} \quad (2)$$

Figure 2-9 shows the normalized deviation values from the mean TMP waveform. The values range from 0.2 and 0.9. The periodic nature of the values indicate that they might be affected by a periodic process such as breathing.

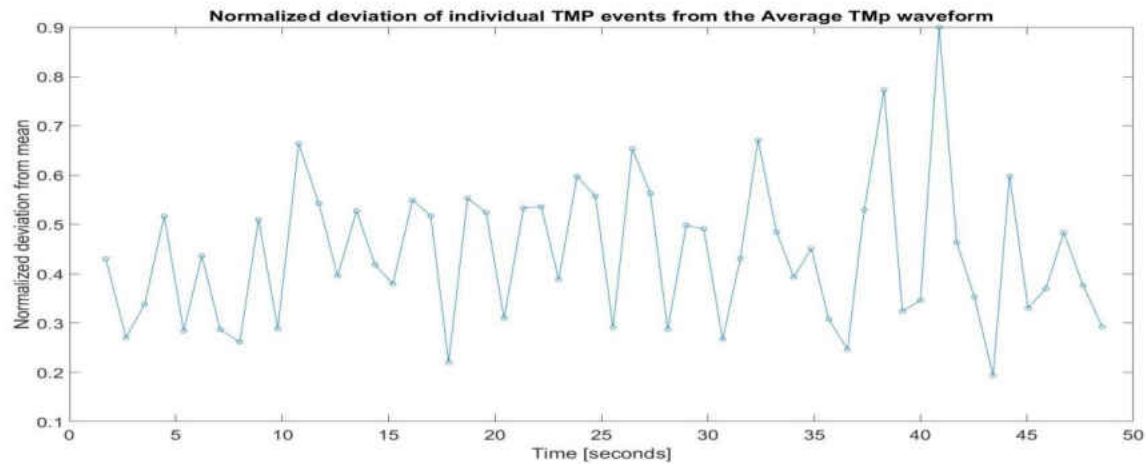


Figure 2-9 Normalized deviation from mean TMP waveforms are plotted. The values range between 0.25 and 0.8. The change in TMP waveform with respect to time might be related to breathing

2.2.7 Effect of Breathing on Tympanic Membrane Pulsations

The values for normalized deviations from the mean indicated that they have fluctuations which are periodic in nature. One possible cause for these fluctuations can be breathing. One way to confirm this possibility is to acquire both TMP and breathing simultaneously and check whether the fluctuations in normalized deviations correlate with breathing. Hence, TMP data was acquired simultaneously with breathing airflow for 5 minutes while the subject rested supine on a tilt table. After data acquisition, the deviation from the mean TMP waveform was determined. The normalized deviation from the mean was plotted along with breathing.

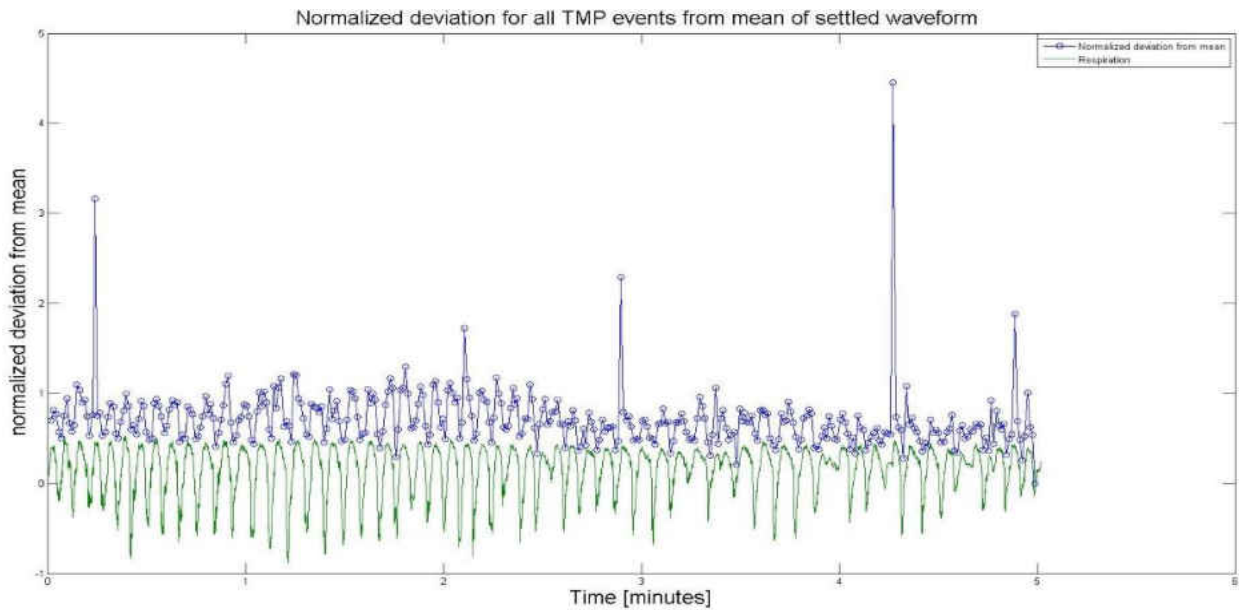


Figure 2-10 Normalized deviation from the settled Tmp for all Tmp waveform (blue line) is plotted along with subject's respiration airflow data (green line). It is evident that the variation in Tmp waveform synchronize with subject breathing

Figure 2-10 shows the variation of Tmp waveforms from the mean Tmp waveforms. The waveform deviation was found to synchronize with the respiratory cycle. This suggests that Tmp waveform is affected by breathing, which may cause small changes to the ICP.

2.2.8 Separating the Tmp Events Based on Lung Volume

The previous section showed that the Tmp waveforms can be affected by breathing. Therefore, to get a better understanding, the individual Tmp waveforms are separated based on airflow data and lung volume. Lung volume was obtained by integrating the airflow data. The normalized deviation from mean was plotted with respect to airflow and lung volume (figure 2-11 and 2-12 respectively).

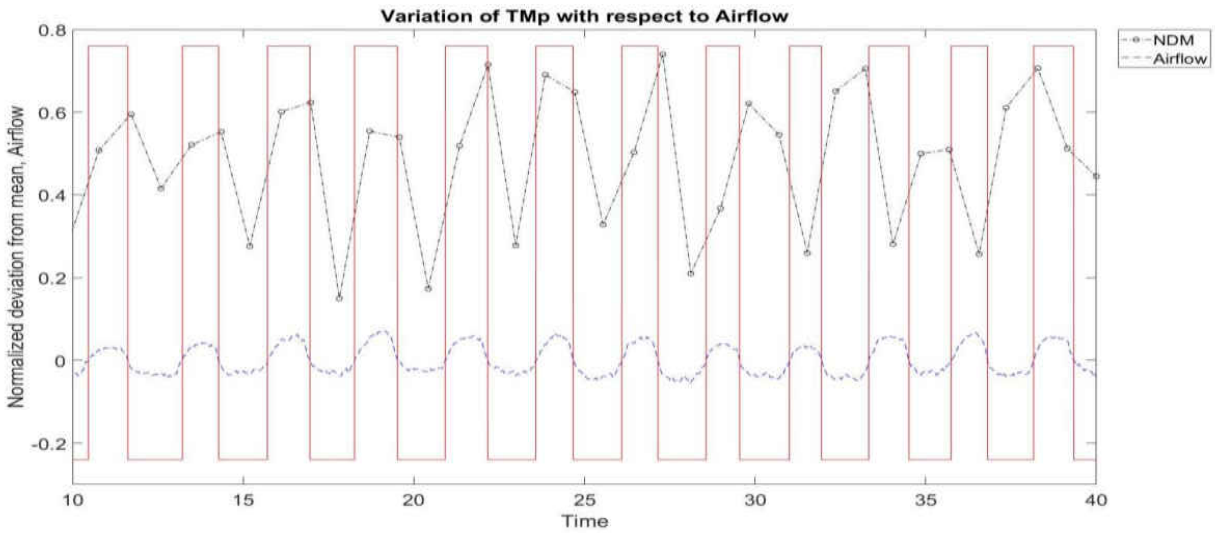


Figure 2-11 Normalized deviation from mean and airflow was plotted together. The red line indicates the regions of inspiration and expiration. The upper flat lines are inspiration region while the lower flat line indicates expiration.

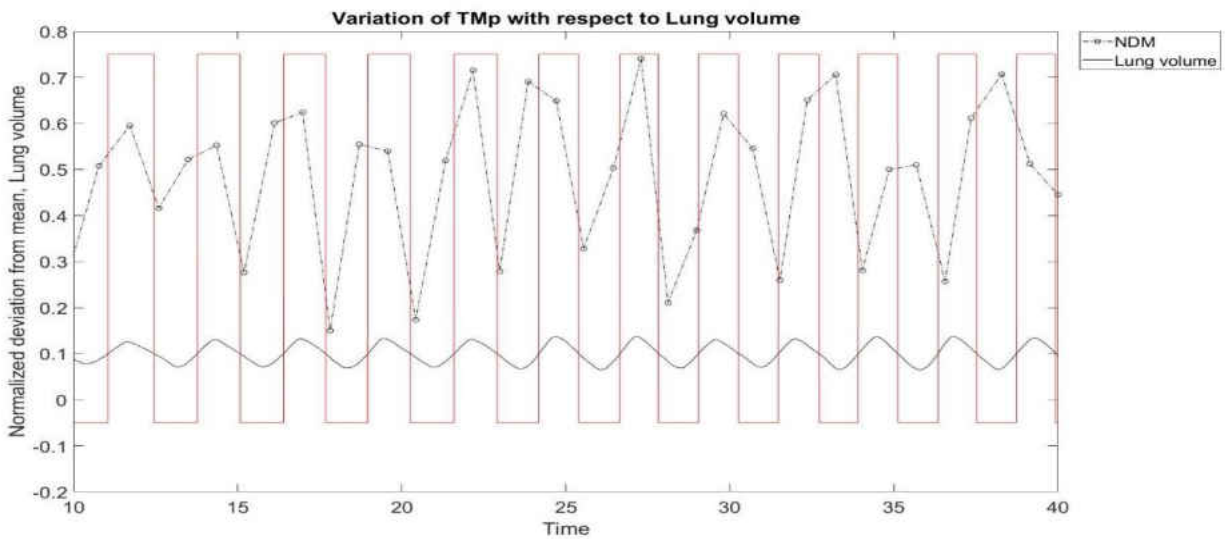


Figure 2-12 Normalized deviation from mean and lung volume data are shown. Red line indicates separation of high and low lung volume event. The regions of upper flat line indicate high lung volume effects while the lower flat line indicates low lung volume events

Figure 2-11 and 2-12 show the variation of TMp events based on airflow and lung volume. While both airflow and lung volume show changes with normalized deviation, lung volume was chosen as it has less noise than airflow (random breathing fluctuations which may create false inspiration or expiration events in the airflow data). More importantly, separation of TMp into two groups was such that similarity of the events in each group was maximized.

The TMp waveform were separated in two groups of high lung volume events or low lung volume events comparable to what has been described in similar studies [27], [28]. To achieve this, the pulse peak locations were used. More specifically, if a pulse peak was during high lung volume, the corresponding TMp waveform was identified as a high lung volume event. Similarly, if the pulse peak was during the low lung volume period, the corresponding TMp waveform was identified as a low lung volume event. Figure 2-13 showed the separation of pulse peaks based on lung volume.

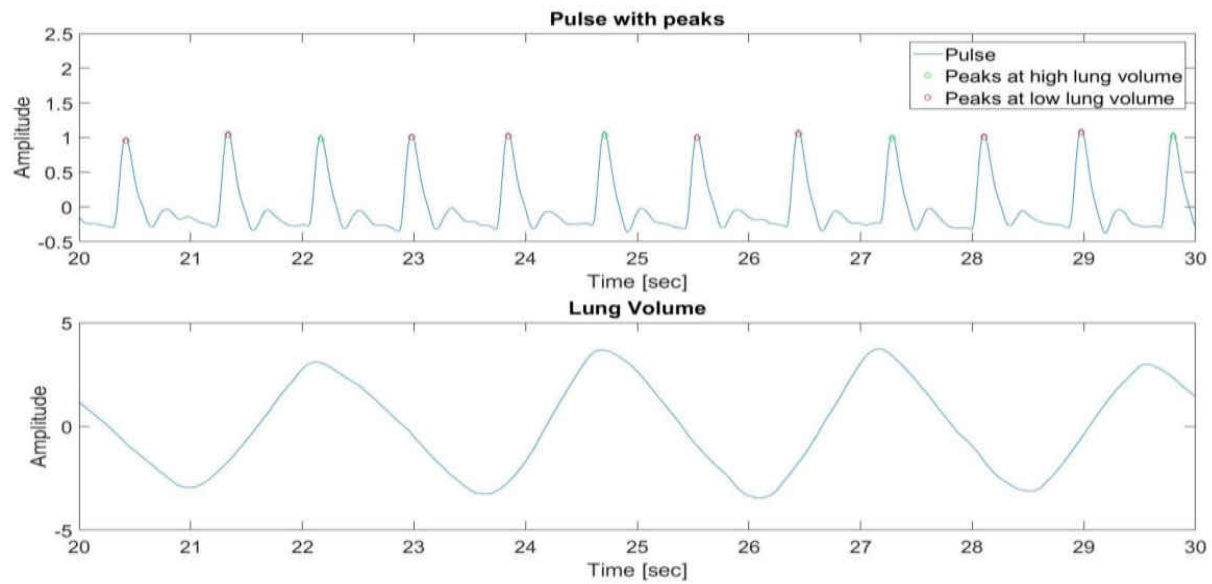


Figure 2-13 Identifying the pulse peaks based on high and low lung volume. The green circle indicates high lung volume event while the red circle indicates low lung volume event.

2.2.9 Mean Tmp for High and Low Lung Volume

Once the Tmp waveforms are separated based on lung volume, the steps from section 2.2.4 to section 2.2.6 were repeated to obtain mean Tmp waveforms for high and low lung volume.

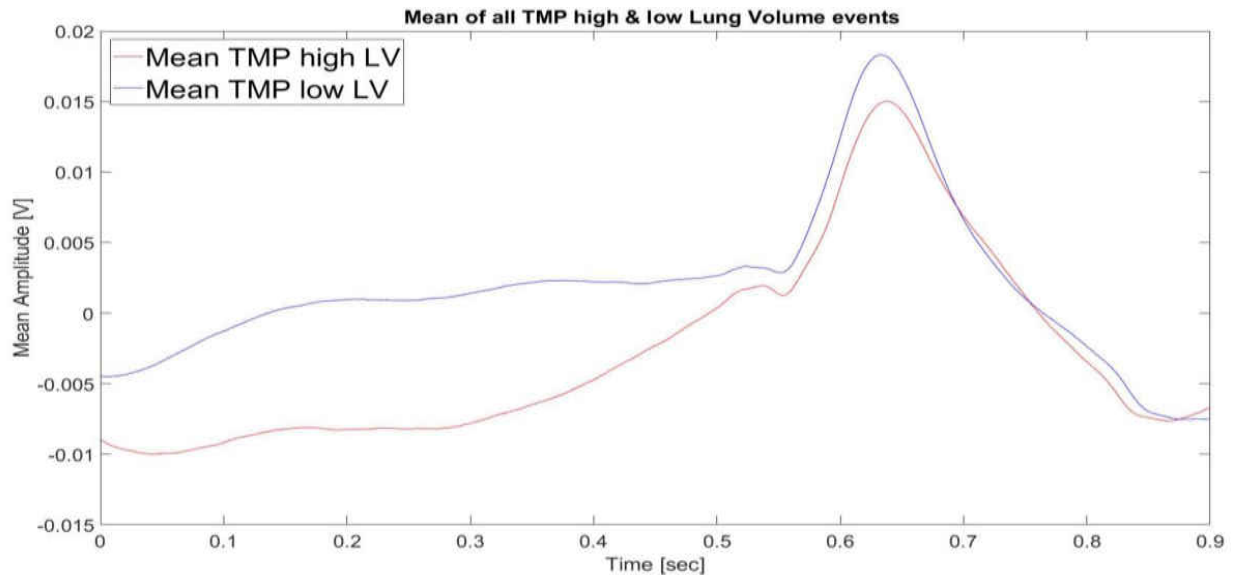


Figure 2-14 Mean Tmp waveforms for high and low lung volume events. Normalized deviation between the two mean waveforms was 0.5102

Figure 2-14 shows the mean Tmp for high and low lung volume event. The normalized deviation between the two was 0.5102. The peak of the high lung volume mean Tmp waveform is about 2-3 mV higher than that of low lung volume event. But at the beginning of the waveform the difference between the waveforms are about 5 mV. The signal peak-peak amplitude was about 25 mV.

2.3 Testing the Tmp Sensor Output Using Mechanical Setup

2.3.1 Experimental Setup

To test the sensor output independent of human factors (i.e., intra and inter subject variability), the sensor was connected to a mechanical setup that has a membrane movement comparable to tympanic membrane movement.

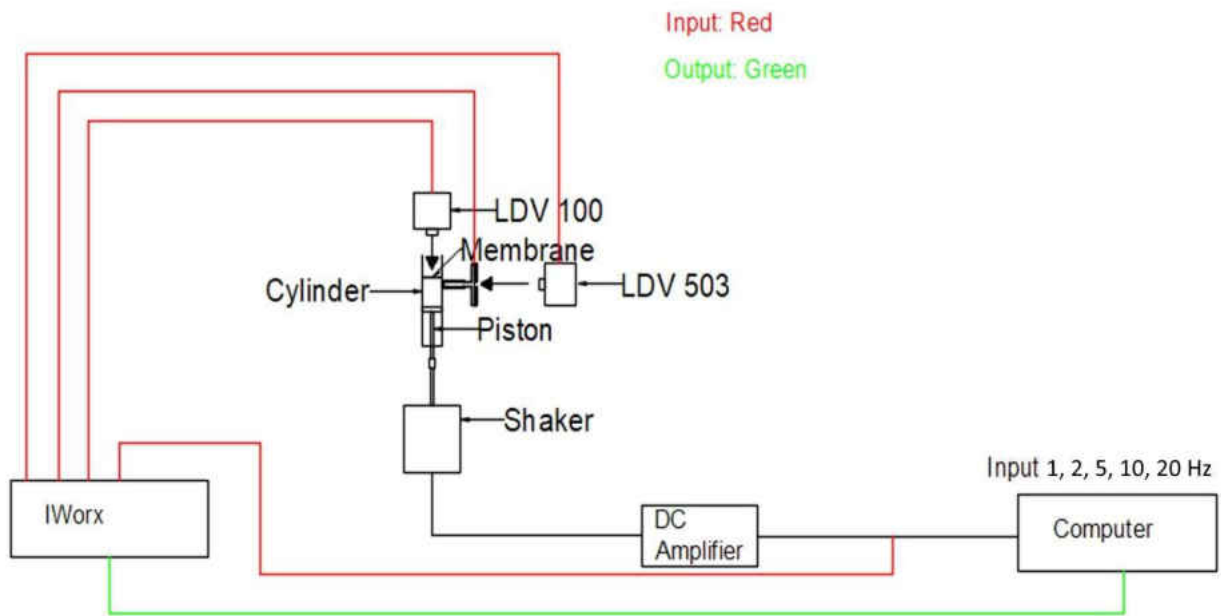


Figure 2-15 Mechanical setup for testing the TMp sensor output independent of human factor

The setup consists of a 5-mm cylinder (close to the dimensions of human external ear canal). A latex membrane is attached at the end of the cylinder length. A piston inside the cylinder can move back and forth to induce a movement of the membrane. The piston is attached to a mechanical shaker. A DC amplifier amplifies the input signal and send the output signal to drive the shaker. A Laser Doppler Vibrometer (LDV 100, Polytec Inc, Hudson, MA, USA) was pointed to the membrane to capture the membrane movement. A pressure port at the side of the cylinder close to membrane allows connection to TMp sensor. Another Laser Doppler Vibrometer (OFV 503, Polytec Inc, Hudson, MA, USA) was pointed towards the back of the piezo disc of the sensor. A computer sends a 1, 2, 5, 10 and 20 Hz cosine signal (with frequency of repetition of 1 Hz) respectively to the amplifier, which moves the shaker like the input signal. The input, both Laser

Doppler Vibrometer (LDV) outputs, and Tmp sensor output are acquired using IWORX data acquisition system.

2.3.2 Testing the sensor output with multiple input signals

The LDV output voltages were converted into velocities using calibration data provided by the manufactures. The velocity values were integrated to get the displacement of the membrane and the piezo disc of the sensor. The membrane displacement, piezo disc displacements were plotted along with piezo output for input signal of 1, 2, 5, 10 and 20 Hz respectively. Sensitivity of the sensor was calculated by the following formula

$$Sensitivity = \frac{Piezo\ Output\ Voltage\ in\ V}{Piezo\ disc\ displacement\ in\ mm} \quad (3)$$

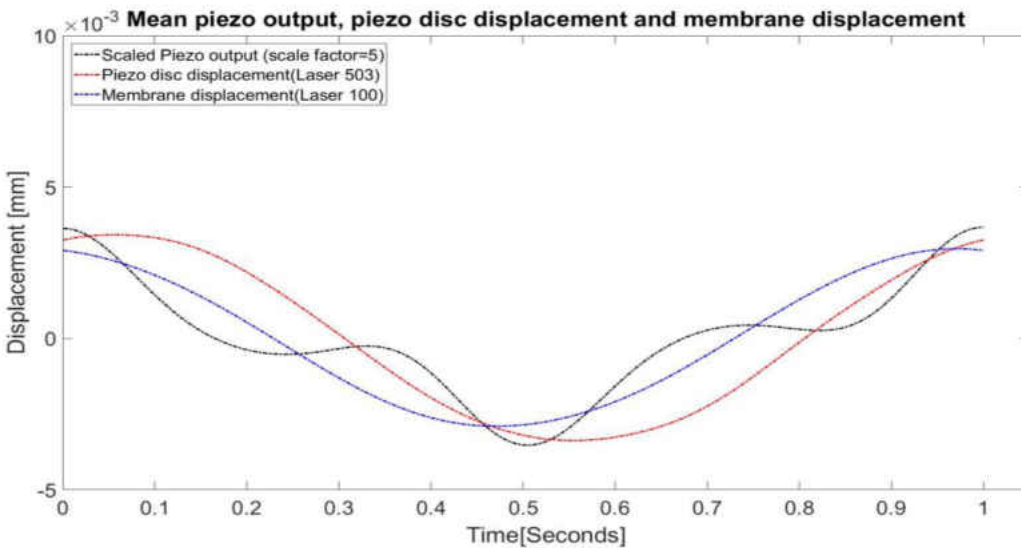


Figure 2-16 Piezo output plotted against piezo disc displacement and membrane displacement at 1Hz cosine input signal. The normalized deviation from mean of piezo displacement was 0.883 and the sensitivity was found to be 0.2117 V/mm

Figure 2-16 shows the piezo output with respect to a 1 Hz cosine input that drives the shaker.

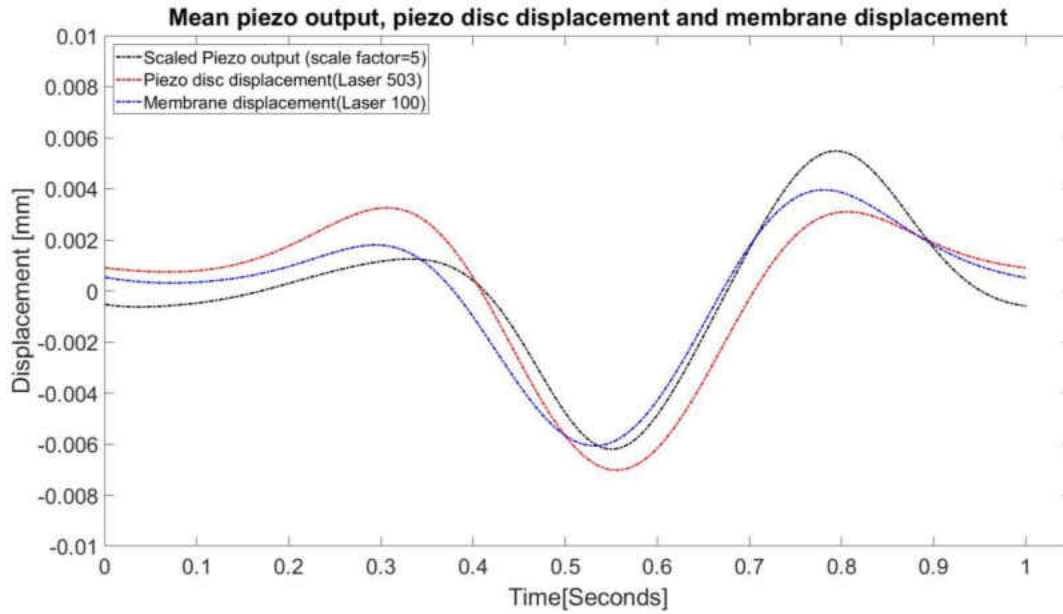


Figure 2-17 Piezo output plotted against piezo disc displacement and membrane displacement at 2Hz cosine input signal. The normalized deviation from mean of piezo displacement was 0.8421 and the sensitivity was 0.2274 V/mm

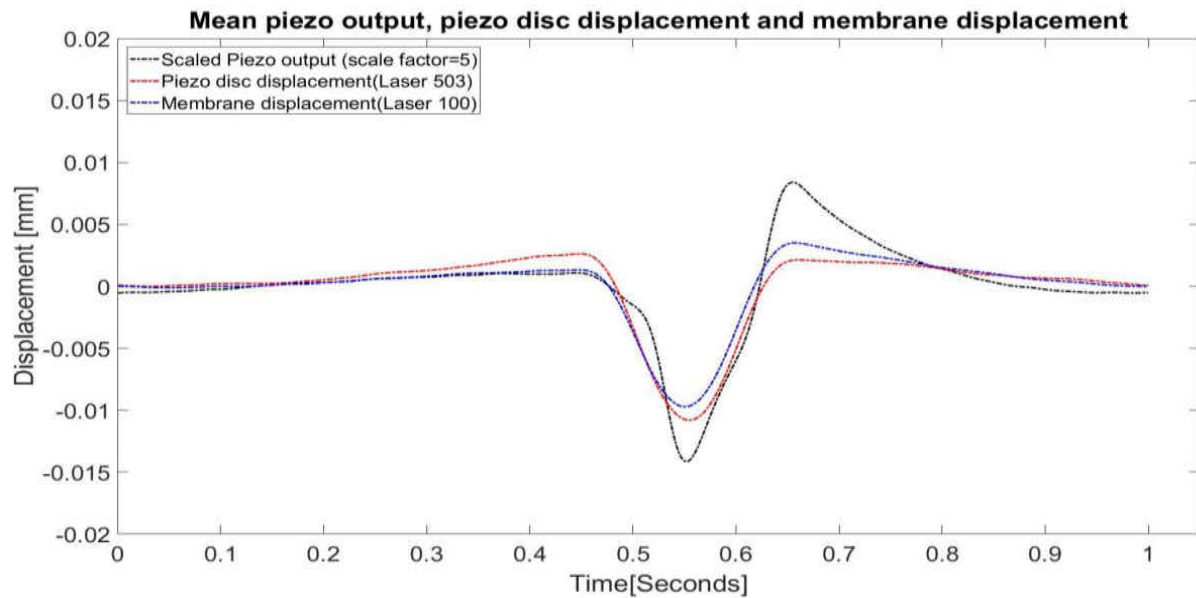


Figure 2-18 Piezo output plotted against piezo disc displacement and membrane displacement at 5Hz cosine input signal. The normalized deviation from mean of piezo displacement was 0.7865 and sensitivity was 0.3358 V/mm

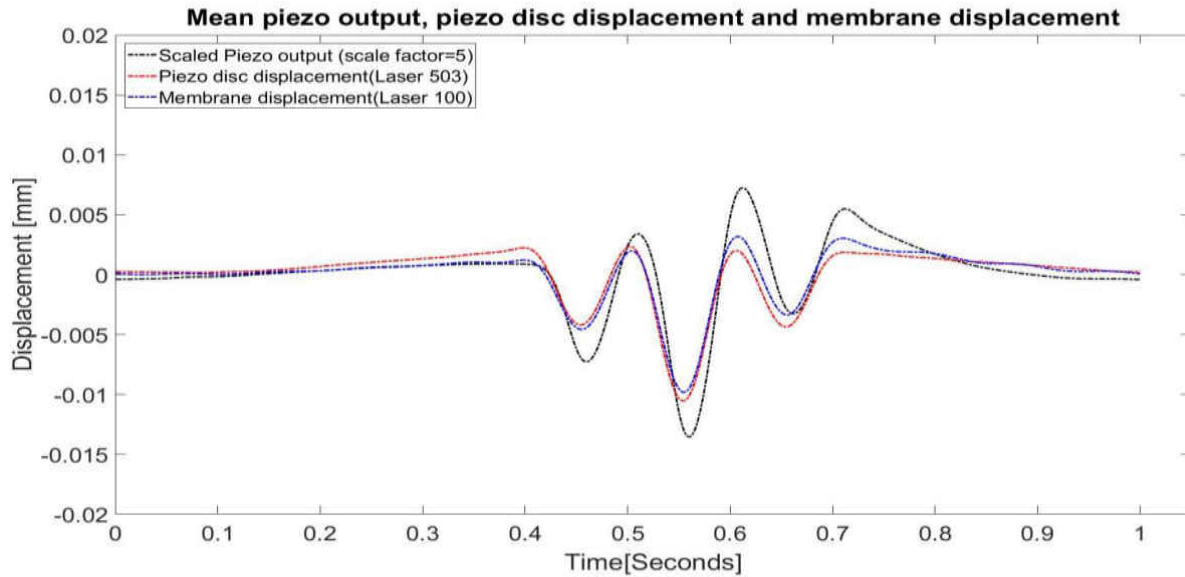


Figure 2-19 Piezo output plotted against piezo disc displacement and membrane displacement at 10Hz cosine input signal. The normalized deviation from mean of piezo displacement was 0.7858 and the sensitivity was 0.3228 V/mm

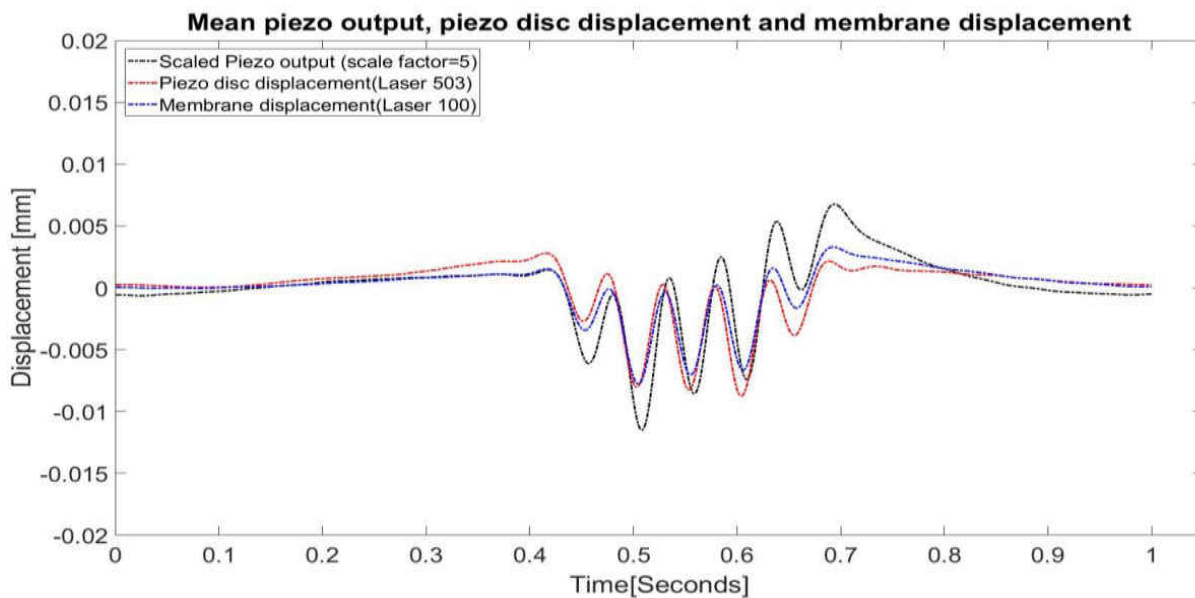


Figure 2-20 Piezo output plotted against piezo disc displacement and membrane displacement at 20Hz cosine input signal. The normalized deviation from mean of piezo displacement was 0.8273 and the sensitivity was 0.3166 V/mm

The sensor output test at varying input frequencies showed that the sensor sensitivity were 0.21, 0.22, 0.33, 0.32, 0.31 V/mm for input signal of 1, 2, 5, 10, 20 Hz respectively. Since the sensitivity had small changes as the input frequency increased (in the 1-20 Hz range), this suggests that the piezo output is representative of a displacement measurement. Testing the sensor with sinusoidal waves will be performed in the future to further confirm this finding.

2.3.3 Testing Repeatability of the Piezo based Tmp Sensor Output

The 5 Hz cosine pulse signal ran continuously from the computer at a repetition rate of 1 Hz. The piezo sensor output was acquired for one minute. The output data was acquired again after 5 minutes and 10 minutes after the first test.

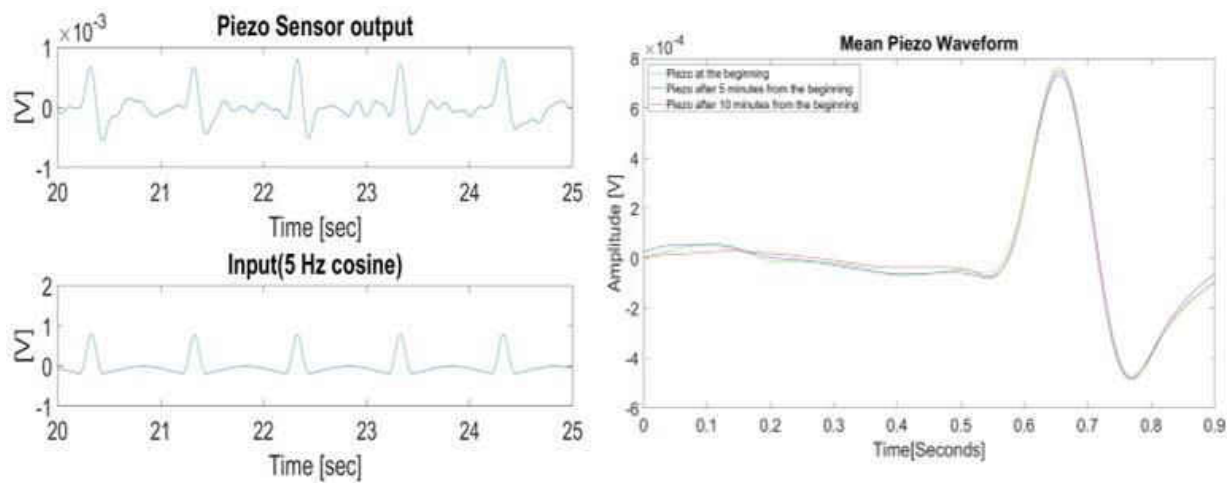


Figure 2-21 Left: Filtered piezo output with 5 Hz cosine input. Right Mean Piezo output waveform at different time. The acquired Tmp sensor output is comparable to the input signal. The normalized deviation from mean is about 0.0736.

Figure 2-21 shows that the Tmp sensor output is comparable to the input signal. The maximum peak to peak amplitude difference is about 1.5% of the peak to peak amplitude of the mean Tmp waveform at the beginning. The normalized deviation from mean is about 0.0736.

2.3.4 Testing the Repeatability of LASER Doppler Vibrometer Output

The output from the LDV is plotted along with the input signal. In addition, the mean waveform for three different time (beginning, after 5 minutes, after 10 minutes from the beginning) was plotted

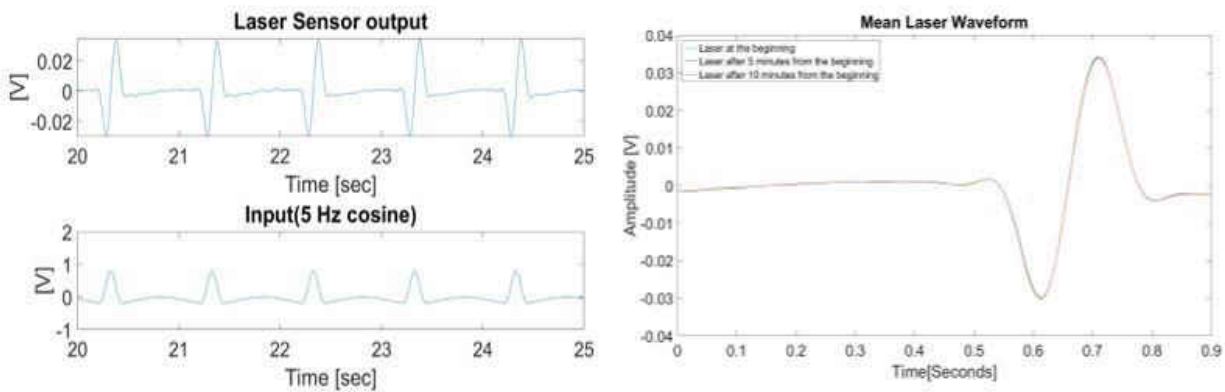


Figure 2-22 Left: Filtered piezo output with 5 Hz cosine input. Right: Mean LDV waveform at different time. The normalized deviation from mean is 0.0135

Figure 2-22 shows that the LDV output measured the velocity of the membrane since the output is showing a sin wave for a cosine wave input. The variability of the mean waveforms for three different time was within 0.9% of the mean waveform at the beginning. The normalized deviation from mean is 0.0135

2.3.5 Testing the Effect of External Pressure on Tmp Sensor Output

The Tmp sensor was tested connected to cylinder of the mechanical setup. The space between cylinder and the sensor cavity was connected to a manometer. External pressure was applied using manometer to test the sensor response at subtle change in pressure. Data acquired for zero, positive 4 cm, positive 8 cm, negative 4 cm and negative 8 cm of water.

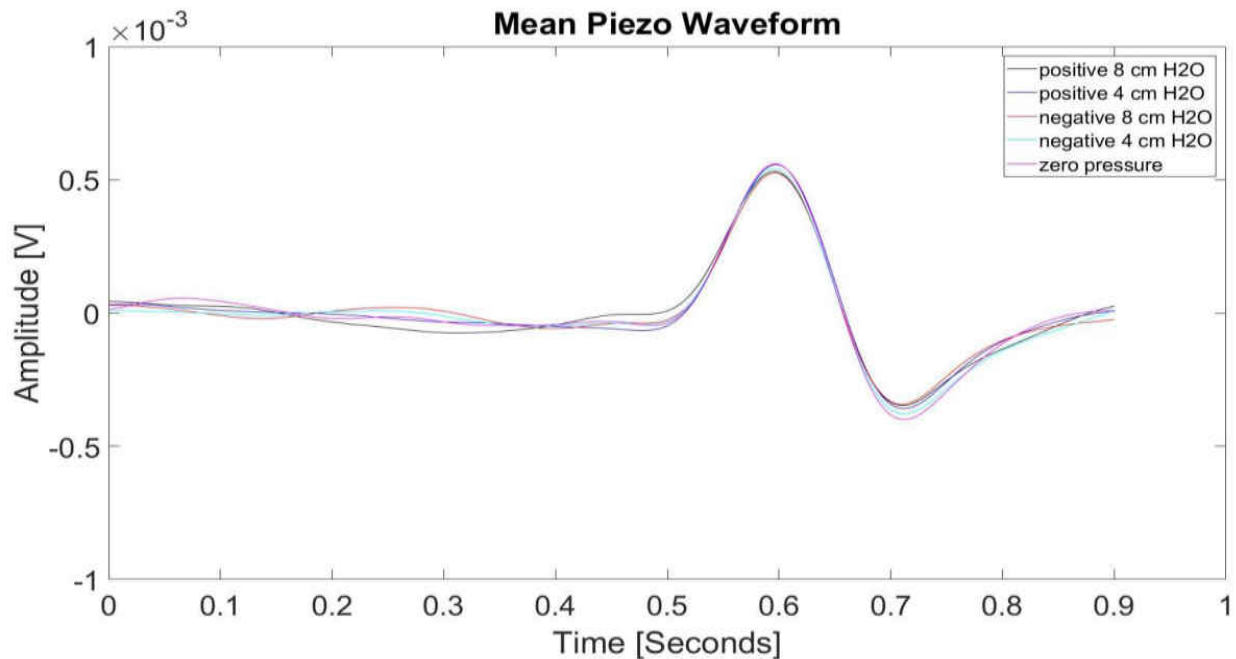


Figure 2-23 Tmp sensor output at different external pressure. The normalized deviation relative to zero pressure for +8, +4, -8 and -4 cm of water were 0.144, 0.102, 0.165, 0.118 respectively.

Figure 2-23 shows that at different external pressure the sensor output didn't change significantly and the maximum peak to peak amplitude difference was found to about 8% of the peak to peak amplitude of Tmp at zero pressure

2.4 Testing the Effect of Dead Space in the System on TMp Signal Output

If the system is sealed, then the space between the piezo disc and the tympanic membrane will be small. The addition of leak testing the valve will increase this dead space. To test the effect of dead space, the sensor assembly was connected to a manometer to test the system leakage. The valve port for manometer connection can be plugged using an occluded hose. Also, the valve can be closed completely to provide complete sealing. Subject is in sitting position while wearing the TMp headset. Left and Right TMp and pulse sensors was connected. Both leak testing valves (of TMp sensors) was gently closed. The left valve remains closed and plugged throughout the experiments. Data was recorded for 1 min. Right valve outlet was plugged, and the valve was opened. Data was recorded for 1 minute. Manometer was connected to right sensor and data was recorded. We measured the dead space that was added to the system when keeping the valve plugged and open when the manometer was connected. The first space consisted of a 1.3 mm diameter and 100 mm long tubing along with 3.5 mm valve internal diameter and 30 mm valve length (total volume= 394.81 mm^3), while the second connection consisted of 1.3 mm diameter and 780 mm long tubing plus the 4.7 mm manometer internal diameter and 150 mm height from the piping connection to the fluid level at zero pressure (Total volume= 4032.548 mm^3). This is about 10 times higher than the first space.

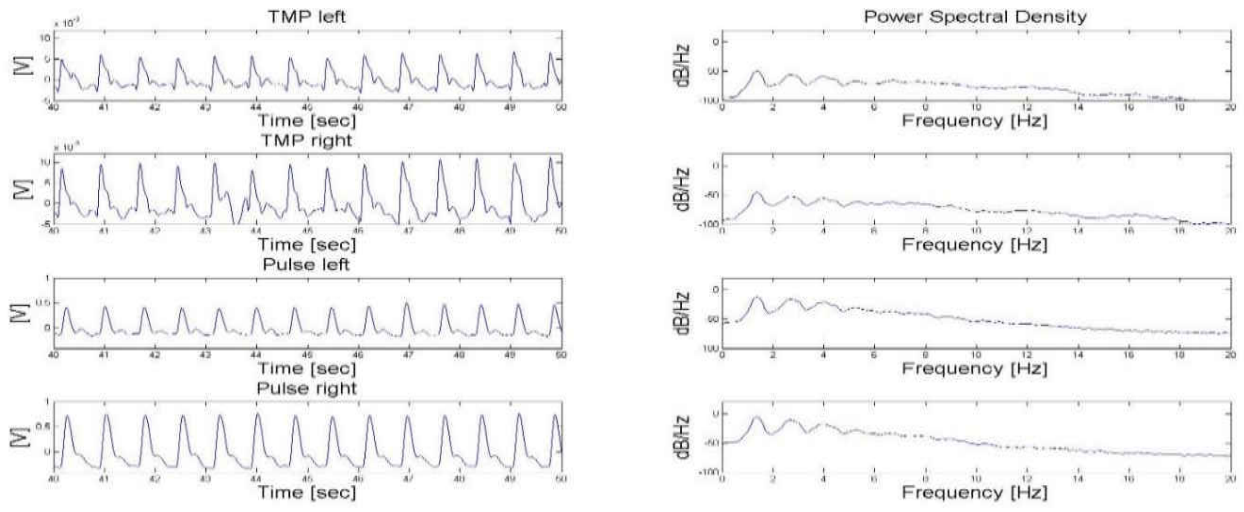


Figure 2-24 Tmp data when both leak testing valve closed and plugged to provide complete seal from the environment. Both left and right Tmp waveform have similarity in shape compared left and right ear lobe pulse.

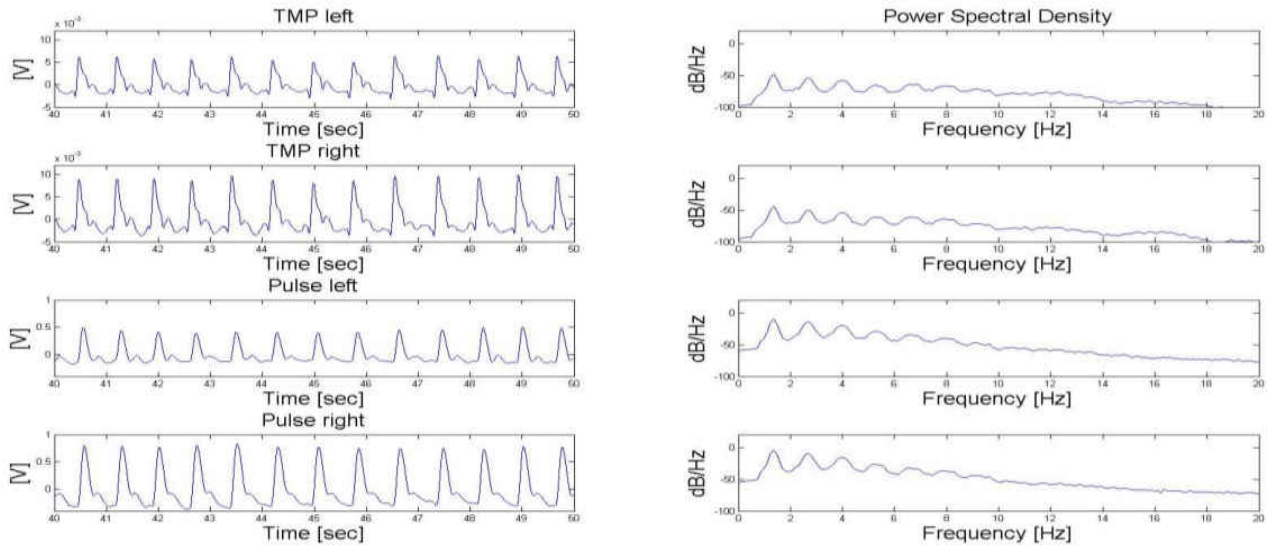


Figure 2-25 Tmp data when left valve is closed and right valve opened and plugged to provide a little dead space. Results show that adding a little dead space didn't significantly change the waveform.

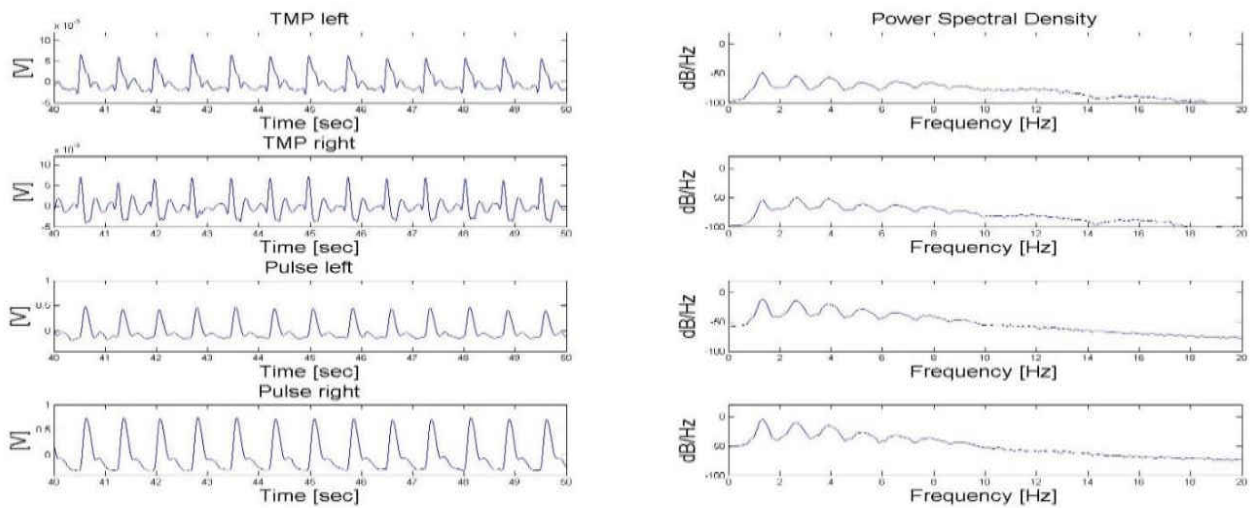


Figure 2-26 Tmp data when right valve is opened and connected to manometer. Although the system is sealed, results show that adding a lot of dead space changed the right Tmp waveform.

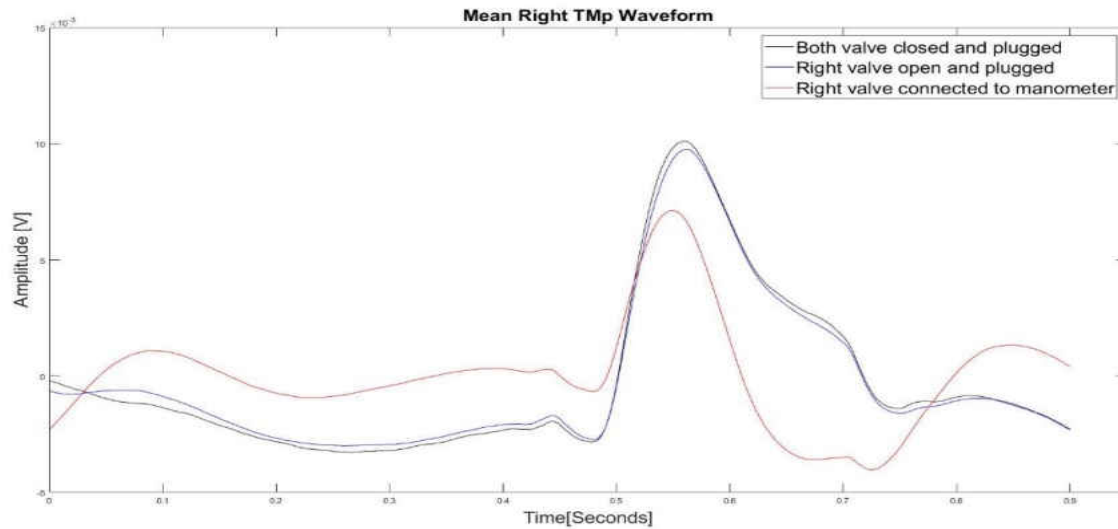


Figure 2-27 Mean waveform showing significant change in waveform when there is considerable dead space between the sensor and tympanic membrane, the amplitude of the waveform decreased and the shape of Tmp waveform changed. The normalized deviation relative to mean for closed and plugged case for open and plugged was 0.0780 and for open and connected to manometer was 0.8825.

The results of the experiment showed that adding a little dead space (the space up to the valve outlet) didn't change the shape and amplitude of the Tmp. But when we added a lot of dead space (tube space from piezo disc to manometer inlet), even though the system is sealed, the waveform changed its shape and amplitude reduced. The normalized deviation for a system with a lot of dead space was significantly higher (0.88) than small dead space (0.07). This suggests that small dead spaces (about 400 mm³) should be used to avoid waveform distortion.

2.5 Testing the effect of leakage on Tmp Signals

To test the effect of leakage, the manometer connection with the valve outlet was removed. The right valve exit was plugged, and the valve was closed gently and completely. Data was recorded for 1 minute. The plug was removed, and the right valve was opened slowly (half a turn) to induce

leakage. Data was recorded for 1 minute. The valve was again repeatedly opened (by half a turn) and the corresponding data recorded to see the effects of leakage of varying degree.

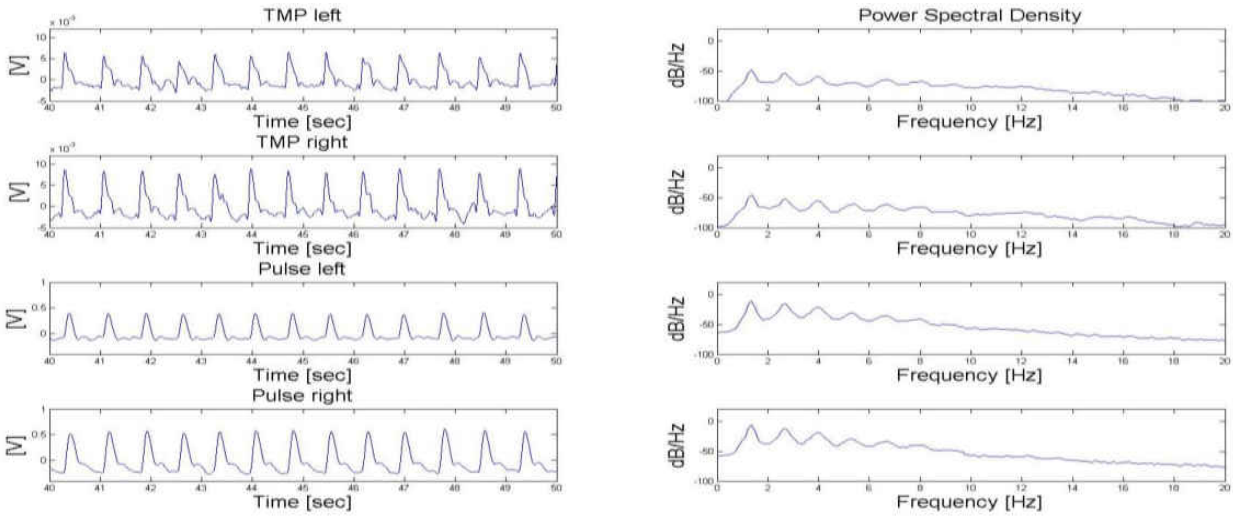


Figure 2-28 Tmp data when both valves are closed. Results show that both Tmp waveform showing similarity in comparison to left and right ear pulse. This waveform with sharp single peak may be an indicator of a sealed system.

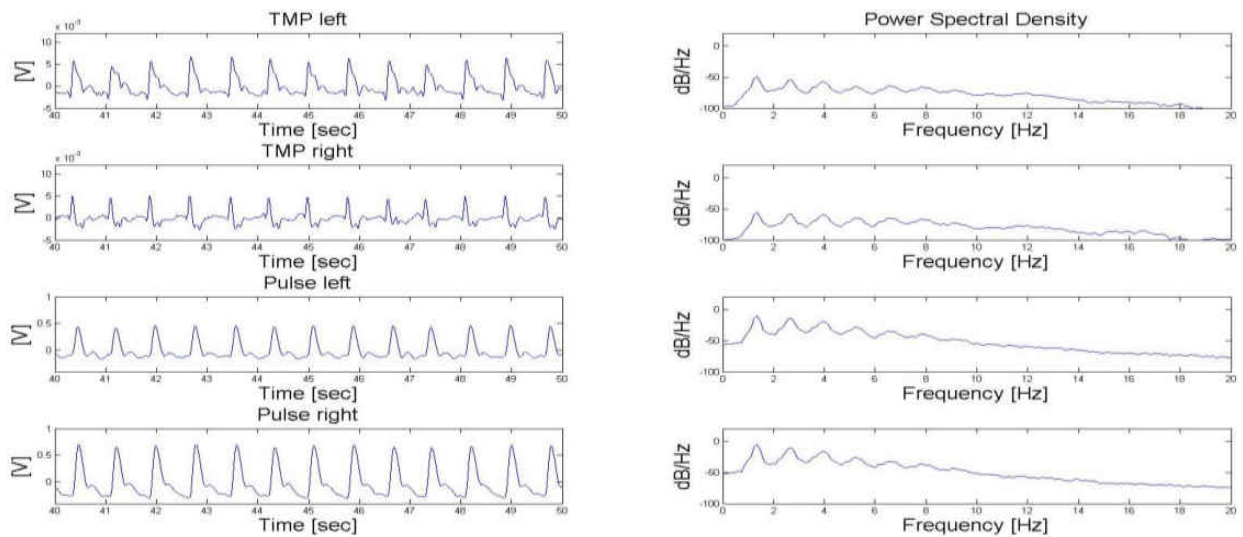


Figure 2-29 Tmp data when the right valve is opened by half way. These results show that the right Tmp waveform started to lose its original shape and amplitude due to leakage of the system.

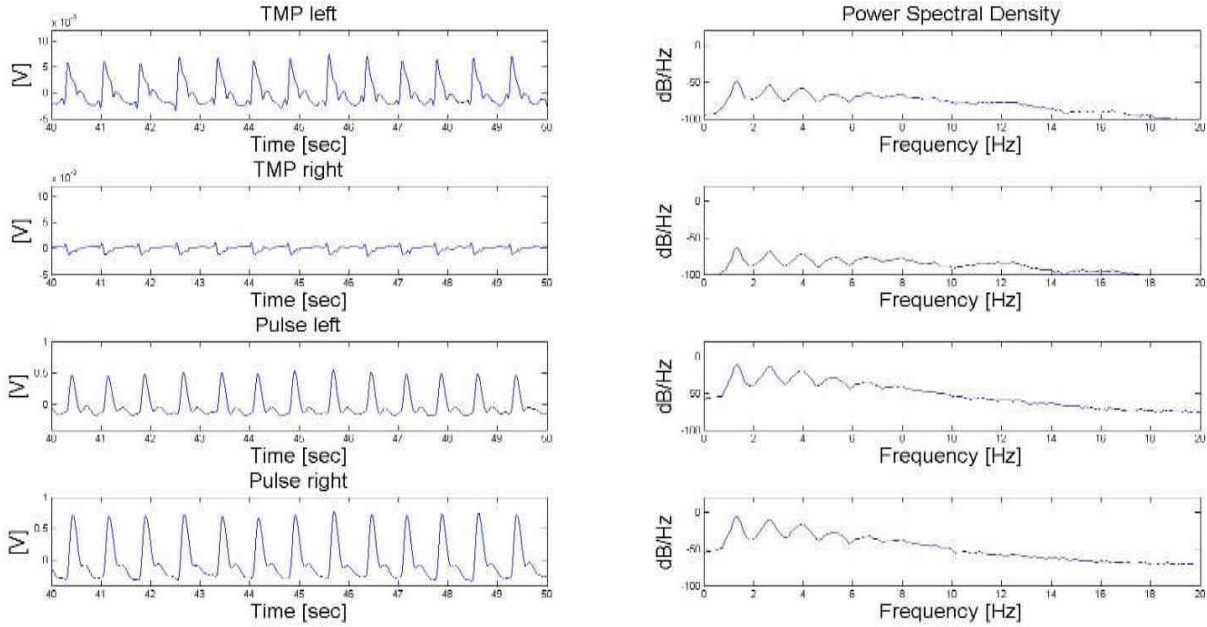


Figure 2-30 Tmp data when the right valve is opened completely to provide a leakage to the right side. The waveform lost in terms of shape and magnitude. This can be an indicator of leakage in the system.

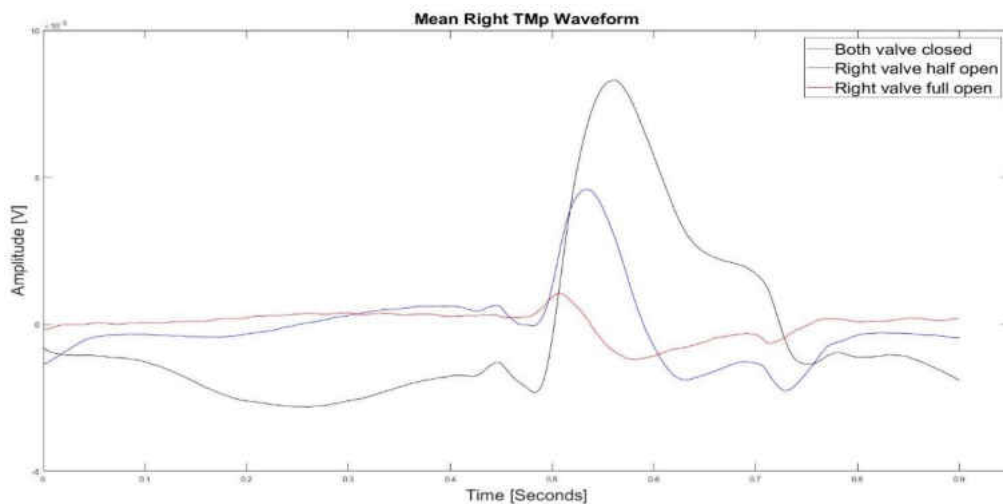


Figure 2-31 Mean Tmp waveform showing the amplitude of the Tmp waveform significantly reduced as the valve position changed from closed to open. The shape of the waveform also changed as leakage introduced to the system. The normalized deviation relative to the mean of completely sealed system for half open and fully open condition was found to be 0.93 and 1.11 respectively.

2.6 Testing the repeatability of the TMp signal

To investigate intra-subject variability of the TMp signal over a period of time, the subject was in the sitting position wearing the TMp sensor. The sealing (the airtightness between the sensor and external ear canal) was then confirmed and data was acquired for one minute. After the data acquisition, the subject removed the TMp sensor from the ear canal. This was repeated after waiting for 5 and 10 minutes.

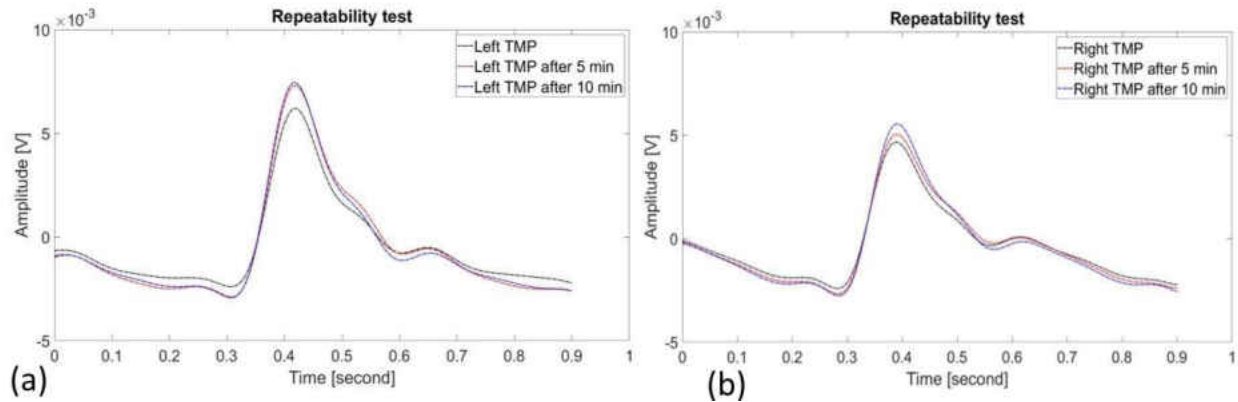


Figure 2-32 Repeatability testing of the TMp signal for left and right ear for same subject over a period. The normalized deviation from mean TMp for left and right 0.216 and 0.194 respectively

Figure 2-32 shows the intra-subject variability of the TMp sensor signal at different times. The normalized deviation was 0.216 for left ear and 0.194 for right ear. This shows that both sensor could acquire repeatable waveforms under same condition. The normalized deviation from mean values were about 3 times higher than what found in mechanical setup (figure 2-19) in section 2.3.3

2.7 Investigating the difference between contralateral ears

To investigate the effect of tympanic membrane pulsation variation between right and left ears, both sensor was switched to the contralateral ear (right sensor placed in the left ear and left sensor in the right ear). Data were acquired for 1 minute following the same procedure as section 2.6

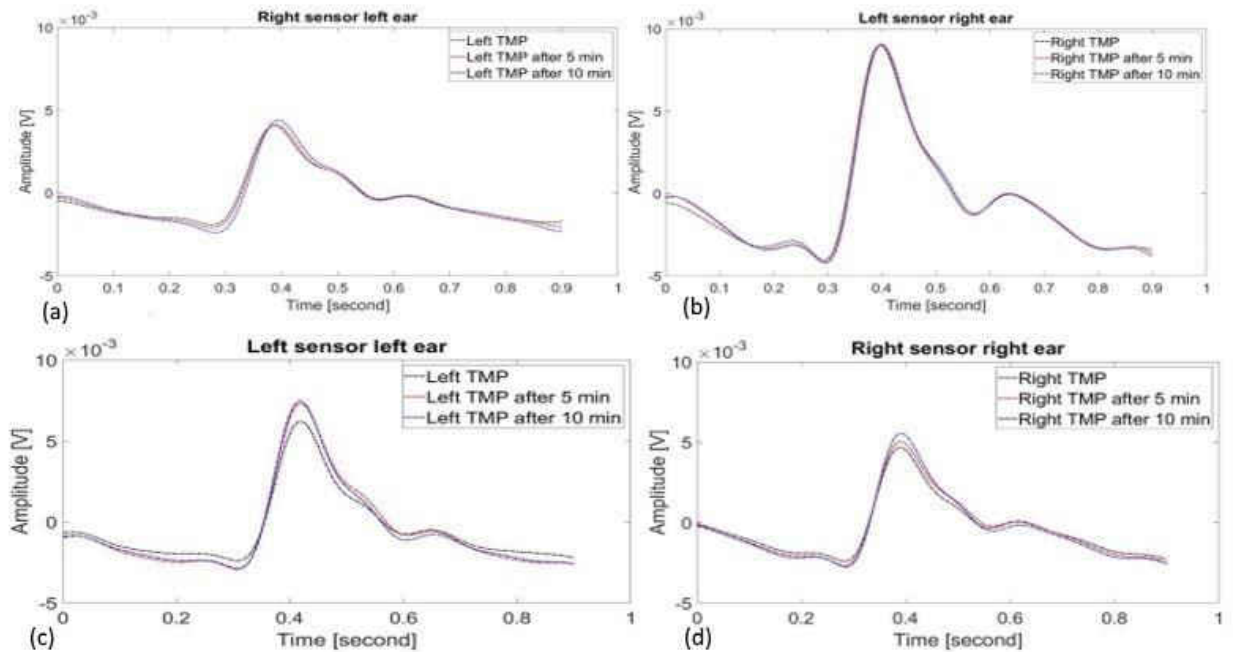


Figure 2-33 Tmp waveform at contralateral ear canal (right sensor in left ear and left sensor in right ear) and ipsilateral (left sensor left ear and right sensor right ear) at different time period. The normalized deviation for left sensor at contralateral and ipsilateral was 0.08 and 0.22 while for right sensor in contralateral and ipsilateral ear was 0.19 and 0.19 respectively.

Figure 2-33 showed that the left sensor normalized deviation from mean increased about three times as sensor was placed from contralateral to ipsilateral ear. While the right sensor normalized deviation from mean didn't change for contralateral and ipsilateral locations.

2.8 Testing the Effect of External Pressures on Tmp Signals

The manometer was connected to the valve outlet. The right valve exit was plugged, and the valve was closed gently and completely. Data was recorded at zero external pressure for 1 minute. The right valve was opened and a positive pressure of 8 cm of water was applied by a syringe in the manometer tubing circuit. Data was recorded for 1 minute. Thirty seconds of wait time was observed after each data acquisition. Data was then acquired for pressures of +4 cm, - 8 cm and - 4 cm of water.

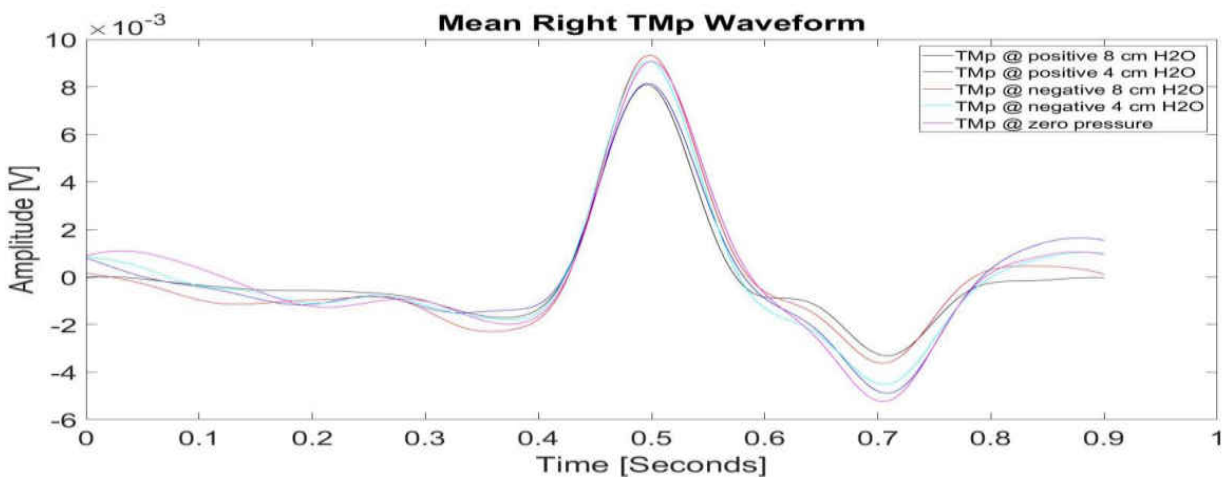


Figure 2-34 Mean Right Tmp waveforms at varying external pressure applied in right external ear canal-Tmp sensor cavity. The maximum peak to peak amplitude difference was about 3 mV found between zero pressure and positive 8 cm of water. This was about 20 % of the peak-to-peak amplitude at zero pressure. The normalized deviations from zero pressure were, 0.3039, 0.1693, 0.2513 and 0.1296 for pressures of 8, 4, -8, and -4 of water, respectively.

Figure 2-34 shows that while the normalized deviation relative to zero pressure was higher at positive 8 cm and negative 8 cm of water, for positive 4 cm and negative 4 cm water the deviation was lower than the values found in the repeatability test (section 2.6). This suggests that changing small external pressures in the ear canal doesn't significantly affect the TMp signal. This result may need to be confirmed in a larger number of subjects.

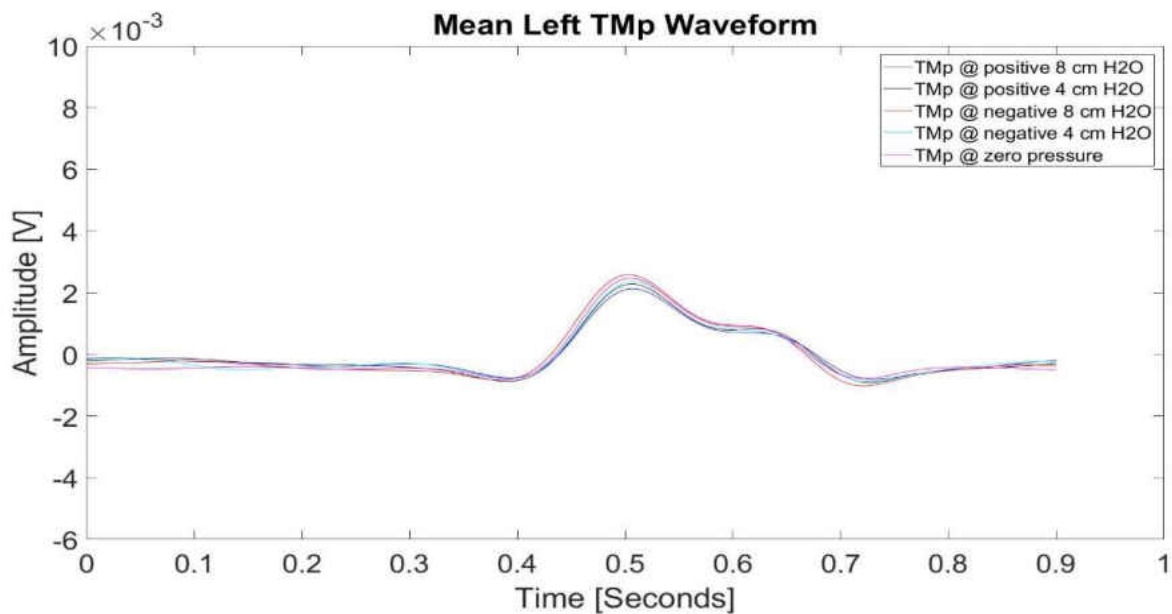


Figure 2-35 Mean TMp waveforms at different external pressures. The maximum peak to peak amplitude difference was about .3 mV found between zero pressure and positive 4 cm of water. This was about 9 % of the peak to peak amplitude at zero pressure. The normalized deviations from zero pressure were, 0.1743, 0.2047, 0.1454, 0.1471 for pressures of 8, 4, -8, and -4 of water, respectively.

Figure 2-35 shows that the normalized deviation relative to zero pressure were found to be similar or lower than the values found in the repeatability test. This suggest changing external pressure caused no significant change in the waveforms for contralateral TMp signal.

CHAPTER 3: TYMPANIC MEMBRANE PULSATIONS AT VARYING TILT ANGLE

3.1 Experimental Procedure

Experimental protocol was approved by IRB of our institution. The subject rested on a tilt table for five minutes. The subject was gently secured by shoulder and waist strap on tilt table to avoid slipping on table while in the downward tilt position. Ear lobe pulse sensors were attached to the subject's both ear lobes. Next, new ear plugs were inserted at the tips of the long pipe of the piezo sensors. The long pipes along with the ear plug were inserted into subject's external ear canals. The air-tightness test valves were connected to the manometer to test the sealing of the ear canal. Once both the ear canal sealing were confirmed, the subject was tilted from 45 degrees upward to supine position. The subject rested for 5 minutes to allow the equalization of cranium pressure to supine position and as well as allowing the subject to be in relaxed state.

Before acquiring the data, a spirometer was put into subject's mouth to measure flow rates. The system was then ready for data acquisition. The subjects were gradually tilted from supine to 45 degrees downward with increments of 15 degree. At each tilt position, there was a 30 second settling time to accommodate equalization of ICP followed by 60 seconds of data acquisition.



Figure 3-1 Experimental setup showing: the data acquisition system, the Piezo sensor assembly, and spirometer assembly (top row). The bottom picture shows the subject wearing piezo sensor headset while the spirometer is put into subject's mouth to acquire the breathing data.

3.2 Results

The acquired Tmp signal was plotted along with ear pulse. The time delay between peaks of both signals was calculated using cross correlation function.

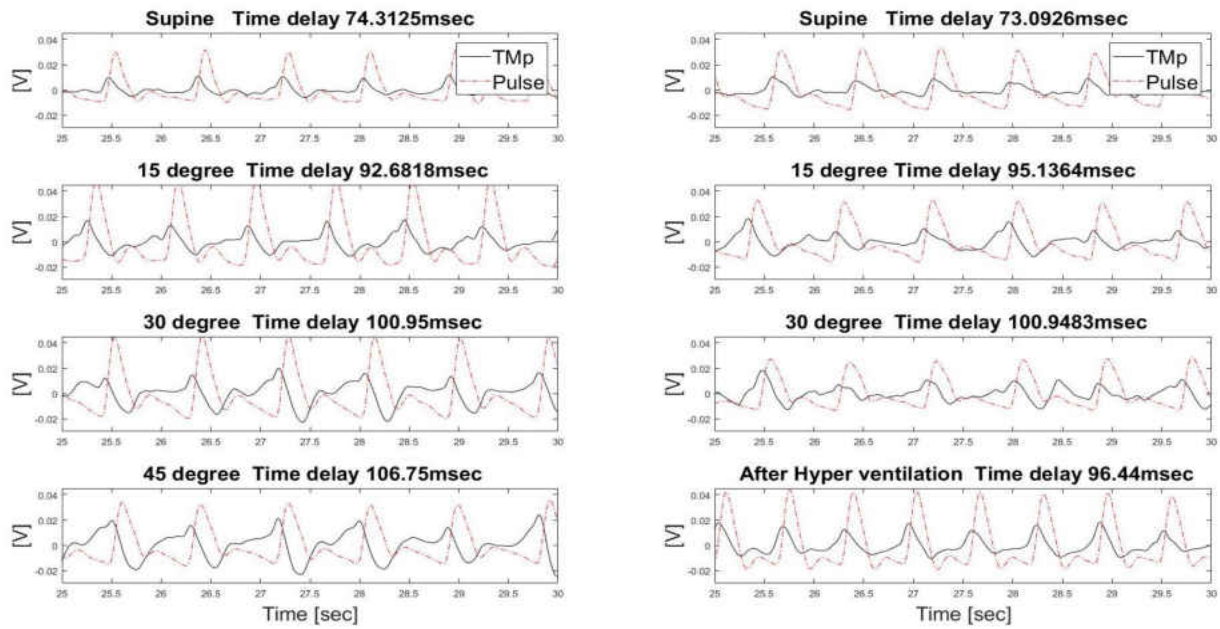


Figure 3-2 Tmp waveform (black continuous line) along with ear lobe pulse (red dotted line) at different tilt positions. Starting at left top figure showing Tmp and Pulse waveform for Supine position followed by 15 degrees, 30 degrees, 45 degrees, after hyper-ventilation at 45 degrees, 30 degrees, 15 degrees, supine again. As ICP increased (by increasing tilt angle) a detectable effect on Tmp waveform was seen. Hyperventilation (which is known to reduce ICP) also affects the Tmp waveform. Tmp appeared to return its supine morphology as the subject was returned to the supine position. (Subject 1)

Figure 3-2 shows that the Tmp waveform changed shape and amplitude as the tilt angle increased gradually from supine to 45-degree downward direction indicating the rise of ICP. The time delay between the signals also increased as ICP increased. To further investigate this phenomenon, both the signals were filtered, and time delay was calculated at the fundamental frequency.

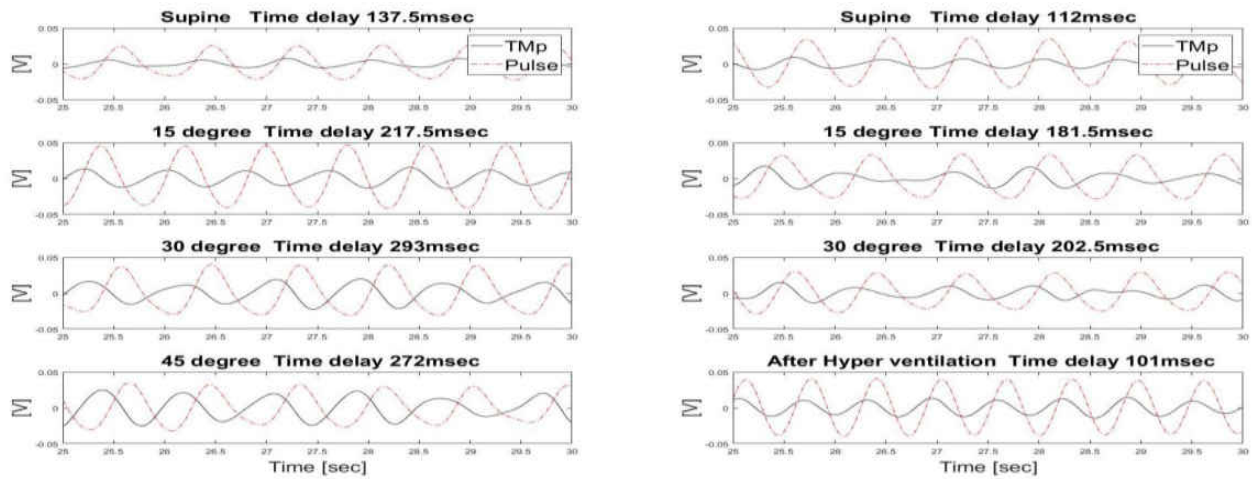


Figure 3-3 Tmp and Ear pulse signal was filtered (bandpass: 1-2 Hz) to calculate the time delay at fundamental frequency. As the tilt angle increased the amplitude of the Tmp waveform increased and the corresponding time delay increased as well.

Figure 3-3 showed that as tilt angle increased, the amplitude of the filtered waveform increased. After hyperventilation, the amplitude of the waveform decreased. In addition, the time delay decreased significantly. This suggests that the CSF pressure dropped after hyperventilation. The waveform amplitude decreased gradually as the tilt angle decreased from downward 45 degrees to supine again.

The time interval between the Tmp and reference ear lobe pulse signal at different tilt angle also plotted.

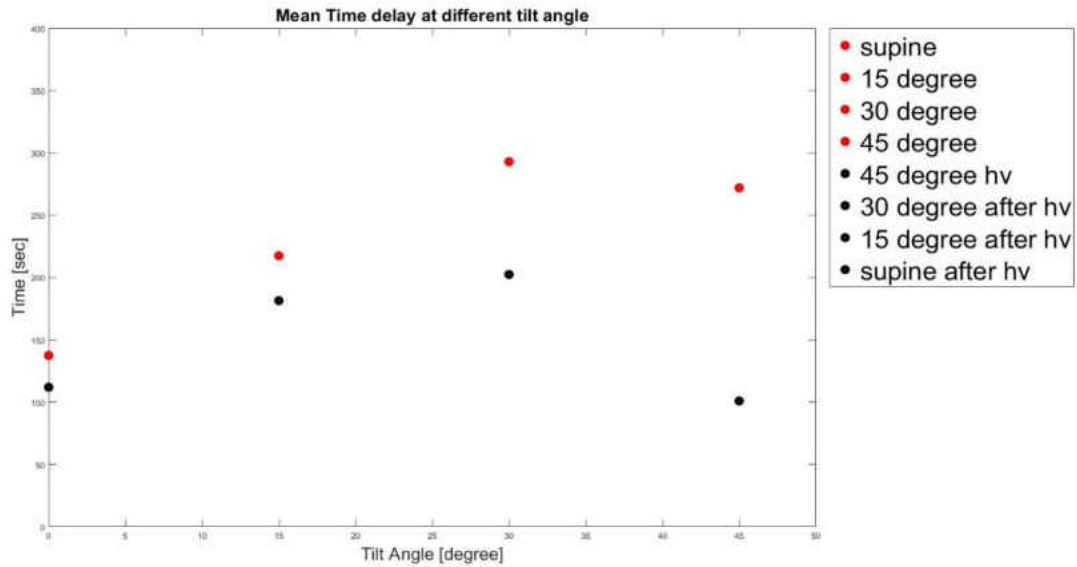


Figure 3-4 Time delay between Tmp signal and earlobe pulse signal at different angle. Time delay changed with tilt angle.

Figure 3-4 shows that the time delay changed with tilt angle, which may be useful in detecting ICP changes. Similar analysis (figure 3-5 to 10) were done from the data acquired from 2 more subjects (subject 2 and 3).

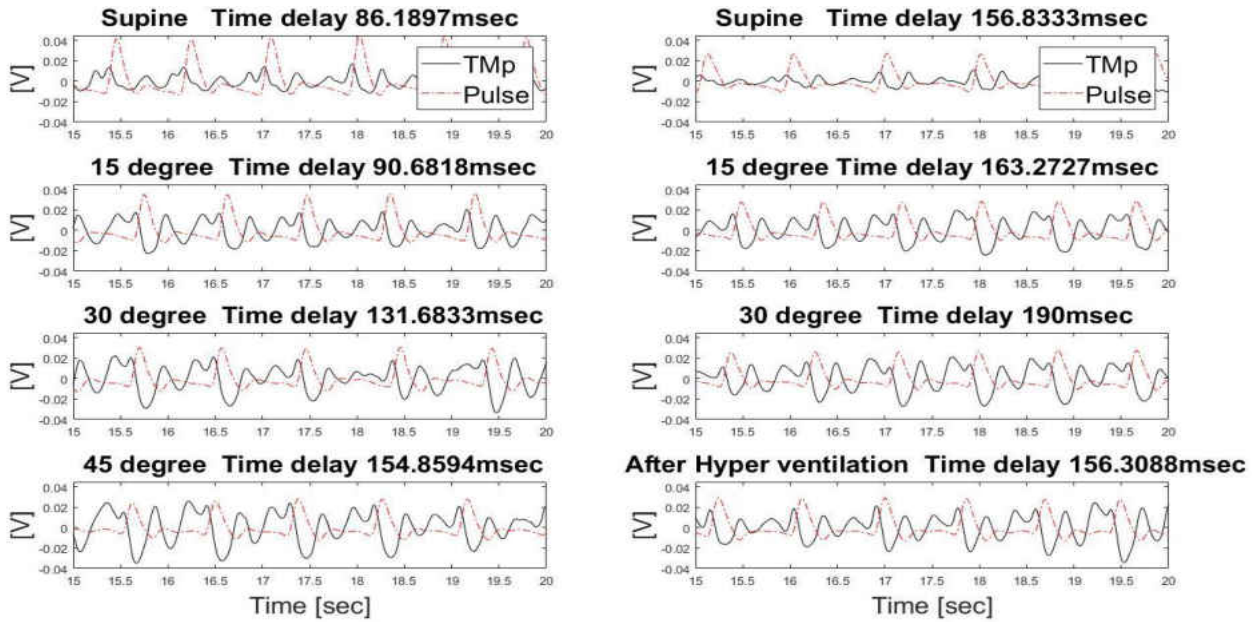


Figure 3-5 Tmp along with earlobe pulse at different tilt angle. The amplitude of the Tmp increased as the tilt angle increased. (Subject 2)

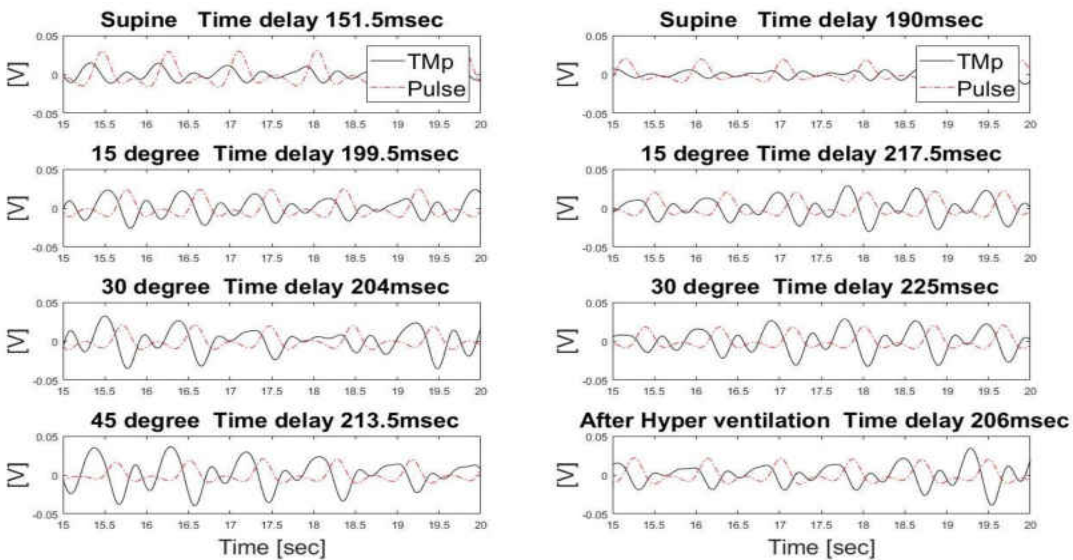


Figure 3-6 Tmp and earlobe pulse filtered at fundamental frequency for different tilt angle (subject 2)

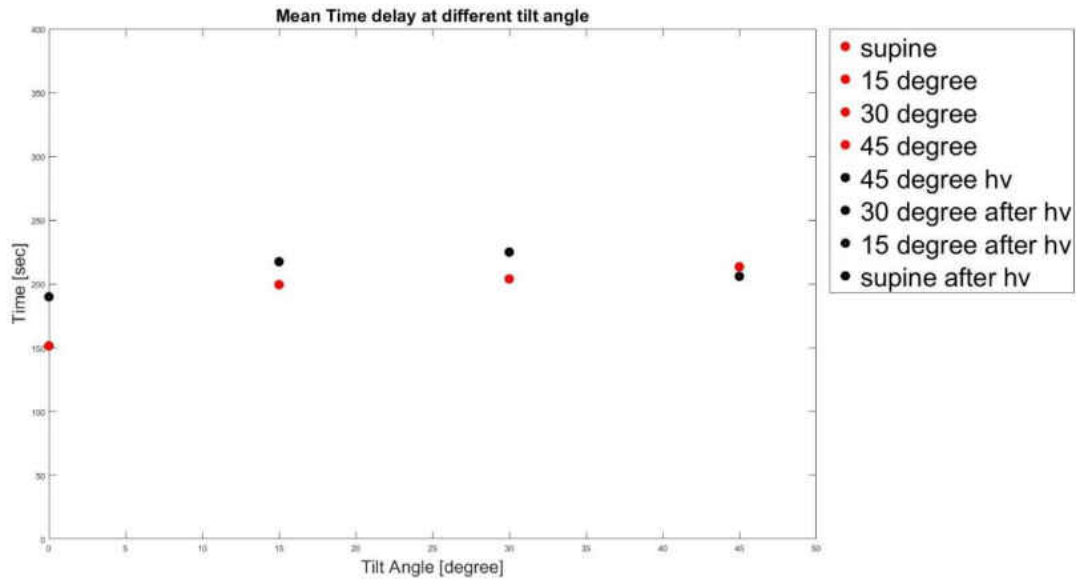


Figure 3-7 Time delay at different tilt angle (subject 2)

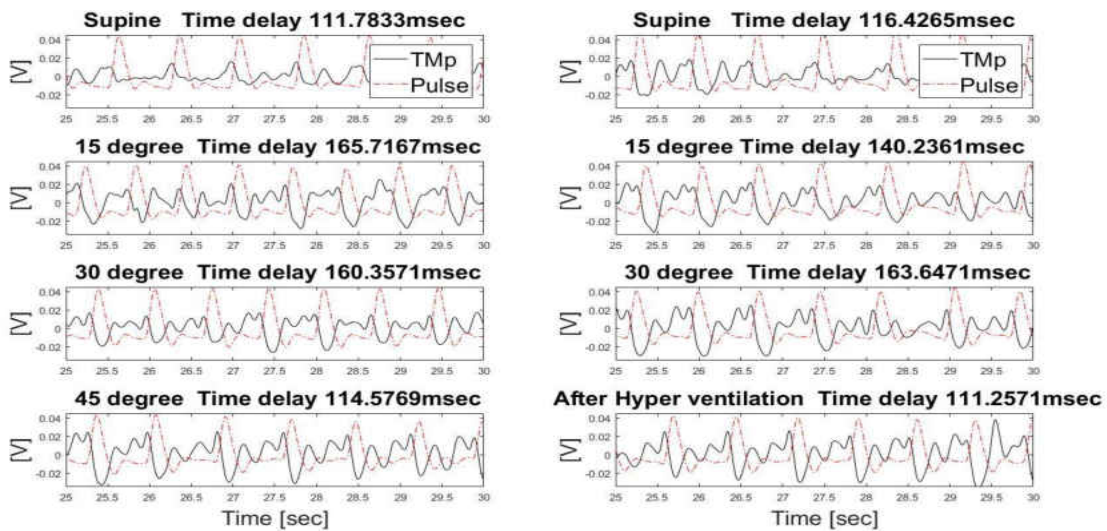


Figure 3-8 Tmp along with earlobe pulse at different tilt angle. The amplitude of the Tmp increased as the tilt angle increased. (Subject 3)

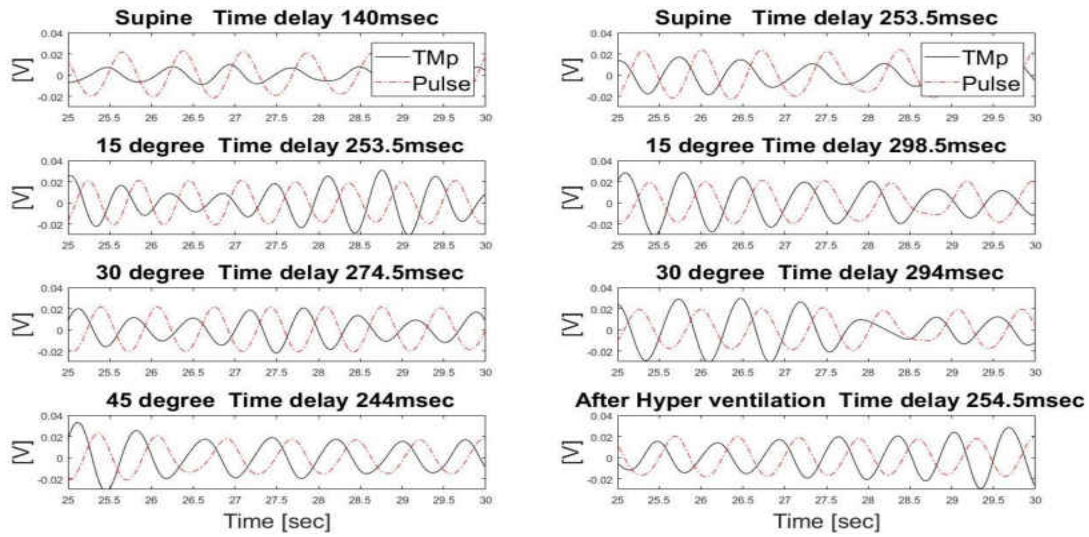


Figure 3-9 Tmp and earlobe pulse filtered at fundamental frequency for different tilt angle (subject 3)

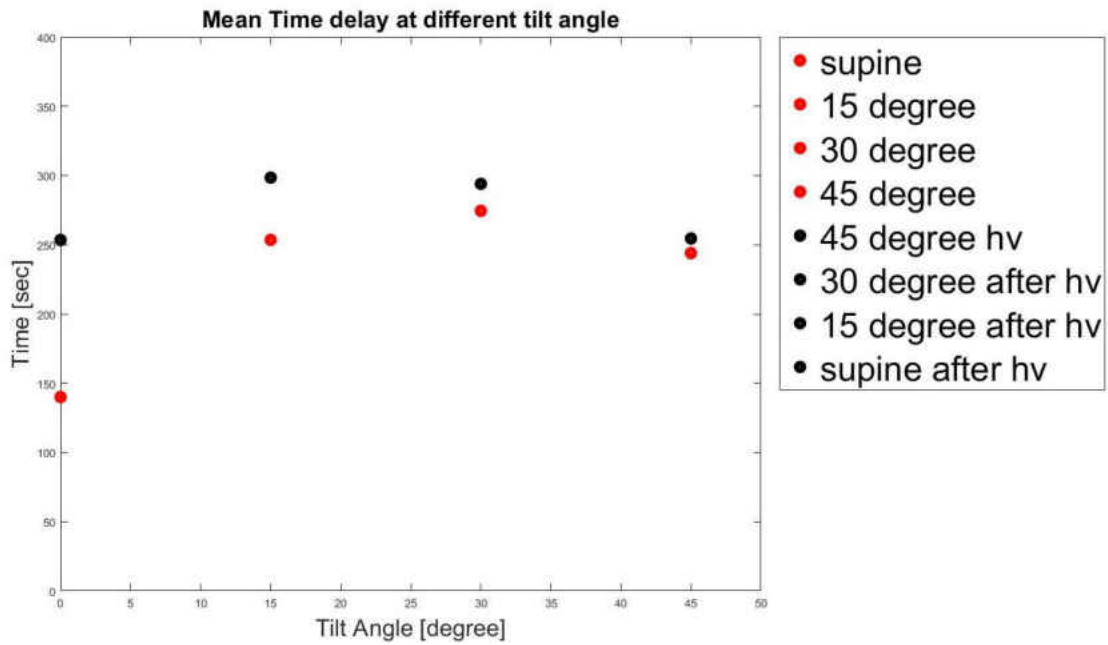


Figure 3-10 Time delay at different tilt angle (subject 3)

3.3 TMp changes with title angle for shorter acquisition and settling times

In the above section, some hysteresis was seen when the subject posture returned to the supine and other positions. Earlier studies used shorter acquisition and settling times and suggest smaller hysteresis effects. To investigate this issue, TMp was acquisition time was shortened to 15 seconds, and the settling time (waiting time between end of posture change and start of acquisition) was kept close to zero. The tilt angle was changed at every 15 seconds from supine to 45 degrees with an increment of 15 degree and back to supine again. Figure 3-11 to 3-19 show the unfiltered, filtered data (band-pass filtered at fundamental frequency) and calculated time delay at the fundamental frequency for different tilt angles. The results suggested that hysteresis was higher in subject 3. The TMp amplitude increased consistently with tilt angle in the 3 subjects. The time delay increased in 2 of the three subjects while time delay changes in the third subject were relatively small.

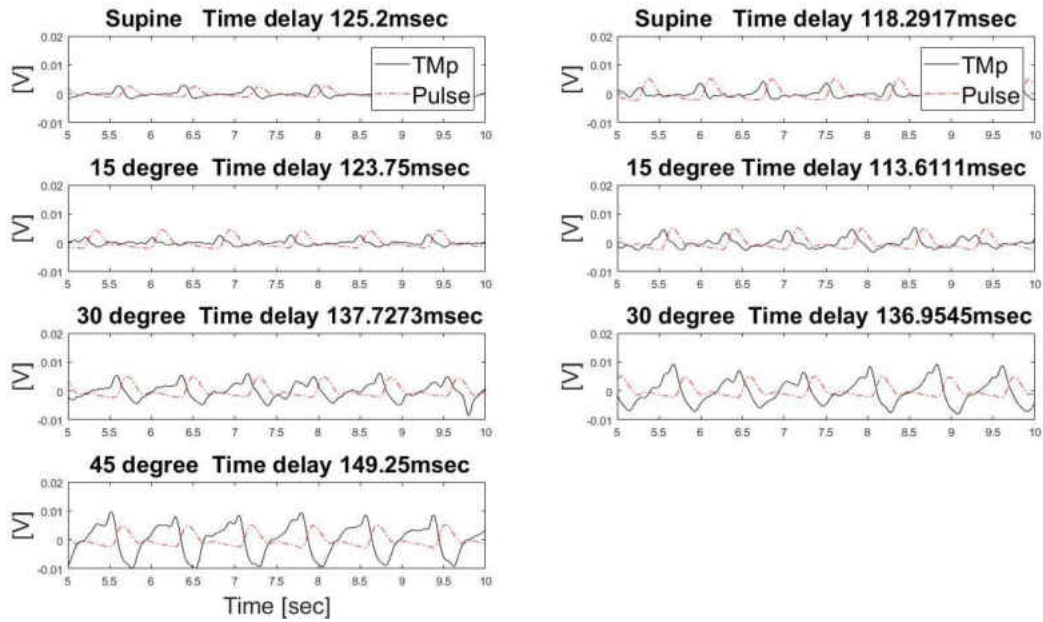


Figure 3-11 Tmp along with ear lobe pulse at different tilt angle, when the latter changed rapidly. The amplitude of the Tmp increased as the tilt angle increased. (Subject 1)

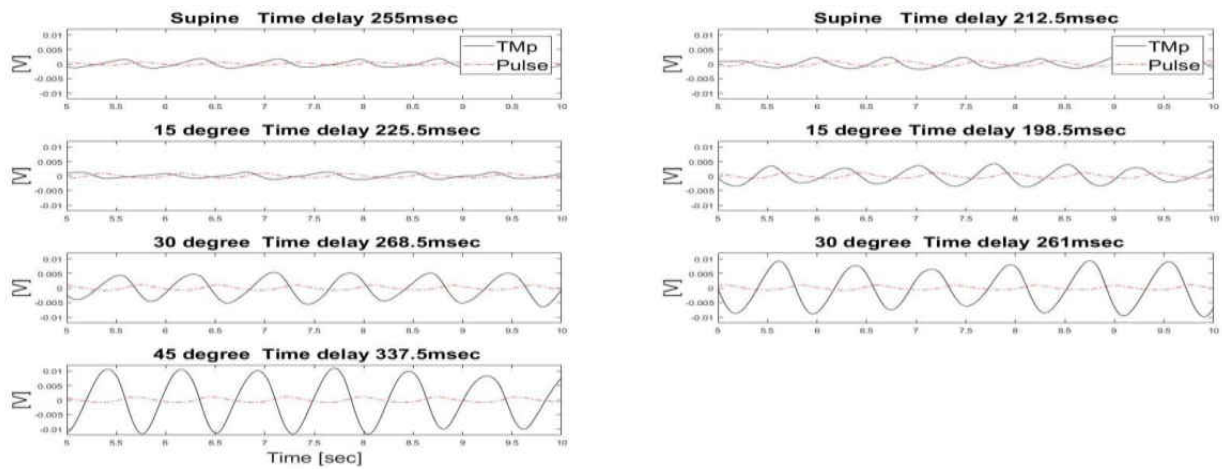


Figure 3-12 Filtered Tmp waveform along with pulse as the tilt angle increased quickly the amplitude of the waveform increased. (Subject 1)

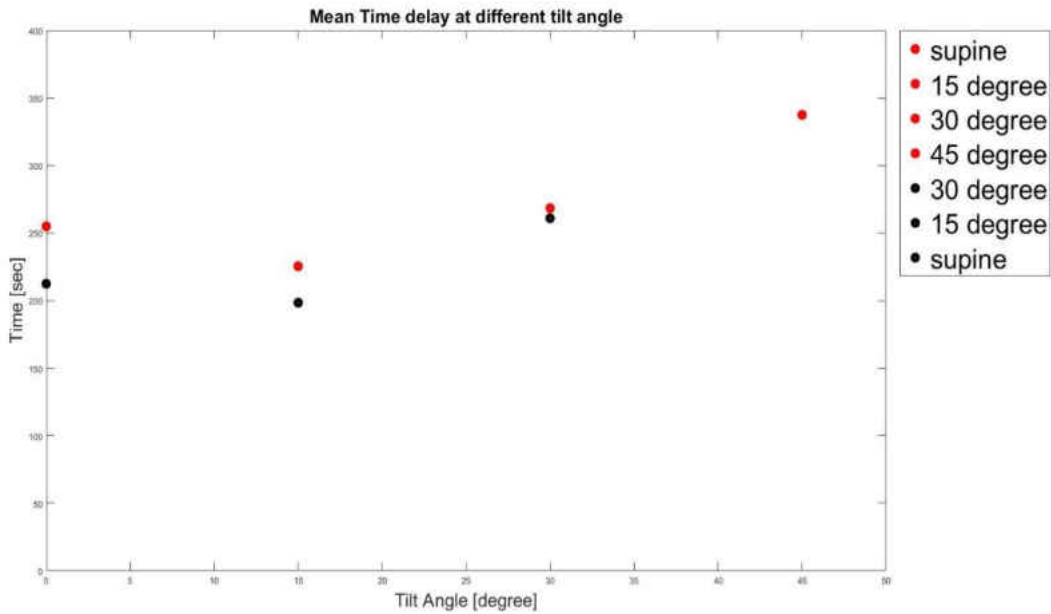


Figure 3-13 Time delay between TMp and Pulse signal at different tilt angle (subject 1). The tilt angle was changed rapidly with a 15 second data acquisition at each angle.

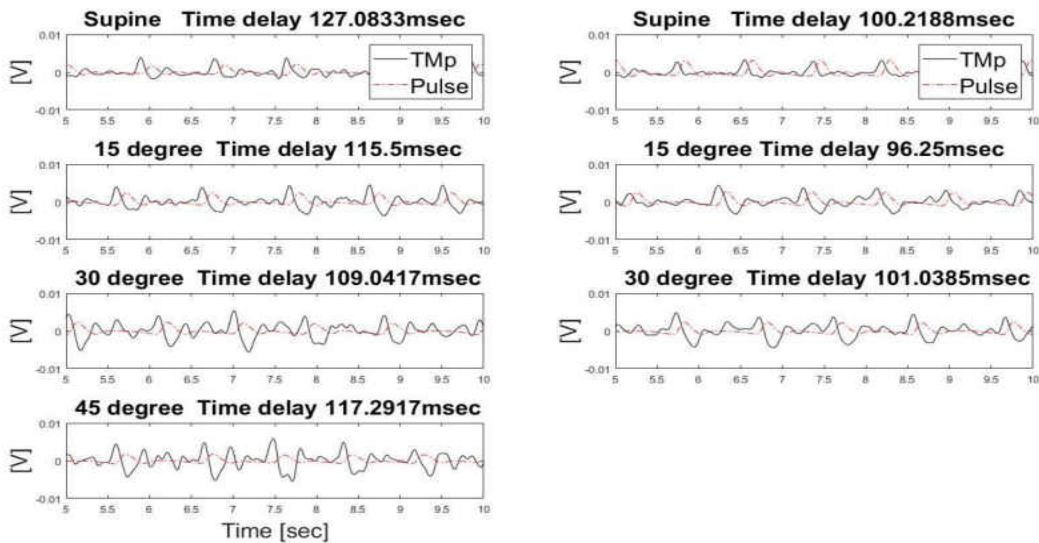


Figure 3-14 TMp along with ear lobe pulse at different tilt angle changed rapidly. The amplitude of the TMp increased as the tilt angle increased. (Subject 2)

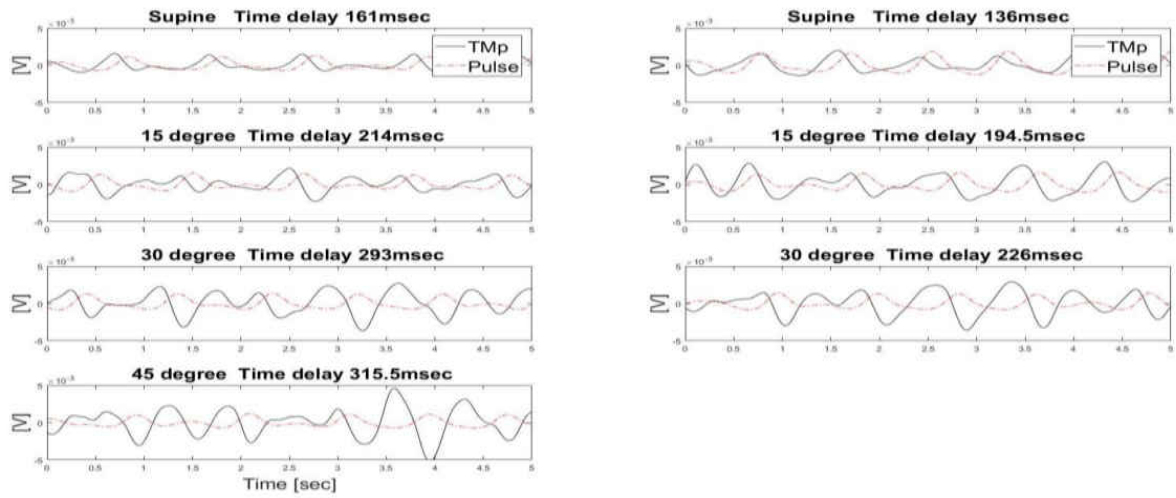


Figure 3-15 Variation of filtered TMP waveform with change in tilt angle (Subject 2). The amplitude and time delay increased with tilt angle

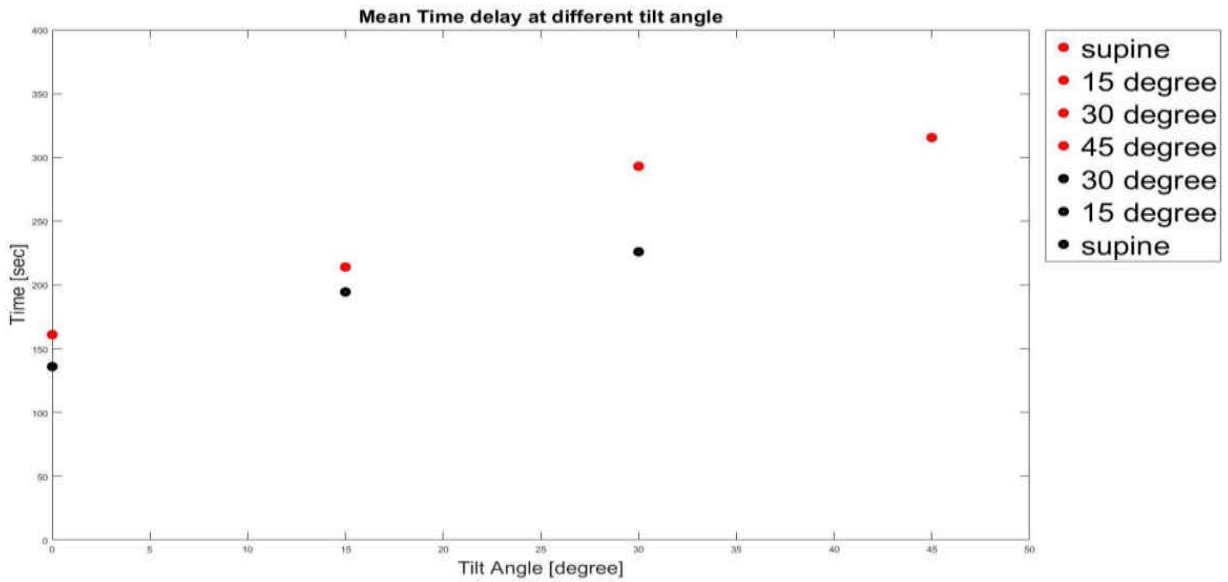


Figure 3-16 Time delay between TMP and Pulse signal at different tilt angle (subject 2). The tilt angle was changed rapidly with a 15 second data acquisition at each angle.

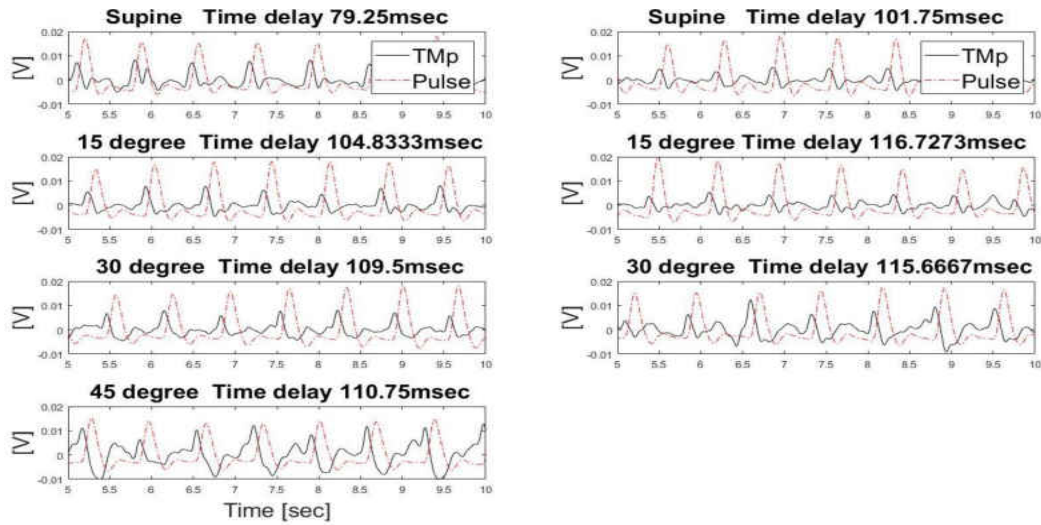


Figure 3-17 TMp along with earlobe pulse at different tilt angle changed rapidly. The amplitude of the TMp increased as the tilt angle increased (Subject 3)

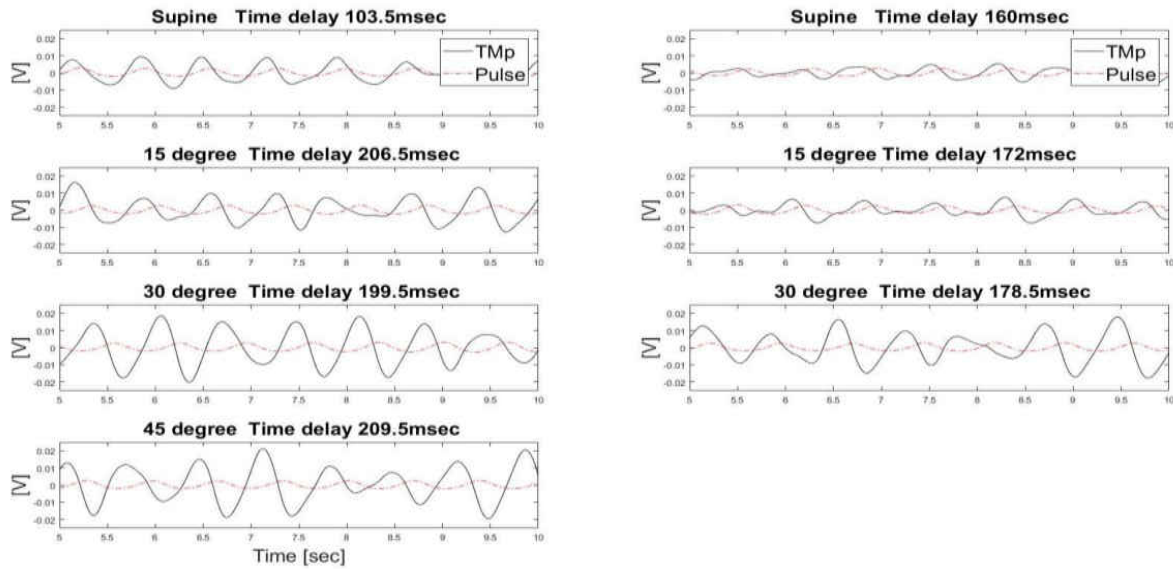


Figure 3-18 Variation of filtered TMp waveform with change in tilt angle (Subject 3). The amplitude and time delay increased with tilt angle

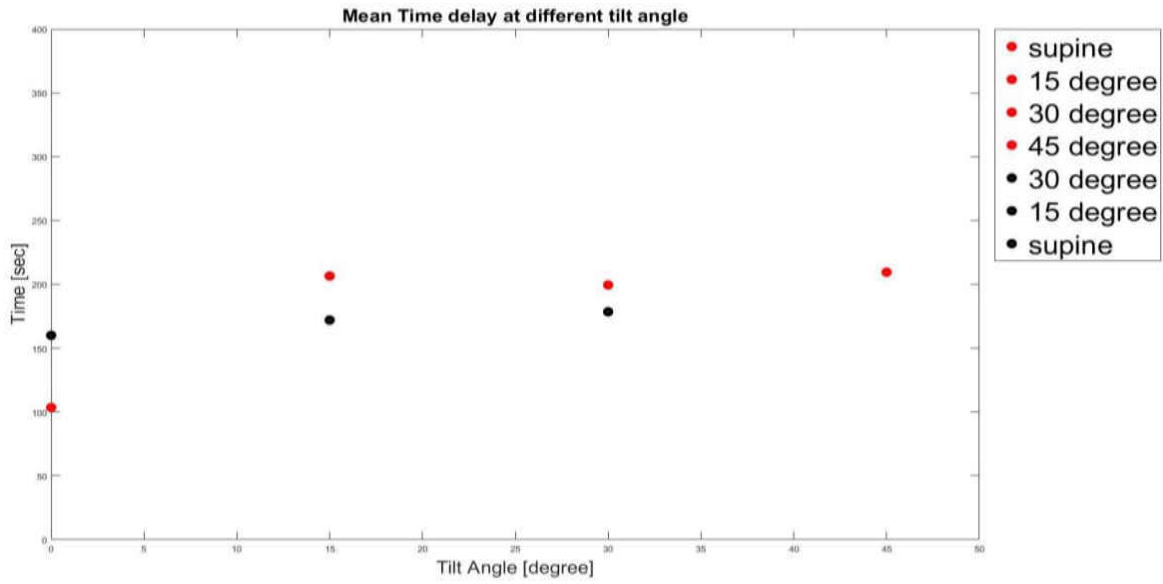


Figure 3-19 Time delay between TMP and Pulse signal at different tilt angle (subject 3). The tilt angle was changed rapidly with a 15 second data acquisition at each angle.

CHAPTER 4: SIMPLIFIED MODEL OF TYMPANIC MEMBRANE PULSATIONS

4.1 Model Geometry

A simplified model (figure 4-1) of CSF-inner ear-tympanic membrane model was developed. The CSF space was assumed to be 140 mL [7] To simplify the model, the CSF space was assumed to be cylinder. Since the cranium is rigid, the other interface of CSF is brain tissue. Hence the CSF wall was assumed to soft tissue with a Young's modulus 60 kPa and a density of 1041 kg/m⁻³. After the CSF cylinder, the cochlear aqueduct was modeled as a cylinder concentric to the CSF cylinder. The channel width was assumed to be 90×10^{-6} m[7]. The wall of the cochlear aqueduct was assumed to be rigid bone and the young's modulus was assumed to be 10 GPa with a density 1900 kg/m⁻³. Next to cochlear aqueduct, is a hollow cylinder with soft tissue wall mimicking cochlea.

The tympanic membrane is assumed to be thin disc with a thickness of 0.2 mm and a Young's modulus 0.1 GPa with a density assumed to be 1000 kg/m⁻³.

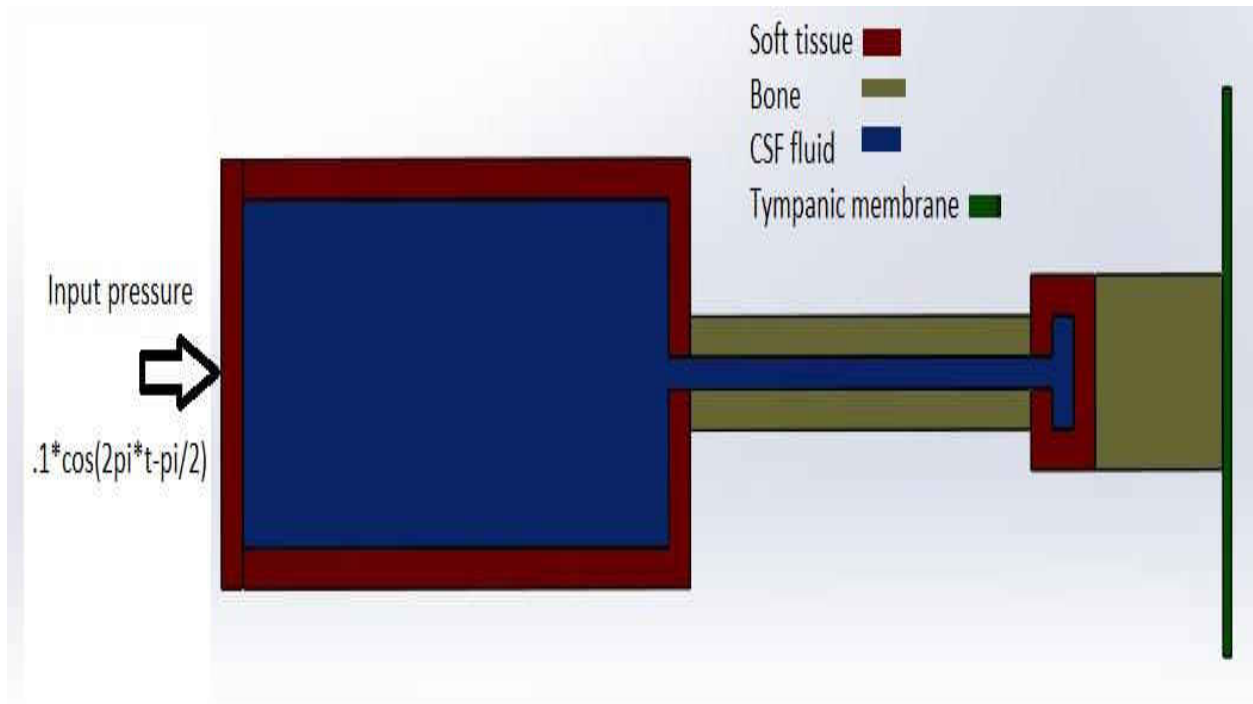


Figure 4-1 Schematic diagram of simplified model of CSF-Cochlea-Middle Ear-Tympanic Membrane. The red color showing the Soft tissue wall mimicking brain tissue, blue color corresponds to CSF fluid. The long bony channel represented by yellow is cochlear aqueduct. After cochlear aqueduct is cochlea surrounded by soft tissue. The green rectangle at the right end is the tympanic membrane. The yellow area between tympanic membrane and the cochlea is middle ear bones. The input is applied at left wall of CSF fluid

The tympanic membrane is fixed at the edge. The cochlear aqueduct and the left CSF wall is assumed to be fixed. An input of 1 Hz half cosine pressure wave with an amplitude of 0.1 Pa was initially applied on the left CSF wall.

4.2 Results

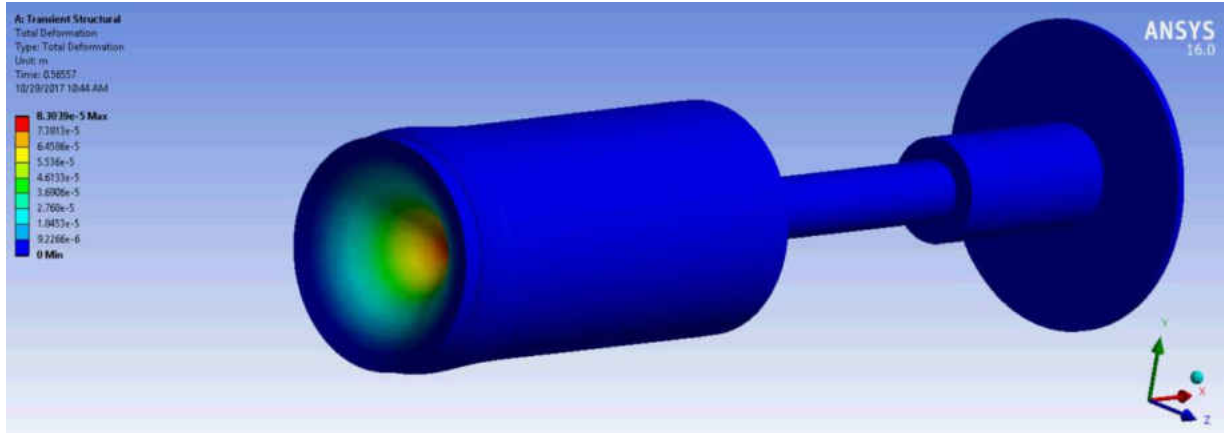


Figure 4-2 The maximum input deformation of the left CSF wall. The other boundaries of the fluid wall also deformed as the pressure travel towards cochlear aqueduct.

Figure 4-2 shows the maximum displacement of the left CSF wall due to the applied input pressure

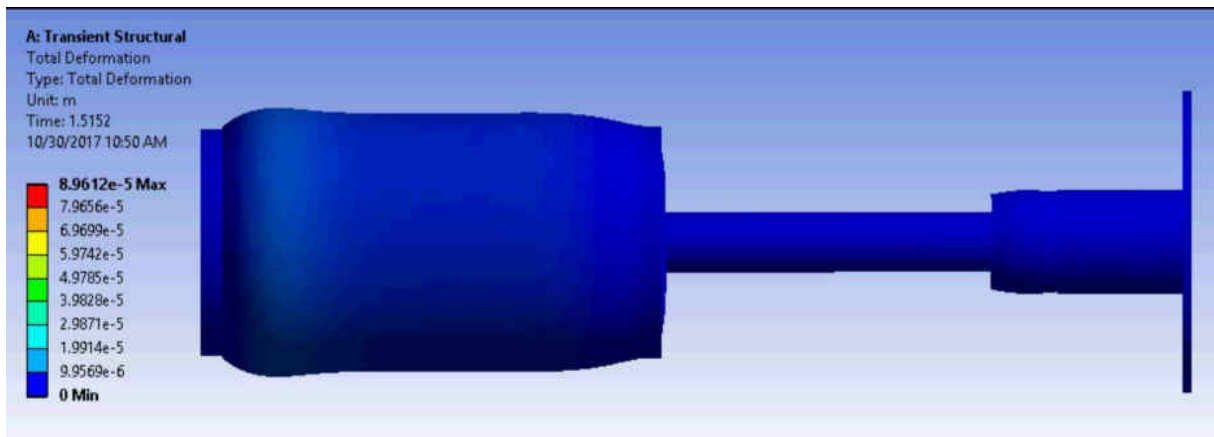


Figure 4-3 Deformation of CSF wall due to pressure input

Figure 4-3 showed that the deformation of CSF wall due to applied pressure wave. In addition, the pressure wave seemed to induce an elastic wave in vessel wall as the wall material was assumed to be soft tissue. Since the cochlear aqueduct is considered a bony rigid channel, the elastic wave

cannot travel through the cochlear aqueduct. Pressure at the end of the CSF cylinder is transmitted to the entrance of the cochlea without any delay.

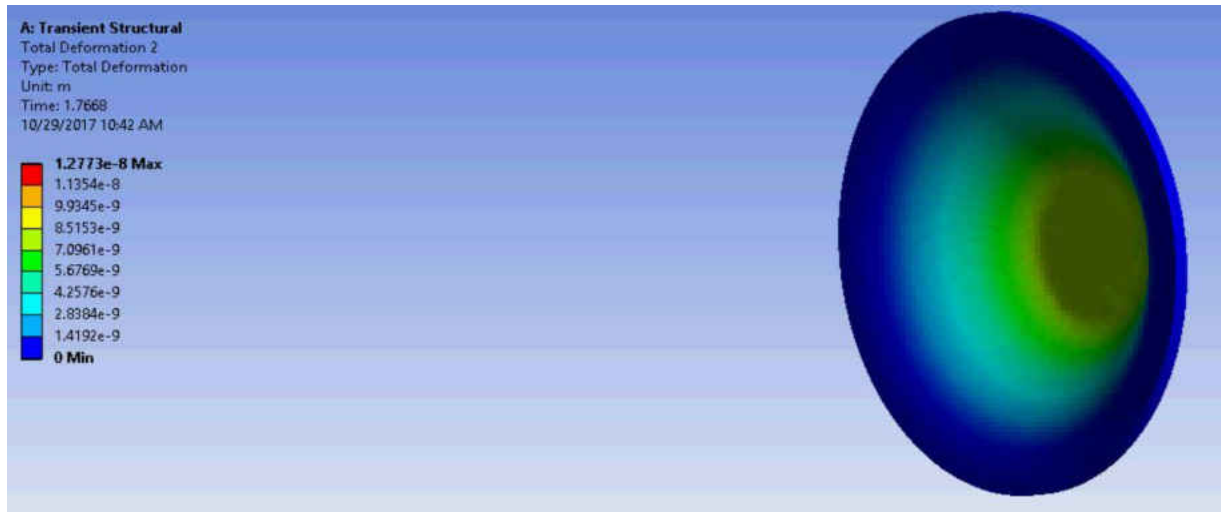


Figure 4-4 Maximum deformation of the TM. Since the edge of the TM is fixed, maximum deformation happened at the center.

The cochlear wall assumed to be soft tissue, hence will undergo deformation due applied pressure.

This pressure is transmitted to the tympanic membrane via middle ear bone.

Figure 4-4 showed the maximum displacement of the tympanic membrane. Since the membrane is fixed at the edge, at the peak input pressure, the membrane will not have any deformation at the edge. Maximum deformation of the tympanic membrane happened at the center. As soon as the tympanic membrane moved to the direction of applied pressure, the elastic behavior of the membrane will pull back the sharply to its equilibrium position.

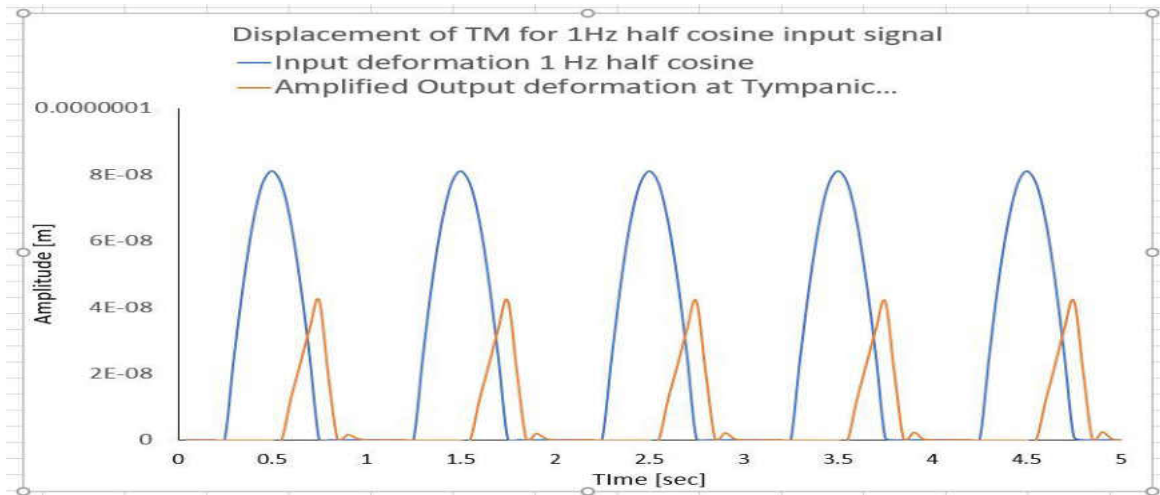


Figure 4-5 Output deformation of tympanic membrane is plotted with input deformation. The output deformation is scaled. Results shows a delay of 250 millisecond between the input deformation and output deformation

Figure 4-5 showed the deformation of the tympanic membrane along with input deformation at the CSF wall due to applied pressure. As the input deformation hits maximum, the membrane deformation remains zero. The membrane deformation builds up as the input deformation decreases. The membrane returns sharply to equilibrium position after the deformation reaches maximum. The delay between input and output deformation is about 250 milliseconds.

CHAPTER 5: DISCUSSION AND CONCLUSION

5.1 Discussion

5.1.1 Other Approaches of TMp Measurement

The current study attempted to utilize various sensors to effectively and reliably capture tympanic membrane pulsations. These included: a LED-photo resistor sensor assembly, a probe microphone, a LDV system, and a piezo disc sensor. The LED-photo resistor sensor consisted of a small white LED light that shine on the tympanic membrane and a photo resistor situated next to the LED to detect changes in reflected light due to the movement of the membrane.

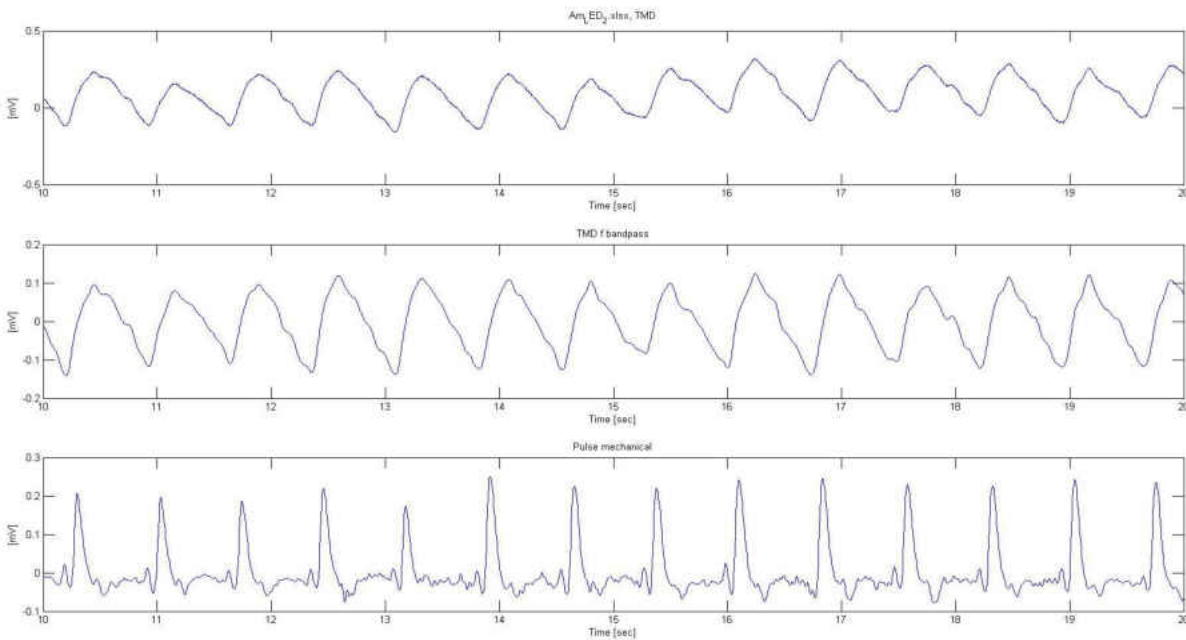


Figure 5-1 Tympanic membrane pulsations using LED & photo resistor assembly. The top figure indicates the raw data from photo resistor output. The middle figure indicates the filtered data (bandpass: 1-95 Hz). The bottom plot corresponds to optical pulse sensor at right hand thumb

Figure 5-1 shows a Tmp signal detected by the photo resistor placed at external ear canal. There were a few advantages of using photo resistor over other approaches. The photo resistor setup doesn't require the external ear canal to be sealed. It is small and convenient to use. The drawback of using LED-Photo resistor assembly was to ensure shining the LED light on the tympanic membrane due to the tortuous nature of external ear canal. In addition, presence of ear hair and wax made the LED-Photo resistor sensor output inconsistent. Any change in the environment light also may affect the output.

Shining a Laser beam directly on the tympanic membrane using a Laser Doppler Vibrometer (LDV) was another approach to capture the membrane movement.

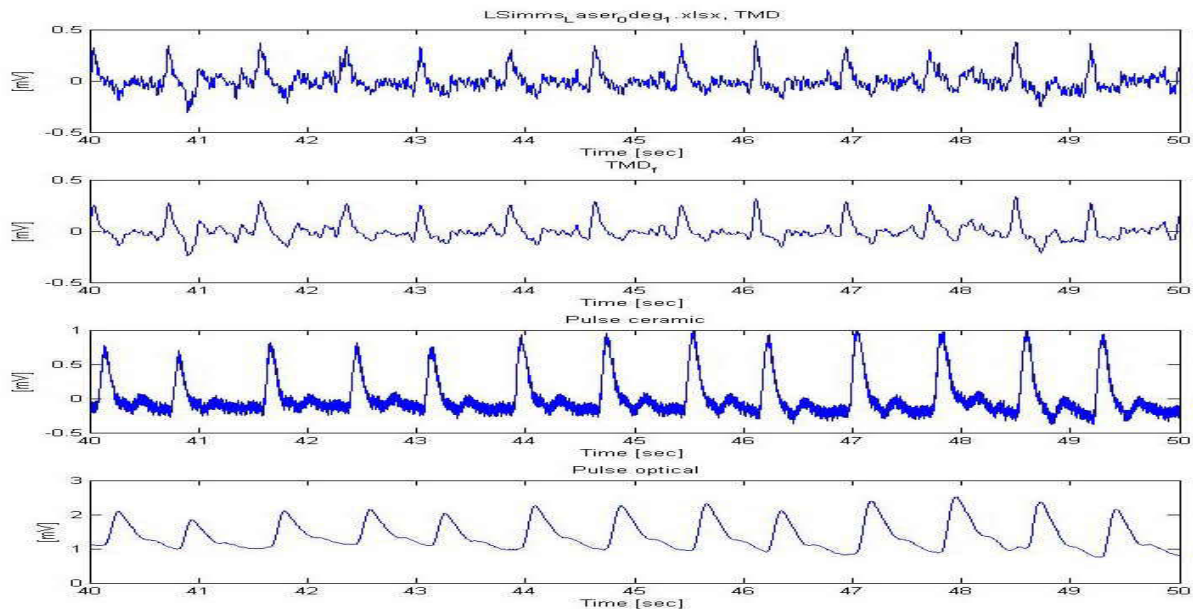


Figure 5-2 Tympanic membrane pulsation using LDV. The top figure shows the raw LDV output. Second from the top figure showing the filtered Tmp data. Third from the top figure showing blood pulsations using mechanical pulse sensor and bottom figure shows blood pulsation using optical pulse sensor.

Advantages of using LDV to acquire Tmp signal is that it is a direct measurement of tympanic membrane movement with a calibrated device. But the presence of ear hair and wax makes it difficult to shine the Laser directly on the membrane. Also, changing Laser direction at different tilt angle was another challenge since it requires time and precision. In addition, the points at the surface of the TM move differently, and aiming the Laser beam at the same point while the subject changes position is difficult to reproduce. These drawbacks made the system unfavorable for measuring Tmp signal at different tilt angles

Another approach was inserting a probe microphone in the external ear canal close to tympanic membrane.

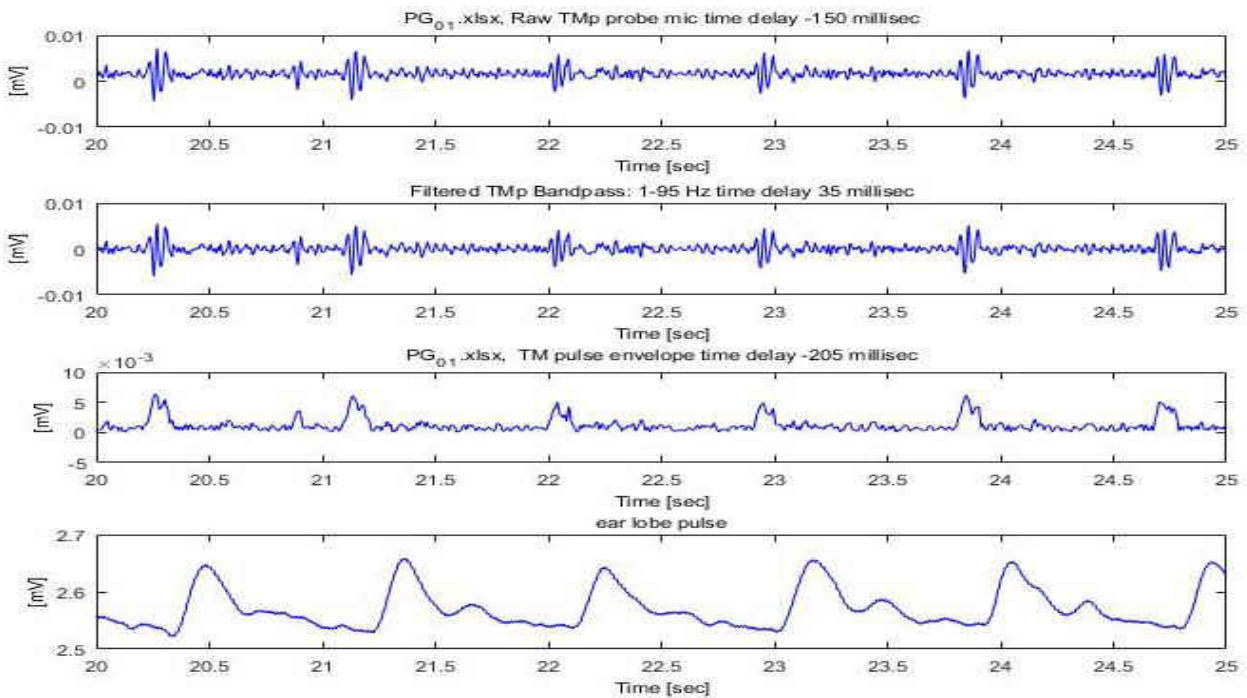


Figure 5-3 Tmp signal using probe microphone along with blood pulse at right thumb. The top figure shows the raw microphone data. The second from the top shows the filtered data. The third figure from the top shows the envelope of the signal using Hilbert transform. The bottom plot shows the blood pulsations at ear lobe.

Probe microphone measured the pressure fluctuations due to the movement of the tympanic membrane. However, maintaining the constant location of the probe for different subject inside the ear canal was a challenge. The signal to noise ratio in some subject was not high. Air tightness (of the space between the probe mic and TM) was needed to improve signal to noise ratio. The sensitivity of this microphone significantly decreased at low frequencies (e.g., <10Hz). The microphone probe also can be clogged by ear wax. These disadvantages made the sensor unfavorable for further use in Tmp acquisition at different tilt angle.

5.1.2 Repeatability of the Piezo Sensor Output

The piezo sensor was tested for its ability to produce repeatable waveform under same conditions using the mechanical setup. The piezo sensor reliably captured the movement of the membrane induced by a shaker. The variability of the sensor output acquired at different time under same condition found to be small (0.02 mV and about 1.5 % of the peak to peak amplitude) compared to the peak-to-peak amplitude of the Tmp signal (Figure 2-21). The corresponding LDV output data suggested that the acquired Tmp signal from piezo sensor corresponds to displacement of the membrane (Section 2.3.2). Since the cylinder cavity in the mechanical setup was comparable to human external ear canal, the ability of the piezo sensor to produce repeatable waveform suggested that the sensor can be a good candidate for acquiring Tmp signal in human subjects. In addition, investigation on the effect of small external pressure inside the sensor-cylinder cavity demonstrated that, changes in external pressure didn't change the sensor output significantly.

5.1.3 Repeatability of TMp signals in Human Subjects

The repeatability tests of TMp signals on several subjects under similar condition showed that although there is a wide inter subject variability in the shape and amplitude of the TMp waveform, intra-subject variability was within (4-8 % of peak to peak amplitude) at the peak of the waveform. The test on switching the sensor to contralateral ear showed that the sensor output remained the same (4-8% in the same ear) in terms of shape and amplitude. The dead space test on the sensor showed that sensor output significantly affected by the amount of dead space in the system. In addition, the leak testing proved that the signal amplitude dropped sharply if there is leakage in the sensor-ear canal cavity. The inclusion of leak testing valve helped greatly to ensure sealed sensor ear canal cavity. The leaked system also induced change in TMp waveform shape. Hence, a sealed system is essential to quantify change in TMp waveform shape and amplitude due to change in ICP. Effect of applying external pressure in the ear canal showed that the TMp waveform amplitude increased when slightly negative pressure was applied. One possible reason may be the compliance of the ear canal which can maximum in slightly negative pressure. The effect of applying external pressure in the contralateral ear didn't show significant change in the TMp waveform shape and amplitude. This suggests that changing pressure in the external ear canal didn't induce any change in ICP and therefore was not detected by the sensor.

5.1.4 Effect of Body Posture on TMp

Studies [14], [16], [17] showed that ICP changes with body posture, where the ICP amplitude increased as the body was tilted in the head down direction. The decrease in ICP waveform amplitude as the body posture moved in head up direction was observed in human and animal

experiments [14]. An earlier study suggested that tympanic membrane movement changed with ICP [19]. Current study showed that as the body tilted downward, the TMp signal amplitude increased gradually. In another experiment, the ICP was changed quickly and each tilt angle duration was approximately 15 seconds with 5 seconds of wait time in between angles. The corresponding TMp waveform showed that the amplitude and shape of the waveform changed as soon as the subject moved to a new tilt angle. Hence it can be said that the TMp sensor assembly can effectively monitor changes in ICP by tracking the changes in TMp waveforms. This can be an effective way of monitoring ICP non-invasively. Another observation was that at fundamental frequency, the time delay between the TMp and reference pulse signal tended to increase as the ICP increased (in 2 of the 3 subjects). After hyper-ventilation, which is expected to cause significant drop in ICP [17], the corresponding time delay between pulse and TMp decreased accordingly. This can be another useful parameter for monitoring ICP non-invasively. Cross correlation function was also used to calculate the time delay between the two signals. This calculation requires signals with better signal to noise ratio. Hence it is paramount to filter the signal at intended frequency. In this case, both signals were filtered using bandpass (1-2 Hz) to keep the fundamental frequency only.

5.1.5 Simplified Numerical Model

Numerical model used in the study was simplified significantly help understand the basic principle of the movement of the tympanic membrane. The soft tissue walls in the model (wall of CSF and cochlea) was assumed to be linearly elastic. In response to an input pressure, the deformation at the simulated ear drum showed a 250 millisecond of delay with respect to deformation at the wall where the input pressure was applied (figure 4-5). This value is comparable with the time delay

values calculated in the experiments. The CSF volume in the cranium is assumed to be constant in the numerical model while the CSF volume in the cranium changes inversely with cerebral blood volume (i.e., as CSF increases the cerebral blood volume decreases) [3], [17]. CSF is assumed to be identical to cochlear fluid in the numerical model. Although the CSF fluid has similar composition as perilymph and endolymph (cochlear fluid), they are separated from CSF. Both perilymph and endolymph also circulate within cochlea. When the stiffness of the CSF wall (Assumed to be brain tissue) was increased in the model didn't yield any change in time delay. Possible reason may be that the brain tissue has hyper viscoelastic properties while the numerical model assumed linear elastic material properties. In addition, the CSF is not in motion in the numerical model while the CSF circulates around the subarachnoid spaces and spinal cord. The entire CSF volume is replaced about four times a day [17]. Therefore, any change in pressure inside CSF in the model would readily transmit to the cochlear wall. Hence changing the wall stiffness didn't change the time delay between input and output. The time step in the numerical modeling was set 5 milliseconds to save computational expense, hence any change in time delay lower than 5 milliseconds would not be detected by the modeling. A lower time step preferably 1 millisecond and a finer mesh may be able to capture the change in time delay due to change in wall stiffness.

5.2 Future Work

Future work includes acquiring TMp data on patients with raised ICP and comparing the data with normal subjects. In addition, acquiring TMp data from patients with ventricular shunt would further illustrate the relation between ICP and TMp. Furthermore, a realistic numerical model with pulsatile blood flow in the blood vessel similar to previous studies [29], [30] along with CSF,

cranium, brain tissue, inner ear, middle ear and tympanic membrane would allow more insight on the movement of tympanic membrane under varying ICP. Also, time-frequency methods [31], [32] of the individual and mean TMp waveforms might be used to identifying new features that would help separate normal ICP from increased ICP.

5.3 Conclusion

The current study investigated the relation between ICP changes and TMp. A sensor system that can reliably acquire tympanic membrane pulse was designed and tested. Results showed that the variation of ICP by changing body posture caused change in the shape of TMp waveforms. Furthermore, as the tilt angle increased the time delay between the TMp waveform and ear lobe pulse waveform increased. After hyper ventilation, the increase in ICP was decreased, which reduced the time delay between TMp and Pulse. After hyperventilation, as the subject gradually returned to supine position the time delay reduced in a similar pattern and was found to be comparable to the time delay values of the supine position at the beginning of the experiment. In addition, the TMp waveform was found to be affected by breathing which is known to affect ICP.

LIST OF REFERENCES

- [1] H. Kristiansson, E. Nissborg, J. Bartek, M. Andresen, P. Reinstrup, and B. Romner, "Measuring Elevated Intracranial Pressure through Noninvasive Methods," *J. Neurosurg. Anesthesiol.*, vol. 25, no. 4, pp. 372–385, 2013.
- [2] B. Blausen, "NOTES - Blausen gallery 2014," *Wikiversity, J. Med.*, vol. 1 (2), no. 3, pp. 144–149, 2014.
- [3] L. Sakka, G. Coll, and J. Chazal, "Anatomy and physiology of cerebrospinal fluid," *European Annals of Otorhinolaryngology, Head and Neck Diseases*, vol. 128, no. 6. pp. 309–316, 2011.
- [4] B. Mokri, "The Monro-Kellie hypothesis: Applications in CSF volume depletion," *Neurology*, vol. 56, no. 12, pp. 1746–1748, 2001.
- [5] P. K. Eide, "Intracranial pressure parameters in idiopathic normal pressure hydrocephalus patients treated with ventriculo-peritoneal shunts," *Acta Neurochir. (Wien)*, vol. 148, no. 1, pp. 21–29, 2006.
- [6] R. W. Baloh, "Dizziness, Hearing Loss, and Tinnitus," in *Dizziness, Hearing Loss, and Tinnitus*, 1998, pp. 73–187.
- [7] R. J. Marchbanks and A. Reid, "Cochlear and cerebrospinal fluid pressure: their inter-relationship and control mechanisms.," *Br. J. Audiol.*, vol. 24, pp. 179–187, 1990.
- [8] A. J. Phillips and R. J. Marchbanks, "Effects of posture and age on tympanic membrane displacement measurements," *Br J Audiol*, vol. 23, no. 4, pp. 279–284, 1989.
- [9] D. A. Sanders, *Auditory perception of speech: An introduction to principles and problems*. Prentice Hall, 1977.
- [10] J. D. Kerth and G. W. Allen, "Comparison of the perilymphatic and cerebrospinal fluid pressures.," *Arch. Otolaryngol. (Chicago, Ill. 1960)*, vol. 77, p. 581, 1963.
- [11] B. I. J. Beentjes, "The Cochlear Aqueduct and the Pressure of Cerebrospinal and Endolabyrinthine Fluids," *Acta Otolaryngol.*, vol. 73, no. 2–6, pp. 112–120, Jan. 1972.
- [12] B. Carlborg, O. Densert, and J. Stagg, "Perilymphatic pressure in the cat. Description of a new method for study of inner ear hydrodynamics.," *Acta Otolaryngol.*, vol. 90, no. 3–4, pp. 209–18, 1980.
- [13] M. Hiipakka, "Measurement Apparatus and Modelling Techniques of Ear Canal Acoustics," *Science (80-.)*, p. 93, 2008.
- [14] K. C. Bradley, "Cerebrospinal fluid pressure," *J. Neurol. Neurosurg. & Psychiatry*, vol. 33, no. 3, p. 387 LP-397, Jun. 1970.
- [15] L. H. Weed, L. B. Flexner, and J. H. Clark, "The effect of dislocation of cerebrospinal fluid upon its pressure," *Am. J. Physiol. Content*, vol. 100, no. 2, pp. 246–261, 1932.
- [16] J. S. Lawley *et al.*, "Effect of gravity and microgravity on intracranial pressure," *J. Physiol.*, vol. 595, no. 6, pp. 2115–2127, 2017.
- [17] D. N. Irani, *Cerebrospinal fluid in clinical practice*. Elsevier Health Sciences, 2009.
- [18] P. H. Raboel, J. Bartek, M. Andresen, B. M. Bellander, and B. Romner, "Intracranial pressure monitoring: Invasive versus non-invasive methods-A review," *Critical Care Research and Practice*, vol. 2012. 2012.
- [19] A. Reid *et al.*, "The relationship between intracranial pressure and tympanic membrane

- displacement,” *Br. J. Audiol.*, vol. 24, no. 2, pp. 123–129, 1990.
- [20] R. Marchbanks, “A study of tympanic membrane displacement.” Brunel University School of Engineering and Design PhD Theses, 1980.
- [21] O. Balédent, M. C. Henry-Feugeas, and I. Idy-Peretti, “Cerebrospinal fluid dynamics and relation with blood flow: a magnetic resonance study with semiautomated cerebrospinal fluid segmentation.,” *Invest. Radiol.*, vol. 36, no. 7, pp. 368–77, 2001.
- [22] A. Taebi and H. A. Mansy, “Time-frequency Analysis of Vibrocardiographic Signals,” in *2015 BMES Annual Meeting*, 2015.
- [23] A. Taebi and H. A. Mansy, “Time-frequency Description of Vibrocardiographic Signals,” in *38th Annual International Conference of the IEEE Engineering in Medicine and Biology Society*, 2016.
- [24] A. Taebi and H. A. Mansy, “Effect of Noise on Time-frequency Analysis of Vibrocardiographic Signals,” *J. Bioeng. Biomed. Sci.*, vol. 6(202), p. 2, 2016.
- [25] A. Taebi and H. A. Mansy, “Noise Cancellation from Vibrocardiographic Signals Based on the Ensemble Empirical Mode Decomposition,” *J. Appl. Biotechnol. Bioeng.*, vol. 2, no. 2, p. 24, 2017.
- [26] A. Taebi, R. H. Sandler, B. Kakavand, and H. A. Mansy, “Seismocardiographic Signal Timing with Myocardial Strain,” in *Signal Processing in Medicine and Biology Symposium (SPMB), 2017 IEEE*, 2017, pp. 1–2.
- [27] A. Taebi and H. A. Mansy, “Grouping Similar Seismocardiographic Signals Using Respiratory Information,” in *Signal Processing in Medicine and Biology Symposium (SPMB), 2017 IEEE*, 2017, pp. 1–6.
- [28] B. E. Solar, A. Taebi, and H. A. Mansy, “Classification of Seismocardiographic Cycles into Lung Volume Phases,” in *Signal Processing in Medicine and Biology Symposium (SPMB), 2017 IEEE*, 2017, pp. 1–2.
- [29] F. Khalili and H. A. Mansy, “Blood Flow through a Dysfunctional Mechanical Heart Valve,” in *38th Annual International Conference of the IEEE Engineering in Medicine and Biology Societ*, 2016.
- [30] F. Khalili, P. P. T. Gamage, and H. A. Mansy, “Hemodynamics of a Bileaflet Mechanical Heart Valve with Different Levels of Dysfunction,” *J. Appl. Biotechnol. Bioeng.*, vol. 2, no. 5, Mar. 2017.
- [31] A. Taebi and H. A. Mansy, “Analysis of Seismocardiographic Signals Using Polynomial Chirplet Transform and Smoothed Pseudo Wigner-Ville Distribution,” in *Signal Processing in Medicine and Biology Symposium (SPMB), 2017 IEEE*, 2017, pp. 1–6.
- [32] A. Taebi and H. A. Mansy, “Time-Frequency Distribution of Seismocardiographic Signals: A Comparative Study,” *Bioengineering*, vol. 4, no. 2, p. 32, 2017.